

© 1972

RAYMOND EDGAR CARHART

ALL RIGHTS RESERVED

A DETAILED THEORETICAL STUDY OF THE  
DIFLUOROMETHANE MOLECULE

Thesis by  
Raymond E. Carhart

In Partial Fulfillment of the Requirements  
For the Degree of  
Doctor of Philosophy

California Institute of Technology  
Pasadena, California

1973

(Submitted September 1, 1972)

## ACKNOWLEDGMENTS

I wish to thank Professors John D. Roberts and William A. Goddard not only for their friendly guidance and encouragement throughout this work, but also for their willingness to let me pursue my own ideas at my own pace. This freedom has aided immeasurably in my scientific maturation.

I am greatly appreciative of the many informative and thought-provoking discussions I have had with various members of the Goddard group, particularly Drs. W. J. Hunt and T. H. Dunning, and of the assistance given by Dana A. Powers in obtaining the IR spectra.

I recognize, too, Mrs. Edi Bierce for her fast and excellent typing of this thesis.

I most gratefully acknowledge the financial support of the National Science Foundation in the form of Graduate Fellowships, and of the Institute in the form of teaching assistantships.

Finally, and most importantly, I thank my dear and understanding wife, Jane, who helped me accept the defeats and enjoy the successes of this work, and my son Kevin who, in his own way, assisted in the speedy completion of this thesis.

To Jane and Boom-Boom

## ABSTRACT

The first chapter describes our theoretical investigation of the potential energy surface of the difluoromethane molecule. The Hartree-Fock (HF) method, with a 73/3 gaussian basis contracted to the double-zeta level, was used, and in many cases, CNDO/2 calculations were included for comparison.

The optimum HF geometry is found to be closer to experiment than that reported by other workers using a minimum (STO-3G) basis set, but it appears that our more flexible basis does little to improve the computed general harmonic force constants, the complete set of which is considered. The stretching constants are found to be in error by +20% to +35%, the bending constants by -4% to +45%. In comparison with HF, the CNDO/2 method grossly overestimates the stretching constants, but mimics rather well the bending and interaction constants.

The theoretical (HF) normal modes and observed vibration frequencies are combined to give a set of semi-empirical force constants (SEFC's) which are used to predict the vibration frequencies of the deuterated difluoromethanes. The synthesis and IR spectrum analysis of these compounds is described, and the SEFC predictions are found to be superior to ones appearing previously in the literature.

The Urey-Bradley potential (UBP) model, with  $1/r^6$  steric terms, is fit to the HF constants and SEFC's. A comparison of the two UBPs indicates that the HF method consistently over-

estimates all parameters but the F-F steric term, which it underestimates.

Anharmonicity in the angular coordinates for large molecular distortions is investigated, and it is found that CNDO/2 mimics HF quite well, except that CNDO/2 underestimates the anharmonicity when the fluorines are quite close together. The UBP model derived from the HF force constants is found to account for most of the anharmonicity in the HF energy variation.

The second chapter describes our investigation of the electronic structure of difluoromethane. The HF method, with the basis set discussed above, and certain configuration-interaction methods, were used.

The localized (HF) molecular orbitals (LMO's) were obtained for the equilibrium geometry using a new, quadratically convergent approach which is useful for cases in which convergence of the Edmiston-Ruedenberg "two-by-two" method is slow. The LMO's are examined in detail, and several methods are used to show that the fluorine lone pairs are delocalized toward carbon, a delocalization which represents an important stabilization in the molecule. It is noted that this effect, which is most pronounced for lone pairs lying in the F-C-F plane, may be the molecular-orbital equivalent of the "double bond-no bond" resonance of valence-bond theory.

An analysis of the LMO's for distorted geometries indicates that the "orbital following" concept does not apply to difluoromethane as the F-C-F angle is altered.

An economical approximation to the generalized valence-bond (GVB) method is developed and is used to give a more detailed picture of the electron pairs in the molecule. The GVB-like pairs are localized, but in this case the localization is a result of the variation principle rather than a physically meaningless localization criterion. They are used to define (in an approximate fashion) "naturally" localized Hartree-Fock orbitals (NLMO's) qualitatively similar to the LMO's.

An analysis of the NLMO's supports the conclusions drawn from the LMO analysis concerning lone-pair delocalization and "orbital following".

## TABLE OF CONTENTS

	<u>Page</u>
ACKNOWLEDGMENTS . . . . .	ii
ABSTRACT . . . . .	iv
Chapter 1 The Potential Energy Surface of Difluoromethane	1
A. Introduction . . . . .	1
B. Geometry Optimization . . . . .	5
C. Quadratic Force Constants . . . . .	13
D. Energy Variation for Gross Angular Distortions	40
E. Summary . . . . .	51
F. Experimental . . . . .	53
G. References . . . . .	74
Chapter 2 The Electronic Structure of Difluoromethane . .	77
A. Introduction . . . . .	77
B. Localized Hartree-Fock Orbitals . . . . .	82
C. Approxiate Generalized-Valence-Bond (GVB) Orbitals . . . . .	124
D. Summary . . . . .	177
E. References . . . . .	180
PROPOSITIONS . . . . .	184

## Chapter 1

## THE POTENTIAL ENERGY SURFACE OF DIFLUOROMETHANE

A. Introduction

The difluoromethane molecule, with 26 electrons, is small enough to be within reach of moderately sophisticated quantum mechanical techniques, yet only a small amount of work on this molecule has been reported (1-3). In none of these investigations has the potential energy surface been considered explicitly, and so we have undertaken such a study using both the semi-empirical CNDO/2 (4) and the ab initio Hartree-Fock-Roothaan (5) methods. There were two major goals in this study: The first was to determine the complete harmonic potential around the theoretical equilibrium geometry; the second was to investigate the molecular energy variation as a function of large changes in the angular coordinates, particularly the F-C-F and H-C-H angles. Several lesser points of interest were also involved, including an investigation of the Urey-Bradley potential model (6), a comparison of the Hartree-Fock and CNDO/2 methods, and the "semi-empirical" prediction of accurate force constants.

In recent years, there has been a great deal of interest in the calculation of molecular geometries and harmonic force constants using ab initio quantum mechanical methods. As noted by Newton et al. (3), the general trend appears to be that the Hartree-Fock

approximation leads to good calculated geometries\* and moderately accurate calculated force constants, even when rather small basis sets of atomic orbitals are employed. In general, stretching constants are overestimated by roughly 20%, bending constants can be either high or low, often in error by 30%, while interaction constants are predicted rather erratically. In much of the work which has been done, only the force constants for symmetric deformation modes have been calculated, although the full set is needed for the prediction of the molecular vibration spectrum and for the testing of various model force fields. The few cases in which a full analysis has been carried out are restricted to molecules of the  $XH_n$  type (7) where X is a first- or second-row atom and n is 2, 3 or 4. Thus, in studying the full potential of  $CH_2F_2$ , we have extended the range of available data to include other than hydrides. In addition, we have used an atomic basis set substantially more flexible than that of Newton et al. (3) (a "double-zeta" rather than a minimum basis set) and have thus been able to verify the basis-set independence of their observations.

As a test of overall accuracy, we have compared the harmonic vibration frequencies derived from these constants with the experimental values. Unfortunately, no reliable force constants are

---

\* The fact that good geometries can be obtained from minimum basis set calculations may be due, in part, to a cancellation of errors. Dunning et al. (39), for example, find that the optimum geometry of  $H_2O$  is rather sensitive to the nature of the basis.

available for direct comparison (8), but we have used the calculated constants in combination with the observed frequencies to give a set of semi-empirical force constants. We have found these to yield good predictions for the vibration frequencies of  $\text{CHDF}_2$  and  $\text{CD}_2\text{F}_2$ , demonstrating that such theoretical calculations can be of value in obtaining true force constants.

In a recent theoretical study of the water molecule, Pitzer and Merrifield found the molecular energy to vary as an essentially parabolic function of the H-O-H angle over a  $30^\circ$  range near the minimum (9). This is reasonable if we assume that the major deviations from parabolicity are due to H-H steric interactions, which should be small. The situation should be quite different in  $\text{CH}_2\text{F}_2$  for two reasons: First, the fluorines are somewhat larger and should show a marked steric effect as the F-C-F angle is varied; second, the tetrahedrally bonded central carbon would be expected to react differently to geometrical changes than would the dihedrally bonded oxygen in  $\text{H}_2\text{O}$ . In order to assess the magnitudes of these effects, we have examined the energy variation as a function of various angular coordinates in difluoromethane. The comparison between Hartree-Fock and CNDO/2 energies is most interesting, giving some indication of the nature of the errors inherent to the CNDO/2 MO method. Also, we have examined the ability of a Urey-Bradley model (6) to account for the Hartree-Fock energy changes, and have found rather good agreement.

Because a large number of individual Hartree-Fock calculations is necessary in a study of this nature, we have chosen to use a small but flexible basis set of gaussian atomic orbitals, a 73/3 set contracted to the double-zeta level. Details of the basis set and of the calculations themselves are included in section F of this chapter. In all cases, sufficient SCF iterations were undertaken to give energies precise to  $1 \times 10^{-6}$  a. u. or better. All CNDO/2 calculations were carried out using program CNINDO, obtained from the Quantum Chemistry Program Exchange (10).

## B. Geometry Optimization

The initial problem in this investigation was the determination of the Hartree-Fock equilibrium geometry for difluoromethane. Newton et al. (3) have done this, but with a basis set substantially different from ours, and our results match the experimental geometry more closely than theirs. They have used an optimization technique which concentrates on only one symmetrized valence coordinate (SVC) at a time; this coordinate is increased and decreased by some small amount and the resulting energy change is fit to a parabolic function. The minimum of this function defines the new value for the coordinate. The SVC's are processed in a cyclic manner until none change by a significant amount. Bratož and Allavena have criticized this numerical type of approach (7d), advocating instead an analytical evaluation of the curvature of the energy surface, but the method is extremely complex for molecules as large as difluoromethane. Thus we have used a method similar to Newton's, with modifications to be discussed below.

During preliminary CNDO/2 calculations, we found that the above method can, during the first few cycles, lead to unreasonable predictions if the starting geometry is very different from the final one. In such cases, the procedure, though convergent, requires many energy evaluations before the solution is reached. The method does not attempt to account for the couplings between SVC's, which is the cause of the problem. In an effort to economize on the number

of Hartree-Fock calculations, we have developed the following rapidly convergent approach. The idea, basically, is to expand the energy as a multidimensional quadratic function of the SVC's and to use the minimum of this function to define the new geometry. Starting from some "guess" geometry, we may expand the energy as a function of small displacements ( $\Delta q_1, \Delta q_2, \dots, \Delta q_n$ ) in the SVC's via a Taylor series:

$$E \cong E_0 + \sum_{i=1}^n \frac{\partial E}{\partial q_i} \Delta q_i + \sum_{i=1}^n \sum_{j=1}^n \frac{1}{2} \frac{\partial^2 E}{\partial q_i \partial q_j} \Delta q_i \Delta q_j. \quad (\text{I})$$

For convenience, we make the substitutions:

$$A_i = \frac{\partial E}{\partial q_i} \quad \text{and} \quad B_{ij} = B_{ji} = \frac{\partial^2 E}{\partial q_i \partial q_j}. \quad (\text{II})$$

And we may express equation (I) concisely in matrix notation as:

$$E \cong E_0 + \underline{A}^T \underline{\Delta q} + \frac{1}{2} \underline{\Delta q}^T \underline{B} \underline{\Delta q}. \quad (\text{III})$$

Here, as throughout this thesis, the underline denotes a column vector, the wavy line denotes a matrix and the superscript T indicates "transpose". We mention in passing that if the "guess" geometry is in fact the equilibrium one, then the vector of first derivatives ( $\underline{A}$ ) is zero and the matrix  $\underline{B}$  represents a portion of the force constant matrix for the molecule. If  $\underline{A}$  and  $\underline{B}$  are known, then we may solve directly for the vector of corrections ( $\underline{\Delta q}$ ) to the SVC's by differentiating (III) with respect to each of the  $\Delta q_i$ 's and setting

the result to zero. This simply locates the minimum of the quadratic function (III). The resulting equations, in matrix form, are:

$$\underline{A} + \underline{B} \underline{\Delta q} \cong \underline{0} \quad (\underline{0} \text{ is the zero vector}) \quad (\text{IV})$$

This yields:

$$\underline{\Delta q} \cong -\underline{B}^{-1} \underline{A}. \quad (\text{V})$$

We evaluate the quantities  $A_i$  and  $B_{ij}$  numerically. To begin, we increase and decrease one of the coordinates (say  $q_m$ ) by some small amount  $\delta$ , then we evaluate the resulting energies, which we call  $E_m^{+\delta}$  and  $E_m^{-\delta}$ , respectively. In this case,  $\Delta q_i = 0$  for  $i \neq m$  and  $\Delta q_m = \delta$ . Formulae (I) and (II) give:

$$E_m^{+\delta} \cong E_0 + A_m \delta + \frac{1}{2} B_{mm} \delta^2 \quad (\text{VI})$$

$$\text{and } E_m^{-\delta} = E_0 - A_m \delta + \frac{1}{2} B_{mm} \delta^2$$

These equations may be solved for  $A_m$  and  $B_{mm}$  to give:

$$A_m = \frac{E_m^{+\delta} - E_m^{-\delta}}{2\delta} \quad \text{and} \quad B_{mm} = \frac{E_m^{+\delta} + E_m^{-\delta} - 2E_0}{\delta^2} \quad (\text{VII})$$

To this point, our method is equivalent to the usual one;  $A_m$  and  $B_{mm}$  define a parabolic function of  $\Delta q_m$  which could be used to generate a new value for  $q_m$ . However, we do not do this yet, but rather we evaluate  $A_m$  and  $B_{mm}$  for each of the SVC's without changing the reference geometry. Next, we simultaneously increase

a pair of SVC's (say  $q_m$  and  $q_n$ ) by  $\delta_m$  and  $\delta_n$ , respectively and we evaluate the energy, which we call  $E_{mn}^{\delta}$ . In this case,  $\Delta q_i = 0$  for  $i \neq m, n$  and  $\Delta q_m = \delta_m$  and  $\Delta q_n = \delta_n$ . Formulae (I) and (II) give:

$$E_{mn}^{\delta} = E_0 + A_m \delta_m + A_n \delta_n + \frac{1}{2} B_{mm} \delta_m^2 + \frac{1}{2} B_{nn} \delta_n^2 + B_{mn} \delta_m \delta_n \quad (\text{VIII})$$

This equation may be solved for  $B_{mn}$  ( $= B_{nm}$ ) because all other values are known. In this way, we evaluate all off-diagonal elements of the matrix  $B$ , these elements representing couplings between the SVC's. At this point, we have fixed all variables necessary for the solution of equation (V) to give the vector  $\Delta q$ , the corrections to be applied to the SVC's. These corrections define a new guess for the optimum geometry. A second cycle of refinement leads to a better guess, and so on.

For a molecule with  $n$  SVC's defining the equilibrium geometry, the above method requires  $1 + (n^2 + 3n)/2$  energy evaluations per cycle, while the usual method needs only  $3n$ . We have assumed that the  $\text{CH}_2\text{F}_2$  molecule has  $C_{2v}$  symmetry, so only four SVC's are required (two bond lengths and two bond angles) to define the geometry. Thus, with  $n = 4$ , our optimization technique uses fifteen separate energies per cycle, as compared to twelve in the usual method. For much larger molecules, our procedure would not be as useful because the number of individual energy calculations increases rapidly as a function of  $n$ .

The geometry optimization for difluoromethane was carried out first using CNDO/2 energies, beginning from the experimental geometry (see Table 1). The parameter increments were taken as  $5^\circ$  and  $0.05\text{\AA}$  for the angular and distance coordinates, respectively. After two cycles, the geometry given in Table 1 was obtained, and a third cycle produced negligible changes. An attempt was made to further refine these values on a "grid" level of  $1^\circ$  and  $0.01\text{\AA}$ , but at this level, the numerical inaccuracy in  $\underline{A}$  and  $\underline{B}$  is rather large due to the small energy variations involved. The results indicate that changing the grid size alters the bond lengths by less than  $.003\text{\AA}$  and the angles by less than  $0.2^\circ$ . As a test of our optimization procedure, we have carried out similar calculations using INDO (11) energies, the results of which are given in Table 1. The INDO geometry differs from that quoted by Pople (12) by about  $0.005\text{\AA}$  and  $0.2^\circ$  in the bond lengths and angles, respectively, and these differences most probably arise from our larger grid size (again,  $5^\circ$  and  $0.05\text{\AA}$  as opposed to  $1^\circ$  and  $0.01\text{\AA}$ ).

For the Hartree-Fock optimization, three starting points were considered. These were: a) the optimum CNDO/2 geometry on the  $5^\circ$ ,  $0.05\text{\AA}$  level; b) the experimental geometry (see Table 1); and c) the optimum Hartree-Fock geometry of Newton et al. (3). Of these, the experimental geometry gave the lowest energy, about  $4.4 \times 10^{-3}$  a. u. lower than a) and  $1.4 \times 10^{-3}$  a. u. lower than c). Thus, with b) as the starting point, we carried out one cycle of optimization using increments of  $0.02\text{\AA}$  for the bond lengths,  $2^\circ$  for

Table 1. - Equilibrium Geometries of Difluoromethane  
( $C_{2v}$  symmetry).

<u>Case</u>	<u>R(C-F)</u>	<u>R(C-H)</u>	<u><math>\theta</math>(F-C-F)</u>	<u><math>\theta</math>(H-C-H)</u>
Experimental <sup>a</sup> (13)	1.358 $\text{\AA}$	1.091 $\text{\AA}$	108.2 $^\circ$	112.1 $^\circ$
CNDO/2	1.345 $\text{\AA}$	1.124 $\text{\AA}$	106.2 $^\circ$	110.7 $^\circ$
INDO	1.348 $\text{\AA}$	1.125 $\text{\AA}$	105.9 $^\circ$	110.9 $^\circ$
Hartree-Fock (3)	1.378 $\text{\AA}$	1.109 $\text{\AA}$	108.7 $^\circ$	108.8 $^\circ$
Hartree-Fock (this work)	1.374 $\text{\AA}$	1.070 $\text{\AA}$	109.0 $^\circ$	112.2 $^\circ$

<sup>a</sup>A more recent experimental study (14) has yielded virtually the same geometry, except for the H-C-H angle, which is reported to be 113.7 $^\circ$ .

the F-C-F angle and  $4^\circ$  for the H-C-H angle. These increments provided energy changes on the order of  $5 \times 10^{-4}$  a. u., substantially above the convergence criterion of  $10^{-6}$  a. u. The predicted parameter changes were on the order of  $0.02\text{\AA}$  and  $1^\circ$ , though the H-C-H angle changed by only  $0.1^\circ$ . A subsequent cycle was undertaken with increments of  $0.02\text{\AA}$  for the bond lengths and  $2^\circ$  and  $3^\circ$  for the F-C-F and H-C-H angles, respectively. In calculating the off-diagonal elements of the  $\underline{B}$  matrix, we used increments of  $0.014\text{\AA}$  for the bond lengths,  $1.4^\circ$  for the F-C-F angle and  $2^\circ$  for the H-C-H angle. These smaller increments were used so that the energy change resulting from the simultaneous alteration of two coordinates would roughly match that resulting from the larger alteration of single coordinates. The second cycle showed negligible parameter corrections (on the order of  $0.001\text{\AA}$  and  $0.05^\circ$ ). Thus, the first-cycle geometry, given in Table 1, was taken as the Hartree-Fock equilibrium geometry for all subsequent studies.

Examining the data in Table 1, we find that our CNDO/2 and INDO results are within  $0.003\text{\AA}$  and  $0.3^\circ$  of one another. Both methods predict the C-H bond length to be quite high, and the C-F bond length to be a bit low. The F-C-F and H-C-H angles are both too low by about  $2^\circ$  and  $1^\circ$  ( $3^\circ$  based on the geometry given in ref. 14) respectively. More interesting is the comparison between our Hartree-Fock geometry and that obtained by Newton *et al.* (3) using the STO-3G minimum basis set. The two methods yield basically the same description of the F-C-F fragment (the C-F distance and

F-C-F angle differ by only  $0.002 \text{ \AA}$  and  $0.3^\circ$ ) while the H-C-H fragment shows substantial change (the distance and angle differ by  $0.039 \text{ \AA}$  and  $3.6^\circ$ , respectively). The minimum basis set is expected to give a rather poor description of the fluorine atom because nearly all of the fluorine basis functions are fully occupied. Our more flexible double-zeta set might be expected to describe the F-C-F fragment rather differently than the STO-3G basis for this reason, and it is surprising to find most of the change at the "other end" of the molecule. We have no explanation for this, but it may be related to the fact that a double-zeta set, with its greater flexibility, is capable of describing types of intra-molecular charge transfer which a minimum basis cannot. We note, finally, that our Hartree-Fock geometry gives the best overall agreement with experiment of any of the theoretical geometries in Table 1.

### C. Quadratic Force Constants

As noted in the previous section, the energy,  $E$ , of a molecule may be approximated as a second-order function of small displacements ( $\Delta q_1, \Delta q_2, \dots, \Delta q_n$ ) of the internal coordinates ( $q_1, q_2, \dots, q_n$ ) which define some reference geometry. These internal coordinates may be any linearly independent set of geometric parameters which define the molecular shape, without reference to its orientation or position in space. A general molecule of  $N$  atoms has  $3N-6$  such parameters ( $3N-5$  for linear molecules). In the event that the reference geometry corresponds to equilibrium, then the linear terms vanish and the energy may be approximated by:

$$E = E_0 + \frac{1}{2} \sum_{i=1}^n \sum_{j=1}^n F_{ij} \Delta q_i \Delta q_j. \quad (\text{IX})$$

The symmetric matrix  $\mathbb{F}$  is the quadratic (or harmonic) force constant matrix for the molecule. It is related to the  $\mathbb{B}$  matrix of equation (III), but  $\mathbb{F}$  refers to all internal coordinates while  $\mathbb{B}$  refers only to those required to define the equilibrium geometry. If a molecule has no symmetry, then  $\mathbb{F}$  and  $\mathbb{B}$  are equivalent, but for symmetrical molecules,  $\mathbb{B}$  is a sub-block of  $\mathbb{F}$ . We shall refer to the diagonal element  $F_{ii}$  as the major force constant (or simply force constant when the context removes ambiguity) for coordinate  $q_i$ , while the off-diagonal element  $F_{ij}$  will be referred to as the interaction constant between coordinates  $q_i$  and  $q_j$ . Also, we shall abbreviate "force constant"

as FC and "interaction constant" as IC.

The numerical values of the FC's depend, of course, upon the coordinates used, but the transformation between different sets of internal coordinates is straightforward: If  $(p_1, p_2, \dots, p_n)$  represents a new set of coordinates, then  $\mathbb{F}'$ , the FC matrix for the  $p$ 's, is related to  $\mathbb{F}$  by

$$\mathbb{F}' = \mathbb{Q}^T \mathbb{F} \mathbb{Q} \quad (\text{X})$$

where the matrix  $\mathbb{Q}$  is defined by

$$O_{ij} = \left. \frac{\partial q_i}{\partial p_j} \right|_{\text{equilibrium}} \quad (\text{XI})$$

The  $\mathbb{Q}$  matrix will generally depend upon the geometry of the molecule as well as the nature of the  $p$ 's and  $q$ 's.

The difluoromethane molecule has five atoms and nine degrees of geometric freedom. Many different coordinate systems are possible, though the set of irrotational, non-translational parameters suggested by Shaffer and Herman (15) are quite useful in the analysis of molecular vibrations. These are rather difficult to picture, however, and do not correspond to "pure" motions such as bond bending and stretching, so we have chosen to use the set of symmetrized valence coordinates described in Table 2 and Figure 1. These are divided into symmetry types according to whether they are totally symmetric ( $a_1$ ), antisymmetric with respect to the F-C-F or H-C-H planes alone ( $b_1$  and  $b_2$  respectively), or antisymmetric with

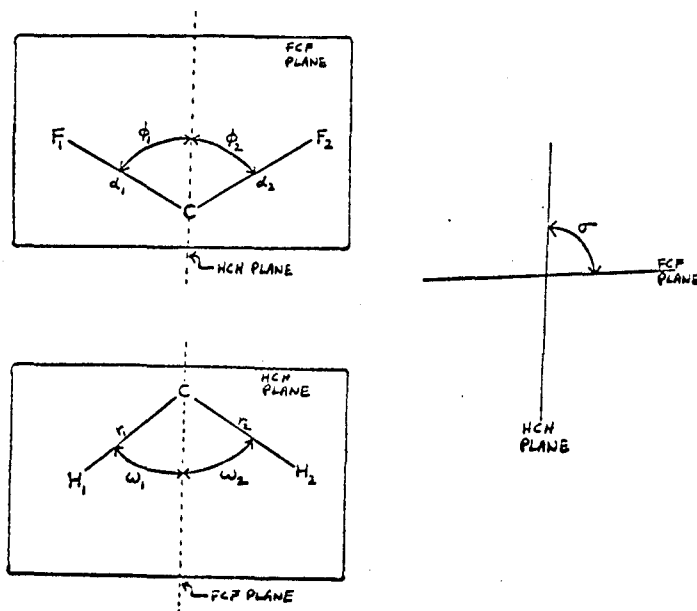
Table 2. Symmetrized Valence Coordinates for Difluoromethane.

<u>Coord.</u>	<u>Symbol</u>	<u>Formula</u> <sup>a</sup>	<u>Description</u>	<u>Symmetry</u>
q <sub>1</sub>	R <sub>f</sub>	(d <sub>1</sub> +d <sub>2</sub> )/2	symmetric C-F stretch	a <sub>1</sub>
q <sub>2</sub>	R <sub>h</sub>	(r <sub>1</sub> +r <sub>2</sub> )/2	symmetric C-H stretch	a <sub>1</sub>
q <sub>3</sub>	Θ <sub>f</sub>	φ <sub>1</sub> +φ <sub>2</sub>	F-C-F angle bend	a <sub>1</sub>
q <sub>4</sub>	Θ <sub>h</sub>	ω <sub>1</sub> +ω <sub>2</sub>	H-C-H angle bend	a <sub>1</sub>
q <sub>5</sub>	D <sub>f</sub>	(d <sub>1</sub> -d <sub>2</sub> )/2	antisymmetric C-F stretch	b <sub>2</sub>
q <sub>6</sub>	ρ <sub>f</sub>	(φ <sub>2</sub> -φ <sub>1</sub> )/2	F-C-F rock	b <sub>2</sub>
q <sub>7</sub>	D <sub>h</sub>	(r <sub>1</sub> -r <sub>2</sub> )/2	antisymmetric C-H stretch	b <sub>1</sub>
q <sub>8</sub>	ρ <sub>h</sub>	(ω <sub>2</sub> -ω <sub>1</sub> )/2	H-C-H rock	b <sub>1</sub>
q <sub>9</sub>	τ	90°-σ	twisting of F-C-F plane relative to H-C-H plane	a <sub>2</sub>

<sup>a</sup>For definition of symbols, see Figure 1.

Figure 1.

Definition of symbols used in the formulas of Table 2.



respect to both planes ( $a_2$ ).

It can be shown (16) that the interaction constants between coordinates of different symmetry types must be zero, and thus the  $\mathbb{F}$  matrix has block-diagonal form with many zero elements. The  $a_1$  block is identical to the matrix  $\mathbb{B}$  of equation (III) for the equilibrium geometry, and may thus be obtained directly from the final cycle of geometry optimization. Only seven force constants remain, two major FC's and one IC for each b-type symmetry block and one major FC for the  $a_2$  "block". These may be evaluated in the same numerical manner as the  $\mathbb{B}$  matrix elements (see equations VII and VIII).

Table 3 presents the Hartree-Fock force constants from our calculations. The totally symmetric FC's were obtained from the second cycle of geometry optimization, while the others were evaluated using distance and angle increments of  $0.02 \text{ \AA}$  and  $2^\circ$ . The errors given for these constants reflect the basic uncertainty in the Hartree-Fock energies ( $\pm 1 \times 10^{-6}$  a. u.), and for some of the IC's this error is a substantial fraction of the constant itself. There are two other sources of error which have not been explicitly evaluated. First, the geometry differs slightly from the true equilibrium one, so the anharmonic terms in the total molecular potential might contribute some small amount to the FC's. Judging from the changes in the  $\mathbb{B}$  matrix from the first to the second optimization cycles and from the small corrections given by the second cycle, we estimate that this source should give errors somewhat less than those quoted for the IC's and major angular FC's, and perhaps two or three times

Table 3. Theoretical Force Constants for CH<sub>2</sub>F<sub>2</sub>

<u>i<sup>b</sup></u>	<u>j<sup>b</sup></u>	<u>F<sub>ij</sub><sup>a</sup></u>		<u>i<sup>b</sup></u>	<u>j<sup>b</sup></u>	<u>F<sub>ij</sub><sup>a</sup></u>	
		Hartree-Fock	CNDO/2			Hartree-Fock	CNDO/2
1	1	14.875±0.044	49.782	2	4	0.270±0.042	0.147
2	2	12.086±0.044	23.422	5	5	12.674±0.044	45.066
1	2	1.155±0.109	1.665	6	6	1.004±0.014	1.027
3	3	1.621±0.014	1.758	5	6	1.099±0.037	1.079
4	4	0.941±0.006	0.939	7	7	11.803±0.044	22.324
3	4	0.093±0.024	0.127	8	8	1.334±0.014	1.355
1	3	0.272±0.060	0.462	7	8	0.250±0.037	0.699
1	4	-0.484±0.042	-0.607	9	9	1.770±0.014	1.873
2	3	-0.145±0.060	-0.290				

<sup>a</sup>The units are md/Å (= 0.22945 a.u./Å<sup>2</sup>), md-Å/radian<sup>2</sup> (= 6.9895 x 10<sup>-5</sup> a.u./degree<sup>2</sup>) and md/radian (= 4.0047 x 10<sup>-3</sup> a.u./Å-degree) for distance-distance, angle-angle and distance-angle constants respectively. The error ranges do not warrant the number of significant figures given, but the constants as written are consistent with the frequencies in Table 4. <sup>b</sup>For a description of the coordinates, see Table 2.

Table 4. Vibration Frequencies for CH<sub>2</sub>F<sub>2</sub> (in cm<sup>-1</sup>).

<u>Sym. type</u>	<u>Experi- mental</u>	<u>Hartree- Fock</u>	<u>Error</u>	<u>Sym. type</u>	<u>Experi- mental</u>	<u>Hartree- Fock</u>	<u>Error</u>
a <sub>1</sub>	532	522± 5	-1.9%	b <sub>1</sub>	1173	1268±10	8.1%
a <sub>1</sub>	1078	1175± 8	9.0%	b <sub>1</sub>	3030	3324± 9	10.8%
a <sub>1</sub>	1508	1729±20	14.7%	b <sub>2</sub>	1089	1228± 4	12.8%
a <sub>1</sub>	2963	3254± 9	9.8%	b <sub>2</sub>	1435	1656±23	15.4%
a <sub>2</sub>	1262	1398± 9	10.8%				

those quoted for the major stretching constants. The second possible error source traces to the fact that our parameter increments were not infinitesimal, so again the anharmonic terms could introduce some error, in this case a basic error in the numerical nature of the FC evaluation. We have tested this to some extent using a Morse potential model (17) for bond stretching and using the actual anharmonic terms for H-C-H and F-C-F angle bending (see section D of this chapter) and have estimated that this error source is negligible. Table 3 also gives the FC's from our CNDO/2 calculations, evaluated using  $5^\circ$  and  $0.05 \text{ \AA}$  increments for angular and distance parameters, respectively. Error estimates are not included, but the errors should not be too different from those for the Hartree-Fock FC's.

With the exception of the stretching constants, we find a good overall parallel between the two methods, particularly for the major angular FC's. All IC's are of the same sign and general magnitude, though in a few cases the CNDO/2 IC's are greater in magnitude by a factor of two. The stretching constants are substantially larger in the CNDO/2 approximation, which agrees with the observation by Segal and Pople (4, 18) that this method often leads to unrealistically high stretching FC's.

In Table 4 we present the harmonic vibration frequencies derived from the Hartree-Fock geometry and FC's, along with the experimental values collected by Meister et al. (19) from a variety of different studies. The classical vibration problem was solved according to the method of Tyson, Claassen<sup>5</sup> and Kim (20). Formally,

the method amounts to solving the necessary matrix equations in the cartesian basis of  $3N$  coordinates ( $N$  is the number of atoms in the molecule). The result is  $3N$  "vibration" frequencies, six of which (five for linear molecules) have zero wavenumber and correspond to the six (five) translations and rotations. It is necessary in this method to express the FC's in terms of cartesian displacement coordinates of the atoms. To do this, we have appended to our list of nine symmetrized valence coordinates a set of six new coordinates corresponding to three rotations and three translations. These are given force and interaction constants of zero since they do not influence the molecular potential energy. Equations (X) and (XI) are applicable in this case with the  $q_i$  as the "appended" valence coordinates and the  $p_i$  as the cartesian coordinates. To carry out the transformation, we need the matrix  $Q$ , which may be viewed as the matrix which expresses first-order changes in the  $q_i$  in terms of  $p_i$  displacements. That is, to first order,

$$\Delta q_i = \sum_{j=1}^n (\partial q_i / \partial p_j) \Delta p_j = \sum_{j=1}^n O_{ij} \Delta p_j. \quad (\text{XII})$$

This matrix is difficult to evaluate analytically, but its inverse, whose elements are simply geometrical parameters representing the changes in cartesian coordinates which result from small changes in valence coordinates, is easy to calculate once the molecular geometry is known. That is, to first order,

$$\Delta p_i = \sum_{j=1}^n (\partial p_i / \partial q_j) \Delta q_j \quad (\text{XIII})$$

but from (XII),

$$\Delta p_i = \sum_{j=1}^n (Q^{-1})_{ij} \Delta q_j \quad (\text{XIV})$$

so we have

$$(Q^{-1})_{ij} = (\partial p_i / \partial q_j) = T_{ij} \quad (\text{XV})$$

and  $T$  is easily obtained from the molecular geometry. It is inverted to give  $Q$ , which in turn is used to carry out the transformation of formula (X).

We have written a FORTRAN IV program to carry out the necessary calculations. The error values for the Hartree-Fock vibration frequencies in Table 4 were obtained by summing the absolute values of the individual frequency changes which took place as each of the Hartree-Fock FC's was allowed to vary over its error range.

The theoretical vibration frequencies are not directly comparable to the experimental values because we have treated only the harmonic portion of the molecular potential. Anharmonicity corrections to the observed frequencies can be made using Dennison's rules, but the application of these is a complex task requiring a detailed knowledge of the fine structure of the molecular vibration

spectrum (21). Such corrections are not available for  $\text{CH}_2\text{F}_2$ , but based on those for  $\text{CH}_3\text{F}$  (22) and  $\text{CH}_4$  (23) we estimate that the errors involved in neglecting anharmonicity are on the order of 5% for C-H stretching modes and about 3% maximum for other modes, with the corrected frequencies higher than the observed ones.

With this in mind, we may examine the values in Table 4. We see that the predicted frequencies are 9-16% higher than the observed, with the exception of the lowest (F-C-F bending mode) which is about 2% low. These errors are outside the range attributable to anharmonicity and we may conclude that, with the exception of F-C-F bending, our Hartree-Fock model describes a molecule which is generally "tighter" than the actual one.\* The vibration frequencies depend roughly on the square roots of the force constants, so we estimate an average error of about +20% to +30% in the major FC's, with perhaps a -4% error in the F-C-F bending constant. Anharmonicity correction would be expected to lower these ranges somewhat, but the general picture would remain the same.

---

\* This is as expected, at least for the stretching modes, because Hartree-Fock wavefunctions do not dissociate properly as bonds are broken, which leads to dissociation energies which are much too high. This is expected to add to the curvature of the energy with respect to bond stretching at equilibrium, and hence a force constant which is too large is obtained.

Similar results for other molecules were obtained by Newton et al. (3) using a minimum basis set. Thus, although our double-zeta set gives a much better equilibrium geometry than Newton's, the general force constant picture does not seem greatly improved.

Ideally, we would like to compare our Hartree-Fock FC's directly with the experimental values, but such values are not available. Meister et al. (19) have given a set of 22 FC's and IC's defined over the set of ten redundant internal valence coordinates, but these were rather arbitrarily determined and certainly do not represent unique values. Most of the constants were transferred from other molecules while only eight IC's were varied to fit the calculated to the observed frequencies. Finally, some of the other constants were varied to improve the fit, but no indication was given as to which constants or how they were varied. Such a procedure is not a reliable one, because even a 1% error in one of the transferred major FC's could lead to substantial errors in the IC's. In addition, the geometry used by Meister was significantly different from the more accurate recent values (13, 14), and this renders their results even more uncertain. We have transformed their values to correspond to our coordinate system using formula (X), which is valid even if the  $q_i$  represent a redundant set of parameters. The Q matrix depends upon the molecular geometry, and for consistency we have used Meister's geometry even though it is incorrect. The resulting transformed "experimental" FC's are given in Table 5.

Table 5. Hartree-Fock FC's vs. Experimental and Semi-Empirical Values.

$i^a$	$j^a$	$F_{ij}^b$		
		<u>Experimental</u> <sup>c</sup>	<u>Hartree-Fock</u>	<u>Semi-Empirical</u>
1	1	13.752	14.875 $\pm$ 0.044	12.924 $\pm$ 0.131
2	2	9.822	12.086 $\pm$ 0.044	10.024 $\pm$ 0.020
1	2	1.012	1.155 $\pm$ 0.109	0.951 $\pm$ 0.083
3	3	1.688	1.621 $\pm$ 0.014	1.649 $\pm$ 0.015
4	4	0.676	0.941 $\pm$ 0.006	0.719 $\pm$ 0.012
3	4	-0.128	0.093 $\pm$ 0.024	0.090 $\pm$ 0.022
1	3	0.616	0.272 $\pm$ 0.060	0.570 $\pm$ 0.044
1	4	-0.220	-0.484 $\pm$ 0.042	-0.403 $\pm$ 0.042
2	3	0.647	-0.145 $\pm$ 0.060	-0.133 $\pm$ 0.043
2	4	0.300	0.270 $\pm$ 0.042	0.219 $\pm$ 0.046
5	5	10.734	12.674 $\pm$ 0.044	9.971 $\pm$ 0.024
6	6	0.885	1.004 $\pm$ 0.014	0.757 $\pm$ 0.009
5	6	1.390	1.099 $\pm$ 0.037	0.858 $\pm$ 0.034
7	7	10.094	11.803 $\pm$ 0.044	9.807 $\pm$ 0.016
8	8	1.193	1.334 $\pm$ 0.014	1.142 $\pm$ 0.006
7	8	0.916	0.250 $\pm$ 0.037	0.215 $\pm$ 0.035
9	9	1.456	1.770 $\pm$ 0.014	1.443 $\pm$ 0.007

<sup>a</sup>For a description of the coordinates, see Table 2.

<sup>b</sup>See footnote a of Table 3 for units and a discussion of the number of significant digits in the constants.

<sup>c</sup>See discussion, p. 22. These are not reliable values.

This situation gives theory a chance to make a few verifiable predictions. In view of the fact that the Hartree-Fock molecule, as noted above, seems to be generally "tighter" than the actual one, we might expect the normal vibration modes to be fairly accurate even though the calculated vibration frequencies are generally about 12% too high. It is possible to determine the FC set which leads to the theoretical modes and the observed frequencies. If the modes are accurate, then this set (which we dub "semi-empirical" force constants, or SEFC's) should represent a good estimate of the actual FC's. The method for calculating SEFC's is given below.

We adopt the notation of Tyson et al. (20), in which  $\underline{X}$  represents a vector of the  $3N$  displacement coordinates ( $N$  is the number of atoms in the molecule),  $\underline{A}$  represents the corresponding FC matrix and  $\underline{M}$  represents the diagonal "mass matrix" ( $M_i$  is the mass of the atom associated with cartesian displacement  $X_i$ ). If  $\underline{A}$  and  $\underline{M}$  are known, the vibration problem is solved by diagonalizing the matrix  $\underline{M}^{-\frac{1}{2}} \underline{A} \underline{M}^{-\frac{1}{2}}$ , that is, by finding an orthogonal matrix  $\underline{U}$  such that

$$\underline{U}^T \underline{M}^{-\frac{1}{2}} \underline{A} \underline{M}^{-\frac{1}{2}} \underline{U} = \underline{\Lambda} = \begin{pmatrix} \lambda_1 & & & 0 \\ & \lambda_2 & & \\ & & \cdot & \\ 0 & & & \cdot \\ & & & & \lambda_{3N} \end{pmatrix} \quad (\text{XVI})$$

The matrix  $\underline{M}^{-\frac{1}{2}} \underline{U}$  has, as its columns, vectors representing the relative displacements of the atoms for the normal modes, and the

$\lambda_i$  are related to the vibration frequencies  $\nu_i$  by

$$\lambda_i = 4\pi^2 c^2 \nu_i^2 \quad (c = \text{speed of light}) \quad (\text{XVII})$$

Now, in our case,  $\mathfrak{A}$  was obtained from the Hartree-Fock FC's in Table 3 and yielded incorrect vibration frequencies, that is, the "wrong" diagonal matrix  $\mathfrak{A}$ . The "right"  $\mathfrak{A}$  matrix has diagonal elements given by (XVII), where the  $\nu_i$  are the correct frequencies. This corrected matrix, which we call  $\mathfrak{A}'$ , may be substituted onto equation (XVII), which may be solved for  $\mathfrak{A}'$ , the SEFC matrix, to give

$$\mathfrak{A}' = \mathfrak{M}^{+\frac{1}{2}} \mathfrak{U} \mathfrak{A}' \mathfrak{U}^T \mathfrak{M}^{+\frac{1}{2}}. \quad (\text{XVIII})$$

This matrix  $\mathfrak{A}'$  gives the same normal modes as did  $\mathfrak{A}$ , but it also yields the correct vibration frequencies. It may be transformed from the cartesian basis to the SVC basis using formula (X) with the transformation matrix  $\mathfrak{Q}$  taken as the  $\mathfrak{T}$  matrix of equation (XV).

If the molecule is not an ideal harmonic oscillator, as is usually the case, then this method should technically be applied to the harmonic rather than the observed frequencies. Anharmonicity corrections on the order of 2%-5% are not uncommon (22, 23), so we might expect force constant errors on the order of 4%-10% if anharmonicity is neglected.

The SEFC's derived from the Hartree-Fock FC's and geometry are given in Table 5. We obtained the error values by

varying each FC over its error range (see Table 3) and summing the absolute values of the SEFC changes thus produced. We have also included, in like manner, terms related to the estimated error in the Hartree-Fock geometry, which we have taken as  $\pm 0.1^\circ$  and  $\pm 0.002 \text{ \AA}$  for the  $a_1$ -type angle and distance coordinates, respectively. In order to test the accuracy of the SEFC's, we have used them, together with the Hartree-Fock geometry, to predict the vibration frequencies of  $\text{CHDF}_2$  and  $\text{CD}_2\text{F}_2$ . We have also synthesized these and assigned their IR spectra (see section F of this chapter). Tables 6 and 7 give the experimental frequencies together with the predictions given by Meister et al. (19) and our SECF predictions. Our predictions are almost invariably better, with average and maximum errors of 1.9% and 6.0%, respectively as compared to 3.4% and 9.8% for Meister's values. We feel that the SEFC's in Table 5 represent the best current estimates of the force constants for difluoromethane.

Table 5 also gives the Hartree-Fock FC's for comparison with the "experimental" FC's and SEFC's. The major Hartree-Fock FC's are higher than the experimental ones by 10%-25% with the exception of the F-C-F bending constant which is about 4% low and the H-C-H constant which is about 40% too high. Using the STO-3G minimum basis, Newton et al. (3) have found that the Hartree-Fock method predicts stretching constants typically 20%-30% higher than experimental values and bending constants typically 15%-70% higher.

Table 6. Calculated and Observed Vibration Frequencies for  $\text{CHDF}_2$ .

<u>Sym.</u>	<u>Designation</u>	<u>Obs.<sup>a</sup></u>	<u>Calc.<sup>b</sup></u>	<u>Error</u>	<u>Calc. (Ref. 19)</u>	<u>Error</u>
a'	$\nu_1$	-	529	-	529	-
a'	$\nu_2$	991	971	-2.0%	954	-3.7%
a'	$\nu_3$	1030	1092	+6.0%	1112	+8.0%
a'	$\nu_4$	1367	1379	+0.9%	1402	+2.6%
a'	$\nu_5$	2230	2199	-1.4%	2197	-1.5%
a'	$\nu_6$	2987	2999	+0.4%	2996	+0.3%
a''	$\nu_7$	943	940	-0.3%	966	+2.4%
a''	$\nu_8$	1103	1113	+0.9%	1090	-1.2%
a''	$\nu_9$	-	1372	-	1366	-

<sup>a</sup>In  $\text{cm}^{-1}$ , estimated accuracy  $\pm 3 \text{ cm}^{-1}$ . <sup>b</sup>From SEFC's and the Hartree-Fock geometry.

Table 7. Calculated and Observed Vibration Frequencies for  $\text{CD}_2\text{F}_2$ . (footnotes as in Table 6)

<u>Sym.</u>	<u>Designation</u>	<u>Obs.<sup>a</sup></u>	<u>Calc.<sup>b</sup></u>	<u>Error</u>	<u>Calc. (Ref. 19)</u>	<u>Error</u>
a <sub>1</sub>	$\nu_1$	-	525	-	520	-
a <sub>1</sub>	$\nu_2$	1032	989	-4.2%	931	-9.8%
a <sub>1</sub>	$\nu_3$	-	1174	-	1254	-
a <sub>1</sub>	$\nu_4$	2128	2142	+0.7%	2170	+2.0%
a <sub>2</sub>	$\nu_5$	-	907	-	908	-
b <sub>1</sub>	$\nu_6$	2284	2259	-1.0%	2222	-2.7%
b <sub>1</sub>	$\nu_7$	963?	953	-1.0%	979	+1.7%
b <sub>2</sub>	$\nu_8$	1159	1186	+2.3%	1099	+3.5%
b <sub>2</sub>	$\nu_9$	1003	971	-3.2%	1050	+4.7%

Notable exceptions are  $\text{CHF}_3$ ,  $\text{NF}_3$  and  $\text{CO}_2$  which give bending constants 10%-30% too low. Our results support these conclusions, suggesting that the greater flexibility of a double-zeta basis does not substantially influence the trends observed in the STO-3G calculations. The agreement between the experimental and Hartree-Fock IC's is fair-to-poor, with two of these IC's showing sign reversal. The IC's are the most questionable of the experimental values though, so it seems meaningless to carry out the comparison at all.

Not surprisingly, there is a better parallel between the SEFC's and the Hartree-Fock FC's, the former being obtained indirectly from the latter. All major Hartree-Fock FC's are in the range of 17%-33% higher than the corresponding SEFC values, except for the F-C-F constant which is about 2% lower. The IC's show a good parallel in both magnitude and sign, with the Hartree-Fock values 5%-30% higher in absolute value. The only exception here is the IC between  $R_f$  and  $\theta_f$ , where the Hartree-Fock value is roughly half the SEFC value. It is interesting that the only Hartree-Fock FC's which are lower than their analogous SEFC's involve only the F-C-F fragment. It may be that electron correlation, which the Hartree-Fock method largely ignores and which might be expected to be especially important in the electron-rich F-C-F fragment, plays a significant role in altering these values. On the other hand, it may simply be an artifact of our basis set.

So far, we have considered FC's defined for the SVC's in Table 3. Though these completely specify the harmonic component

of the energy near the equilibrium geometry, they are not directly comparable to FC's in related molecules of different symmetry. We would like to believe that the energy behavior of molecules can be understood in terms of some relatively simple model which refers to bond angles and interatomic distances, and that the parameters for such a model are equal, or at least of comparable magnitude, for similar interactions in chemically different molecules. Several such models have been proposed (24), and one of the most successful has been that suggested by Urey and Bradley (6a) and further investigated by Shimanouchi (6b). It is assumed, using this model, that the energy varies as an independent parabolic function of each bond length and angle, but is augmented by steric terms between non-bonded pairs of atoms. As originally proposed (6a), the model steric terms were approximated by repulsive potentials of the form

$$E_{ij}^{\text{steric}} = k/r_{ij}^n \quad (\text{XIX})$$

where  $r_{ij}$  is the distance between atoms  $i$  and  $j$ . It was found that a value of about  $n = 6$  lead to fairly good overall molecular potentials for a variety of molecules. This is the form of the Urey-Bradley potential which we have investigated, though in its more recent modification (6b), the nature of the steric term is not considered explicitly. Rather, only the first- and second-derivative portions of each interaction with respect to the interatomic distance are considered, and these derivatives are not assumed to be related as they

must be for the steric term given in equation (XIX).

Figure 2 gives the description of the coordinates we have used in defining the model. The energy,  $U$ , is approximated by the following formula.

$$\begin{aligned}
 2U = & 2U_0 + 2s_F(r_{F1} + r_{F2}) + f_F(r_{F1}^2 + r_{F2}^2) \\
 & + 2s_H(r_{H1} + r_{H2}) + f_H(r_{H1}^2 + r_{H2}^2) \\
 & + 2s_{FF}\theta_F + f_{FF}\theta_F^2 + 2s_{HH}\theta_H + f_{HH}\theta_H^2 \\
 & + 2s_{FH}(\phi_1 + \phi_2 + \phi_3 + \phi_4) \\
 & + f_{FH}(\phi_1^2 + \phi_2^2 + \phi_3^2 + \phi_4^2) \\
 & + 2k_{HH}/d_H^6 + 2k_{FF}/d_F^6 \\
 & + 2k_{HF}(1/d_1^6 + 1/d_2^6 + 1/d_3^6 + 1/d_4^6)
 \end{aligned} \tag{XX}$$

It should be noted that the model is not stated in terms of displacement coordinates, as is usually the case. The transformation to displacement coordinates involves nothing more than replacing terms of the form

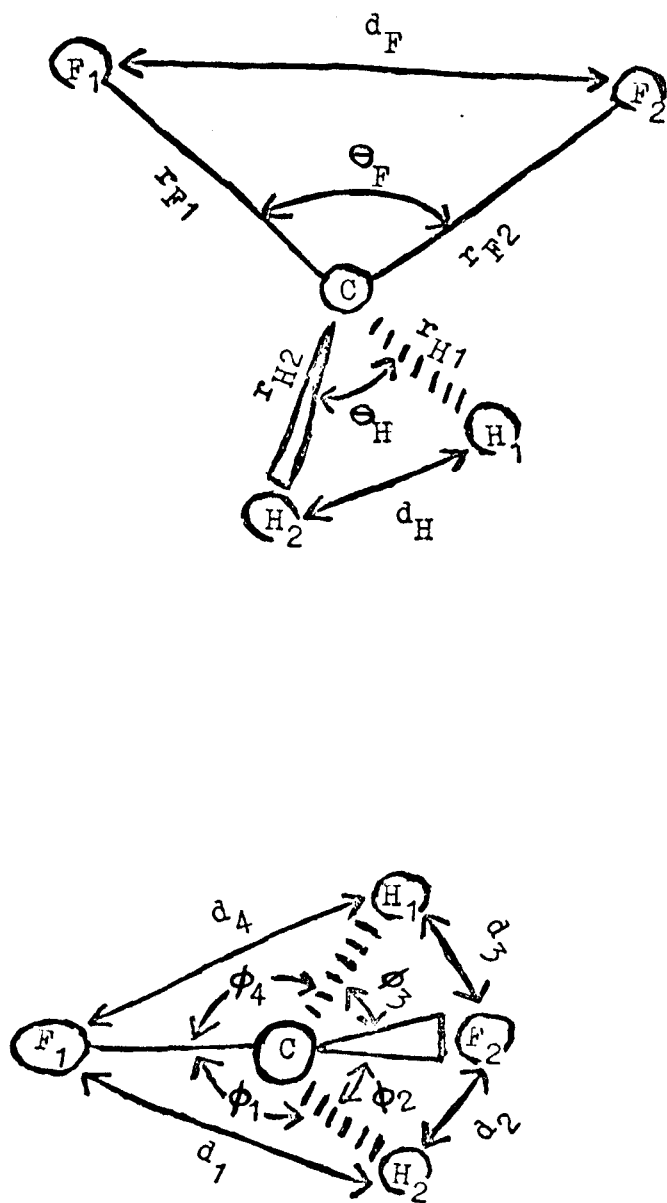
$$k_x/d_x^6$$

by

$$(21k_x/d_{x,0}^8)(\Delta d_x)^2 - (12k_x/d_{x,0}^7)\Delta d_x$$

where  $d_{x,0}$  is the equilibrium value of  $d_x$ , and by replacing terms of the form

Figure 2. Description of Coordinates used in the Urey-Bradley model for  $\text{CH}_2\text{F}_2$



$$2s_x P_x + f_x P_x^2 \quad (P \text{ represents } r, \Theta \text{ or } \phi)$$

by

$$2(s_x + f_x P_{x,0}) \Delta P_x + f_x (\Delta P_x)^2$$

where  $P_{x,0}$  is the equilibrium value of  $P_x$ . The transformed formula agrees to second order with (XX), and hence will yield the same results for harmonic force constants, but (XX) is in a form which will be quite useful in the subsequent section on large molecular distortions.

The thirteen parameters of the Urey-Bradley potential (UBP) model are not independent, because we require that the force on each atom be zero in the equilibrium geometry. Mathematically, this may be stated as

$$\left. \partial U / \partial q_i \right|_{\text{equilibrium}} = 0 \quad i = 1, 2, \dots, 9 \quad (\text{XXI})$$

where the  $q_i$ 's are the nine SVC's of Table 3. Our model has an inherent symmetry which guarantees the above condition for the five SVC's which are not totally symmetric, but we are left with four conditions upon the thirteen UBP parameters. For  $q_1$ , which is  $R_f$ , equation (XXI) gives

$$\begin{aligned}
0 &= \partial U / \partial R_f |_{\text{eq.}} = s_F (\partial r_{F1} / \partial R_f + \partial r_{F2} / \partial R_f) & (\text{XXII}) \\
&+ f_F [r_{F1} (\partial r_{F1} / \partial R_f) + r_{F2} (\partial r_{F2} / \partial R_f)] \\
&- (6 k_{FF} / d_F^7) (\partial d_F / \partial R_f) \\
&- (6 k_{HF} / d_1^7) (\partial d_1 / \partial R_f + \partial d_2 / \partial R_f + \partial d_3 / \partial R_f + \partial d_4 / \partial R_f)
\end{aligned}$$

where all quantities are to be evaluated at equilibrium and where we have made use of the equilibrium relationship  $d_1 = d_2 = d_3 = d_4$ . A bit of trigonometry and calculus gives

$$\begin{aligned}
\partial r_{F1} / \partial R_f &= \partial r_{F2} / \partial R_f = 1 \\
\partial d_F / \partial R_f &= 2 \sin(\theta_F / 2) & (\text{XXIII}) \\
\partial d_1 / \partial R_f &= \partial d_2 / \partial R_f = \partial d_3 / \partial R_f = \partial d_4 / \partial R_f \\
&= 2 R_f + 2 R_h \cos(\theta_F / 2) \cos(\theta_H / 2)
\end{aligned}$$

where we have used the fact that, at equilibrium,  $r_{F1} = r_{F2} = R_f$  and  $r_{H1} = r_{H2} = R_h$ . Substituting the expressions (XXIII) into (XXII) and solving for  $s_F$  we obtain

$$\begin{aligned}
s_F &= -R_f f_F + 6 k_{FF} \sin(\theta_F / 2) / d_F^7 & (\text{XXIV}) \\
&+ 24 k_{HF} [R_f + R_h \cos(\theta_F / 2) \cos(\theta_H / 2)] / d_1^7.
\end{aligned}$$

Relationships similar to (XXIV) may be derived for  $s_H$ ,  $s_{FF}$  and  $s_{HH}$  by differentiating (XX) with respect to  $q_2$ ,  $q_3$  and  $q_4$  (that is,  $R_h$ ,  $\theta_f$  and  $\theta_h$ ), respectively. The nine remaining UBP constants ( $f_H$ ,  $f_F$ ,

$f_{\text{HH}}, f_{\text{FF}}, s_{\text{HF}}, f_{\text{HF}}, k_{\text{FF}}, k_{\text{HH}}$  and  $k_{\text{HF}}$ ) are thus the truly independent parameters of the model.

Now, the force constant related to  $q_i$  and  $q_j$  is  $F_{ij}$ , and is defined by

$$F_{ij} = \partial^2 U / \partial q_i \partial q_j. \quad (\text{XXV})$$

The second partial derivatives with respect to  $q$ 's may be evaluated explicitly beginning from formula (XX), though quite a bit of involved manipulation is necessary. The net result is that each of the seventeen unique nonzero SVC force constants can be expressed in terms of the nine independent model parameters. That is,

$$F_{ij} = \sum_{k=1}^9 T_{ij,k} f_k \quad (\text{XXVI})$$

where  $f_k$  is a generic symbol for one of the nine UBP constants and each  $T_{ij,k}$  is a function of the equilibrium geometry of the molecule. If we consider  $ij$  to be a single index, say  $\ell$ , running from 1 to 17 (the number of SVC FC's), we have

$$F_{\ell} = \sum_{k=1}^9 T_{\ell k} f_k \quad (\text{XXVII})$$

or, in matrix notation,

$$\underline{F} = \underline{T} \underline{f} \quad (\text{XXVIII})$$

We wish to fit the UBP model to some set of known FC's, which means we wish to find  $\underline{f}$  such that  $\underline{F}$  is as close as possible to the actual vector of FC's, which we call  $\underline{F}_0$ . This is a standard problem in least-squares analysis (25) and the  $\underline{f}$  which gives the best rms fit between  $\underline{F}$  and  $\underline{F}_0$  is

$$\underline{f} = (\underline{T}^T \underline{T})^{-1} \underline{T}^T \underline{F}_0 \quad (\text{XXIX})$$

Some care must be exercised here, though, because the resulting  $\underline{f}$  may depend upon the units used for  $\underline{F}_0$ . For example, if two FC sets differ in the units of the angle constants only, one having units of md-Å/deg<sup>2</sup> and the other having units of md-Å/rad<sup>2</sup>, the first will have numeric values roughly 3300 times smaller than the second. Clearly, the simple rms criterion will weight the angle constants quite differently in the two cases. To overcome this, one may either weight the rms fit appropriately or one may choose units which put the various FC's on a fairly uniform numerical level. The units used in Table 5 give constants whose absolute errors are comparable, so we have used these units and an unweighted rms fit in the current work.

We have written a FORTRAN IV program to calculate the  $\underline{T}$  matrix of equation (XXVIII) from the molecular geometry and to carry out the least-squares analysis. The nine independent UBP parameters thus obtained are used in the program to calculate the four dependent constants. Table 8 gives the "best-fit" UBP

Table 8. Urey-Bradley Model Parameters Derived from Force Constants.

<u>Parameter</u>	<u>Value obtained from least-squares fit</u>			<u>Units</u>
	<u>Using Hartree-Fock FC's</u>	<u>Using SEFC's</u>		
$s_F$	-8.005	-6.244		md
$s_H$	-5.748	-4.780		md
$s_{FF}$	-1.492	-1.139		md-Å <sup>0</sup> /rad
$s_{HH}$	-1.290	-0.957		md-Å <sup>0</sup> /rad
$s_{HF}$	-1.371	-1.106		md-Å <sup>0</sup> /rad
$f_F$	6.127	(4.376) <sup>a</sup>	4.864	md/Å <sup>0</sup>
$f_H$	5.594	(4.298) <sup>a</sup>	4.649	md/Å <sup>0</sup>
$f_{FF}$	0.776	(0.484) <sup>a</sup>	0.647	md-Å <sup>0</sup> /rad <sup>2</sup>
$f_{HH}$	0.565	(0.380) <sup>a</sup>	0.416	md-Å <sup>0</sup> /rad <sup>2</sup>
$f_{HF}$	0.663		0.539	md-Å <sup>0</sup> /rad <sup>2</sup>
$k_{FF}$	10.475	(19.99) <sup>a</sup>	14.302	md-Å <sup>7</sup>
$k_{HH}$	0.382	(0.802) <sup>a</sup>	0.303	md-Å <sup>7</sup>
$k_{HF}$	2.821		2.325	md-Å <sup>7</sup>

<sup>a</sup>The values in parentheses were derived from the experimental UBP constants for CH<sub>4</sub> and CF<sub>4</sub> in ref. 26. See text.

parameters derived from the Hartree-Fock FC's and SEFC's.

Table 9 shows these sets of constants in comparison to those given by the UBP models. In both cases, the Hartree-Fock geometry was used in the calculation of  $\mathcal{T}$ .

Table 9 shows that the UBP model is capable of duplicating the actual FC's fairly well, with most errors less than 0.3 units. The worst errors occur in  $F_{56}$ ,  $F_{24}$  (the only constant showing the wrong sign) and, for the SECF's,  $F_{13}$ , which correspond to the  $(D_f, \rho_f)$ ,  $(R_h, \theta_h)$  and  $(R_f, \theta_f)$  IC's, respectively. Of the major FC's, the rocking coordinates  $\rho_h$  and  $\rho_f$  show the greatest errors, with both roughly 10% off but in opposite directions. These two motions involve much the same relative H-F displacements and H-C-F angle changes, and the model thus predicts similar FC's for the two. They are, in fact, rather different, which points up the necessity of including, in a truly accurate model, hybridization parameters such as occur in the HOFF method (27). Considering the simplicity of the UBP model, we believe that the overall agreement in Table 9 is quite good.

In Table 8 we see that there is a good overall parallel between the model parameters derived from the Hartree-Fock FC's and those derived from the SEFC's. In every case but one, the Hartree-Fock values are 20%-35% higher in absolute value, the exception being the F-F steric constant, which is about 26% lower. This is a most interesting result, for it implies that the anomalously low value for  $F_{33}$ , the major force constant for  $\Theta_f$ , in the

Table 9. Comparison of UBP Model Force Constants with Actual Values.

<u>i<sup>a</sup></u>	<u>j<sup>a</sup></u>	<u>F<sub>ij</sub><sup>b</sup></u>			
		<u>Hartree-Fock values</u>		<u>Semi-empirical values</u>	
		<u>Actual</u>	<u>Best UBP fit</u>	<u>Actual</u>	<u>Best UBP fit</u>
1	1	14.9	14.8	12.9	12.8
2	2	12.1	12.2	10.0	10.1
1	2	1.2	1.4	1.0	1.1
3	3	1.6	1.6	1.6	1.6
4	4	0.9	0.9	0.7	0.7
3	4	0.1	0.0	0.1	0.0
1	3	0.3	0.5	0.6	0.9
1	4	-0.5	-0.3	-0.4	-0.2
2	3	-0.1	-0.2	-0.1	-0.2
2	4	0.3	-0.1	0.2	-0.1
5	5	12.7	12.8	10.0	10.1
6	6	1.0	1.1	0.8	0.9
5	6	1.1	0.5	0.9	0.4
7	7	11.8	11.7	9.8	9.7
8	8	1.3	1.2	1.1	1.0
9	9	1.8	1.8	1.4	1.5

<sup>a</sup>For a description of the coordinates, see table 2.

<sup>b</sup> See footnote a of table 3 for the units. The FC's have rounded to facilitate comparison.

Hartree-Fock set is caused by an underestimation of the F-F steric repulsion rather than by anything unusual in the F-C-F fragment. Shimanouchi et al. (26) have obtained the stretching, bending and steric constants for the UBP model of CH<sub>4</sub> and CF<sub>4</sub>. They have used a somewhat different formula for the steric term, and their derived constants are defined slightly differently than ours: Their angle constants are scaled by the bond lengths included in the angle, and their steric constants refer to the second derivative of the steric term. We have transformed their values to conform to our nomenclature using the formulas

$$f_{\text{XX}} = r_{\text{X}}^2 H_{\text{X}} \quad (\text{XXIX})$$

and

$$k_{\text{XX}} = (d_{\text{XX}}^8/42) F_{\text{X}} \quad (\text{XXX})$$

where H and F are Shimanouchi's angle and steric terms, respectively,  $r_{\text{X}}$  is the C-X distance and  $d_{\text{XX}}$  is the X-X distance. These values appear in Table 8, and we see that our UBP constants derived from SEFC's are of quite reasonable magnitude in comparison with them. The differences may be due to non-transferability, but we think it more likely that they arise either from the differences between Shimanouchi's model and our own or from inherent errors in the SEFC's.

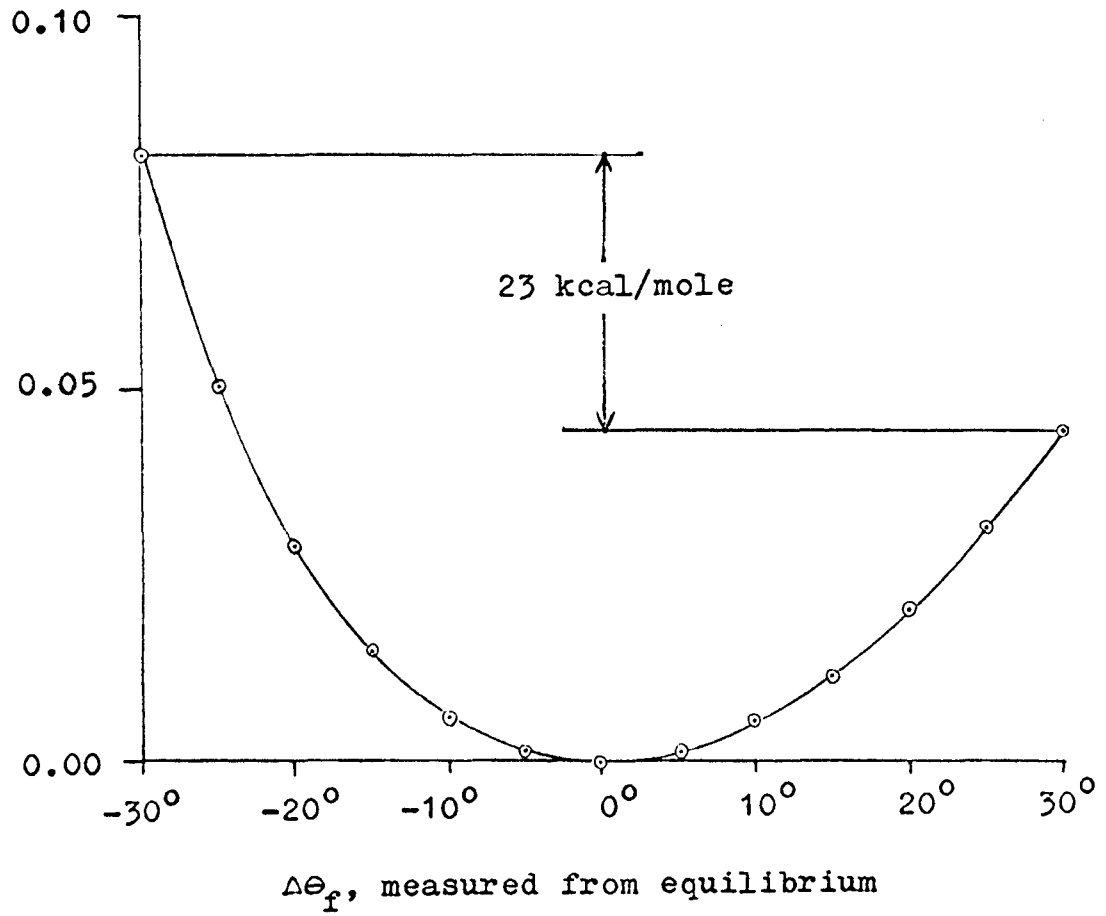
#### D. Energy Variation for Gross Angular Distortions

The difluoromethane molecule is the simplest saturated aliphatic molecule in which a geminal steric interaction between first-row atoms is possible. We would expect the F-F interaction to show up most dramatically in the energy curve which results from the variation of the F-C-F angle, because this motion substantially alters the F-F distance. Figure 3 shows the Hartree-Fock energy of  $\text{CH}_2\text{F}_2$  as a function of the F-C-F angle (the molecule is distorted from the Hartree-Fock equilibrium geometry), and we can see that there is indeed a marked asymmetry in the curve. As the angle is decreased by  $30^\circ$ , the energy increase is about 0.037 a. u. larger than it is when the angle is increased by a like amount. This is a chemically significant quantity, over 22 kcal/mole, and the asymmetry is consistent with the concept of F-F steric repulsion. We shall investigate this asymmetry, then, in an effort to learn a bit about this repulsion within the Hartree-Fock framework.

Initially, however, we must consider another possible contribution to the noted anharmonicity. As the F-C-F angle is changed, the carbon hybridization must change, and we have no guarantee that this will contribute only harmonic terms to the energy variation. In terms of a "ball-and-spring" model, for example, the F-C-H angle does not change proportionately to the F-C-F angle, so that quadratic terms from the former may contribute anharmonicity to the latter. Using reasonable values for the F-C-H force

Figure 3. Hartree-Fock energy of  $\text{CH}_2\text{F}_2$  as a function of the F-C-F angle.

$E_{\text{Hartree-Fock}}$  in a. u. above equilibrium value (-237.523925 a. u.)



constant, for example  $f_{\text{HF}}$  from Table 8, we have found that this source should not affect the asymmetry of Figure 3 very much, but is of sufficient magnitude to warrant consideration.

If we assume that steric terms involving hydrogen are small, then we may estimate the magnitude of this "rehybridization anharmonicity" by investigating the energy variation as a function of the H-C-H angle. We have calculated the CNDO/2 energy of  $\text{CH}_2\text{F}_2$  as a function of this angle over a  $60^\circ$  range symmetric about the CNDO/2 equilibrium value, using  $5^\circ$  increments. Figure 4 shows the deviation of this curve from a parabola fit to the three lowest values ( $\Delta\theta_{\text{h}} = +5^\circ, 0^\circ, -5^\circ$ ), though the parabolic portion of a fourth-order polynomial fit to the five lowest values yields the same results. Such a curve will be called a DFP (deviation-from-parabolicity) curve. We see that the deviations are quite modest, less than 2 kcal/mole at the worst. The Hartree-Fock energies for the  $\Delta\theta_{\text{h}} = +30^\circ$  and  $-30^\circ$  cases (measured from the Hartree-Fock equilibrium geometry) have also been obtained, and the endpoints of the Hartree-Fock DFP curve calculated. The parabola in this case was fit to the  $\Delta\theta_{\text{h}} = +3^\circ, 0^\circ, -3^\circ$  energies used in the computation of the H-C-H force constant. We note that the two MO methods give nearly identical results at these endpoints, and we have drawn an approximate Hartree-Fock DFP curve in Figure 4 assuming that this parallel holds over the entire range. Figure 5 shows the DFP curve for  $\text{H}_2\text{O}$  derived from the calculations of Pitzer and Merrifield (9) though their energy values were quoted to only five decimal places, which

Figure 4. Hartree-Fock and CNDO/2 deviation-from-parabolicity (DFP) curves for  $\text{CH}_2\text{F}_2$ ; H-C-H bending.

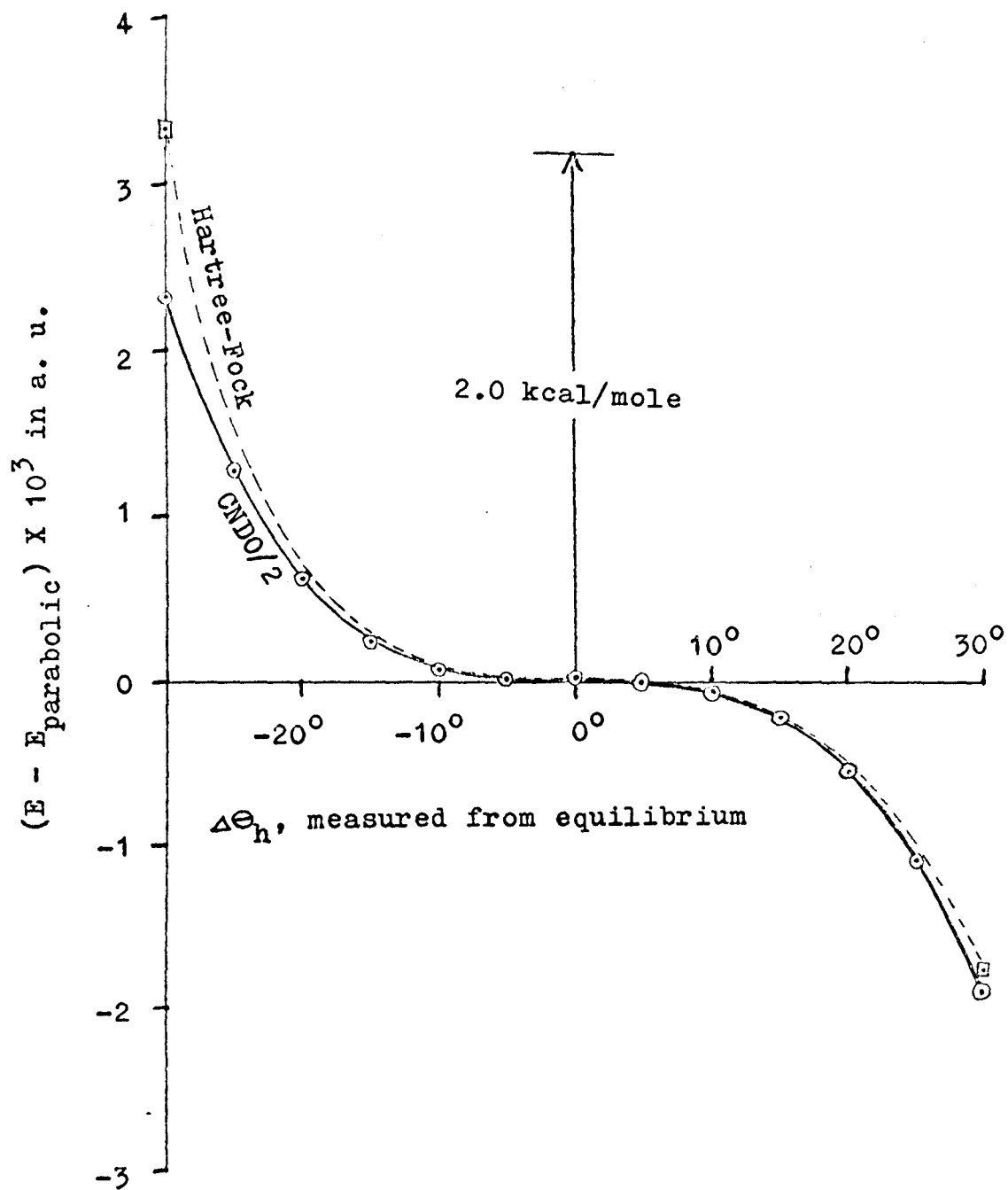
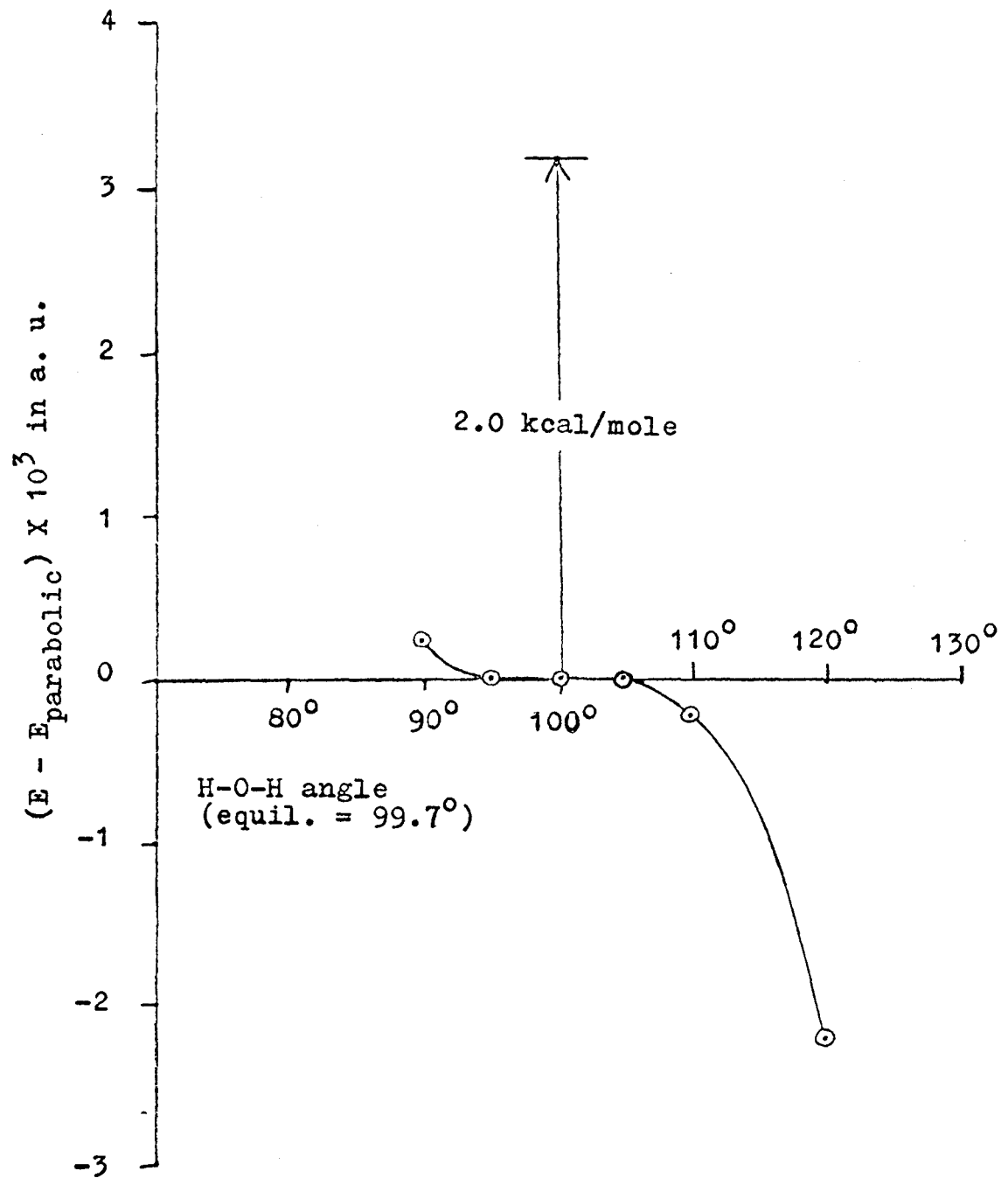


Figure 5. Hartree-Fock DFP curve for  $H_2O$ ; H-O-H bending.



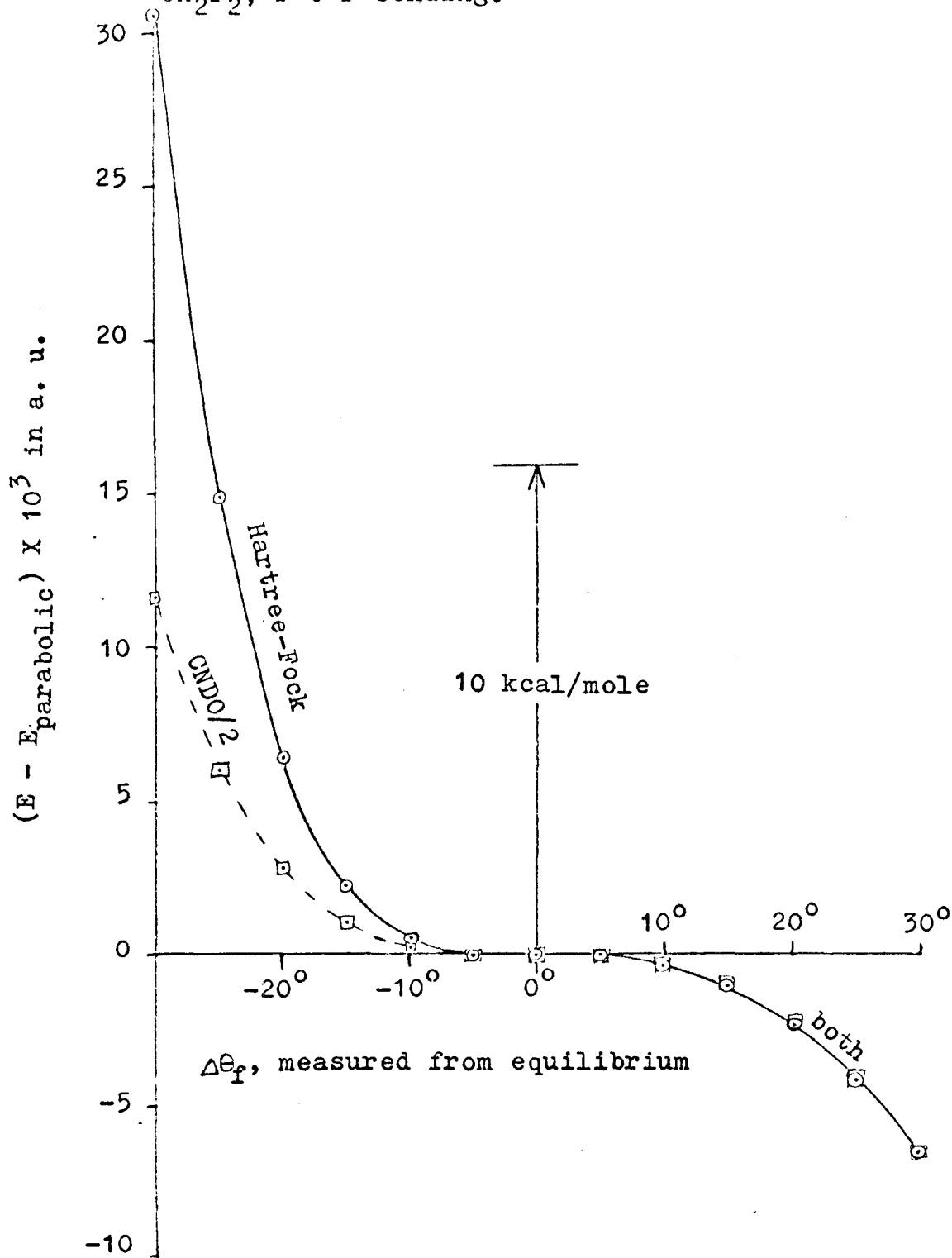
renders the curve somewhat imprecise.\* We see that the energy variation in our case shows greater harmonicity, which may be due in part to the greater flexibility of our basis set.

Figure 6 shows the DFP curve for the F-C-F angle variation, using both Hartree-Fock and CNDO/2 energies. In these calculations, the angle was varied from its equilibrium value in  $5^\circ$  increments up to a total distortion of  $+30^\circ$  and  $-30^\circ$ . The comparison between the two MO methods is most interesting. Qualitatively, the Hartree-Fock curve is similar to that for CNDO/2, with both methods giving a positive deviation as the F-C-F angle is closed and a negative one when it is opened. For  $\Delta\theta_f > 0$ , they yield almost identical results, but in the region  $\Delta\theta_f < 0$ , the Hartree-Fock values are considerably larger. This is most likely due to the approximate manner in which CNDO/2 treats the two-centered integrals, the net effect of which appears to be an underestimation of the F-F repulsion for small values of  $\theta_f$ . The fact that CNDO/2 predicts an F-C-F angle which is too small by a few degrees is consistent with this notion that CNDO/2 underestimates the F-F steric repulsion.

---

\* Using a substantially larger and more flexible basis, Ermler and Kern (40) have computed the cubic term in the H-O-H anharmonicity. Their value suggests that the deviations in Figure 5 are too large by a factor of about two.

Figure 6. Hartree-Fock and CNDO/2 DFP curves for  $\text{CH}_2\text{F}_2$ ; F-C-F bending.



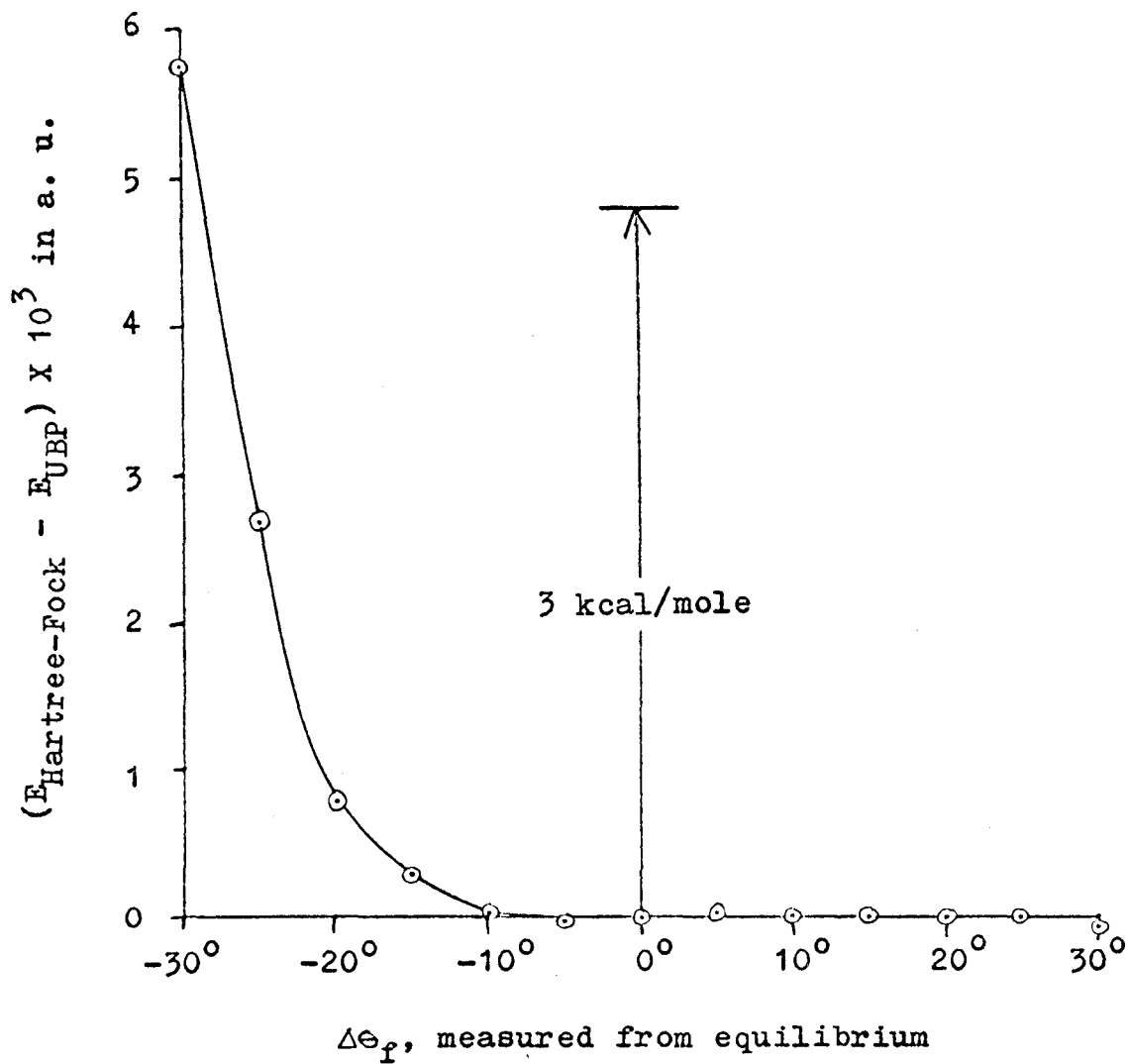
Comparing Figures 4 and 6, we see that the F-C-F anharmonicity is greater than the H-C-H anharmonicity by an order of magnitude, which suggests that the F-F interaction is almost entirely responsible for the shape of the F-C-F DFP curve. If we assume, as we did in the Urey-Bradley potential model, that this interaction is a repulsive one of the form

$$E_{\text{F-F, steric}} = k/r_{\text{FF}}^6$$

then we may estimate the a value for k by scaling the DFP curve for  $1/r_{\text{FF}}^6$  (expressed as a function of  $\Delta\theta_{\text{F}}$ ) so that it matches the Hartree-Fock curve at  $\Delta\theta_{\text{F}} = -30^\circ$ . We have done this, obtaining a scaling factor (k) of 2.91 a. u.- $\text{\AA}^6$  or 12.7 md- $\text{\AA}^7$ , which is only about 20% higher than the value we obtained from the UBP fit of the Hartree-Fock FC's. In view of the fact that these values were obtained using quite different methods, the agreement is surprisingly good.

The above suggests that the UBP model of equation (XX) might be rather accurate in accounting for the anharmonicity in the F-C-F curve, and we have found this to be the case. Figure 7 shows the deviation of the Hartree-Fock energy from the UBP model defined by the Hartree-Fock parameters in Table 8. We see that 80% of the DFP curve in Figure 6 has been accounted for, and that the remaining deviation, little more than 3 kcal/mole at worst, shows up only when the fluorines are rather close together. The H-C-H angle fares rather well, too, giving deviations from the UBP model of 1.31 and

Figure 7. Deviation of the Hartree-Fock energy from the UBP model as a function of  $\Theta_f$ .



$-1.85 \times 10^{-3}$  a. u. (0.82 and -1.16 kcal/mole) for  $\Delta\theta_h = +30^\circ$  and  $-30^\circ$ , respectively.

We have not investigated the non-totally symmetric angular coordinates extensively using the Hartree-Fock method, but we have carried out several CNDO/2 calculations. All three of these coordinates ( $\rho_h$ ,  $\rho_f$  and  $\tau$ ) show very little deviation from parabolic energy behavior as they are varied from  $0^\circ$  to  $30^\circ$ . As we have noted above, DFP curves derived from CNDO/2 energies match those from Hartree-Fock energies quite well except when the F-F distance is small, so we would expect the Hartree-Fock energy to vary as an essentially parabolic function of these three coordinates. We have tested this for the coordinate  $\rho_f$ , finding that the energy at  $\rho_f = 30^\circ$  differs by  $0.43 \times 10^{-3}$  a. u. (0.27 kcal/mole) from the value predicted by the harmonic Hartree-Fock force constant, an error on the order of only 1%. The UBP model predicts that these coordinates should be quite harmonic, but we recall that the model has some difficulty in duplicating their force constants. Thus, we find the Hartree-Fock energy at  $\rho_f = 30^\circ$  to be  $3.37 \times 10^{-3}$  a. u. (2.12 kcal/mole) below the model value, an error of about 11%. Assuming parabolicity for  $\rho_h$  and  $\tau$ , we estimate the energies at  $30^\circ$  to be about 0.004 a. u. above and 0.001 a. u. below the model values, respectively. These correspond to respective errors of about 10% and 2%.

We conclude that the UBP model mimics rather well the Hartree-Fock energy variation in difluoromethane as the angular coordinates are distorted up to  $30^\circ$  from their equilibrium values, with maximum errors on the order of 3 kcal/mole and 10%.

### E. Summary

The following six points summarize the findings we have obtained in the study of the potential energy surface of difluoromethane:

- 1) The flexibility of a double-zeta basis set over a minimum basis set improves the calculated Hartree-Fock geometry, with the major differences between our calculations and those of Newton et al. (3) appearing in the H-C-H fragment.
- 2) This same flexibility does little to improve the accuracy of the calculated FC's, judging either from the predicted vibration frequencies or from a comparison of the theoretical with the (somewhat dubious) experimental or semi-empirical values. The calculated major FC's are roughly 20%-35% too large except for the F-C-F angle constant, which is a few per cent low. Newton et al. (3) have found similar errors for the totally symmetric coordinates in other molecules, though our results refer to all coordinates.
- 3) In spite of these FC errors, useful semi-empirical constants derived from observed frequencies and calculated normal modes may be obtained. These SEFC's predict the observed frequencies for the deuterated difluoromethanes rather well, and give UBP parameters

reasonably close to those in  $\text{CH}_4$  and  $\text{CF}_4$ .

- 4) Within the framework of the UBP model, the Hartree-Fock method appears to consistently overestimate all parameters except for the F-F steric repulsion, which it underestimates. This leads to the anomalously low value for the F-C-F angle constant, and in view of the fact that Newton et al. (3) calculate a low symmetric bending constant for  $\text{CHF}_3$ , we suspect that this effect may apply to other molecules as well.
- 5) The CNDO/2 method gives FC's and IC's which parallel rather well the Hartree-Fock values, except for the major stretching constants, which are much too large. As the F-C-F angle is decreased, CNDO/2 appears to underestimate the anharmonicity due to F-F steric interaction.
- 6) The UBP model, using  $k/r^6$  steric terms, is capable of fitting the Hartree-Fock FC's and SEFC's fairly well, and it forms a good model for the Hartree-Fock energy variation in difluoromethane as the angular coordinates are grossly altered. Particularly, the model accounts for 80% of the marked anharmonicity in the F-C-F angle.

## F. Experimental

### Details of calculations

All CNDO/2 calculations were done using program CNINDO (10) on the IBM 360/75 and 370/155 computers. To facilitate the large number of calculations, a subroutine was included which read in the SVC's of Table 2 and computed the cartesian coordinates for  $\text{CH}_2\text{F}_2$ .

The Hartree-Fock calculations were done using the CIT modification (28) of the POLYATOM program package (29) on the IBM 360/75 and 370/155 computers. Here, as in the CNDO/2 case, a subroutine was included to compute the cartesian coordinates (in a.u.) from the SVC's of Table 2. The SVC distance coordinates are given in angstroms, and the conversion to a.u. was accomplished using a value of  $0.529167\text{\AA}$  for the Bohr radius. The current accepted value (30) of  $0.52917715 (\pm 1.5 \text{ ppm}) \text{\AA}$  differs negligibly from this.

The basis set of atomic orbitals consisted of seven s-type gaussians and, for each axis, three p-type gaussians on each first-row atom, and three s-type gaussians on each hydrogen. The orbital exponents for C and F were obtained from Whitman and Hornback's recent study (31), while those for hydrogen were obtained via an Huzinaga fit (32) of a 1s Slater function with an orbital exponent of 1.2. This basis set was contracted (i. e., some of the gaussians were combined in fixed linear combinations) to a "double-zeta" set, which is a set containing four s-type and two p-type functions on each

first-row atom and two s-type functions on hydrogen. The Dunning criteria (33) were used in choosing the sets of gaussians to be combined, and the contraction coefficients were obtained from Whitman and Hornback's atomic calculations (31) and from the above-mentioned Huzinaga fit. Table 10 summarizes our orbital exponents and contraction coefficients.

Unland et al. (1), using a very similar but uncontracted basis and a very slightly different experimental geometry, obtained a molecular energy of -237.54 a.u. as compared to our value of -237.52 a.u., indicating that the contraction of the basis set influences the energy very little. As noted by them, this energy is at least 0.4 a.u. above the (sp) Hartree-Fock limit.

Three geometries were treated initially, corresponding to the experimental, CNDO/2 and previous Hartree-Fock (3) geometries of Table 1. Energies of -237.52292849, -237.51866426 and -237.52168377 were obtained, respectively, and the energy change during the last SCF cycle was less than  $9 \times 10^{-8}$  in each case. The energies obtained during the first geometry optimization cycle are summarized in Table 11. Table 12 gives the analogous values for the second cycle, along with the energies used in computing the non-totally symmetric FC's and in investigating the gross angular distortions of the molecule.

The calculation of molecular vibration frequencies was carried out using a double-precision program (FIBBER) written in FORTRAN IV for the IBM 360/75 and 370/155 computers. This program is

Table 10. Orbital Exponents and Contraction Coefficients

<u>Atom</u>	<u>Type</u>	<u>Grouping</u>	<u>Exponent</u>	<u>Con. coeff.<sup>a</sup></u>	<u>Con. coeff.<sup>b</sup></u>
F	s	}	2723.	0.0059	0.0094676
F	s		416.4	0.0420	0.0673966
F	s		97.73	0.1792	0.2875587
F	s		27.87	0.4544	0.7291666
F	s		8.712	1.0000	1.0000000
F	s		1.396	1.0000	1.0000000
F	s		.4209	1.0000	1.0000000
F	p		10.53	0.1270	0.2299053
F	p		2.188	0.4784	0.8660371
F	p		.4785	1.0000	1.0000000
C	s	}	994.7	0.0072	0.0115293
C	s		160.0	0.0473	0.0757411
C	s		39.91	0.1819	0.2912750
C	s		11.82	0.4474	0.7164181
C	s		3.698	1.0000	1.0000000
C	s		.6026	1.0000	1.0000000
C	s		.1817	1.0000	1.0000000
C	p		4.279	0.1093	0.2095240
C	p		.8699	0.4597	0.8812276
C	p		.2036	1.0000	1.0000000
H	s	}	6.481	0.0705	0.1563558
H	s		.9810	0.4079	0.9046456
H	s		.2180	1.0000	1.0000000

<sup>a</sup>Raw.    <sup>b</sup>After basis function normalization.

Table 11. Hartree-Fock Energies Used in the First Geometry Optimization Cycle.

$R_f^a$	$R_h^a$	$\epsilon_f^a$	$\Theta_h^a$	$(E+237) \cdot 10^3$ (a.u.)	$(E-E_0)^b \cdot 10^3$ (a.u.)	Convergence <sup>c</sup> (a.u.)
1.358 <sup>d</sup>	1.091 <sup>d</sup>	108.2 <sup>d</sup>	112.1 <sup>d</sup>	-522.92849	0	$8 \times 10^{-8}$
1.358	1.091	<u>110.2</u>	112.1	-522.93392	0.0054	$2 \times 10^{-8}$
1.358	1.091	<u>106.2</u>	112.1	-522.43915	-0.4893	$1 \times 10^{-8}$
1.358	1.091	108.2	<u>116.1</u>	-522.24214	-0.6864	$1 \times 10^{-9}$
1.358	1.091	108.2	<u>108.1</u>	-522.56375	-0.3647	$1 \times 10^{-9}$
1.358	<u>1.111</u>	108.2	112.1	-521.46738	-1.4611	$2 \times 10^{-8}$
1.358	<u>1.071</u>	108.2	112.1	-523.41947	0.4910	$1 \times 10^{-8}$
<u>1.378</u>	1.091	108.2	112.1	-523.30435	0.3759	$1 \times 10^{-8}$
<u>1.338</u>	1.091	108.2	112.1	-521.05131	-1.8772	$8 \times 10^{-9}$
<u>1.338</u>	<u>1.071</u>	108.2	112.1	-523.86940	0.9409	$5 \times 10^{-8}$
1.358	1.091	<u>110.2</u>	<u>108.1</u>	-522.62935	-0.3045	$2 \times 10^{-8}$
<u>1.378</u>	1.091	<u>110.2</u>	112.1	-523.25138	0.3229	$3 \times 10^{-8}$
1.358	<u>1.071</u>	<u>110.2</u>	112.1	-523.41419	0.4857	$3 \times 10^{-8}$
<u>1.378</u>	1.091	108.2	<u>108.1</u>	-522.76391	-0.1646	$9 \times 10^{-9}$
1.358	<u>1.071</u>	108.2	<u>108.1</u>	-522.98415	0.0567	$8 \times 10^{-9}$

<sup>a</sup>For description of coordinates, see Table 2. Units are angstroms for R, degrees for  $\Theta$ . Underlined are the coordinates which are changed from experimental values.

<sup>b</sup>Here,  $E_0$  is the energy of the experimental geometry.

<sup>c</sup>Energy change during the final SCF iteration.

<sup>d</sup>Experimental geometry from ref. 13.

Table 12. Hartree-Fock Energies for Distortions from First Cycle Equilibrium Geometry.

Magnitude and type of distortion <sup>a</sup>	(E+237) x10 <sup>3</sup> (a.u.)	(E-E <sub>0</sub> ) <sup>b</sup> x10 <sup>3</sup> (a.u.)	Convergence <sup>c</sup> (a.u.)
none <sup>d</sup>	-523.92501	0	5 x 10 <sup>-8</sup>
$\Delta\theta_f = -2^\circ$	-523.70300	0.2210	2 x 10 <sup>-8</sup>
$\Delta\theta_f = +2^\circ$	-523.69305	0.2320	2 x 10 <sup>-8</sup>
$\Delta\theta_h = +3^\circ$	-523.63139	0.2963	5 x 10 <sup>-8</sup>
$\Delta\theta_h = -3^\circ$	-523.62603	0.2990	1 x 10 <sup>-8</sup>
$\Delta R_h = +0.02\text{\AA}$	-523.42807	0.4969	2 x 10 <sup>-7</sup>
$\Delta R_h = -0.02\text{\AA}$	-523.31273	0.6123	1 x 10 <sup>-7</sup>
$\Delta R_f = +0.02\text{\AA}$	-523.27877	0.6462	1 x 10 <sup>-7</sup>
$\Delta R_f = -0.02\text{\AA}$	-523.20604	0.7190	1 x 10 <sup>-7</sup>
$\Delta\theta_h = +2^\circ, \Delta R_f = +0.014\text{\AA}$	-523.54052	0.3845	8 x 10 <sup>-8</sup>
$\Delta R_h = +0.014\text{\AA}, \Delta R_f = +0.014\text{\AA}$	-523.33273	0.5923	6 x 10 <sup>-8</sup>
$\Delta\theta_h = +2^\circ, \Delta R_h = +0.014\text{\AA}$	-523.53346	0.3915	6 x 10 <sup>-8</sup>
$\Delta\theta_f = -1.4^\circ, \Delta R_f = +0.014\text{\AA}$	-523.53028	0.3947	2 x 10 <sup>-7</sup>
$\Delta\theta_f = -1.4^\circ, \Delta\theta_h = +2^\circ$	-523.70620	0.2188	2 x 10 <sup>-7</sup>
$\Delta\theta_f = -1.4^\circ, \Delta R_h = +0.014\text{\AA}$	-523.57519	0.3498	2 x 10 <sup>-7</sup>
$D_h = 0.02\text{\AA}$	-523.38341	0.5416	2 x 10 <sup>-9</sup>
$\rho_h = 2^\circ$	-523.73859	0.1864	1 x 10 <sup>-8</sup>
$D_h = 0.02\text{\AA}, \rho_h = 2^\circ$	-523.15692	0.7681	1 x 10 <sup>-8</sup>
$D_f = 0.02\text{\AA}$	-523.34337	0.5816	8 x 10 <sup>-8</sup>
$\rho_f = 2^\circ$	-523.78461	0.1404	3 x 10 <sup>-9</sup>
$D_f = 0.02\text{\AA}, \rho_f = -2^\circ$	-523.37906	0.5460	9 x 10 <sup>-8</sup>

(continued)

Table 12. (continued)

Magnitude and type of distortion <sup>a</sup>	(E+237) x10 <sup>3</sup> (a.u.)	(E-E <sub>0</sub> ) <sup>b</sup> x10 <sup>3</sup> (a.u.)	Convergence <sup>c</sup> (a.u.)
$\tau=2^\circ$	-523.67768	0.2473	2 x 10 <sup>-8</sup>
$\Delta\theta_f=-5^\circ$	-522.46939	1.4556	4 x 10 <sup>-8</sup>
$\Delta\theta_f=+5^\circ$	-522.53677	1.3882	4 x 10 <sup>-8</sup>
$\Delta\theta_f=-10^\circ$	-517.72199	6.2030	1 x 10 <sup>-7</sup>
$\Delta\theta_f=+10^\circ$	-518.56832	5.3567	1 x 10 <sup>-7</sup>
$\Delta\theta_f=-15^\circ$	-508.94045	14.9846	1 x 10 <sup>-7</sup>
$\Delta\theta_f=+15^\circ$	-512.17620	11.7488	1 x 10 <sup>-7</sup>
$\Delta\theta_f=-20^\circ$	-494.93016	28.9948	1 x 10 <sup>-7</sup>
$\Delta\theta_f=+20^\circ$	-503.46086	20.4641	1 x 10 <sup>-7</sup>
$\Delta\theta_f=-25^\circ$	-473.80603	50.1190	2 x 10 <sup>-7</sup>
$\Delta\theta_f=+25^\circ$	-492.49889	31.4261	1 x 10 <sup>-7</sup>
$\Delta\theta_f=-30^\circ$	-442.60119	81.3238	4 x 10 <sup>-7</sup>
$\Delta\theta_f=+30^\circ$	-479.36148	44.5635	2 x 10 <sup>-7</sup>
$\Delta\theta_h=-30^\circ$	-490.96280	32.9622	1 x 10 <sup>-6</sup>
$\Delta\theta_h=+30^\circ$	-496.63400	27.9210	8 x 10 <sup>-7</sup>
$\rho_f=30^\circ$	-492.77198	31.1530	9 x 10 <sup>-6</sup>

<sup>a</sup>For a description of the coordinates, see Table 2.

<sup>b</sup>Here, E<sub>0</sub> is the energy of the undistorted geometry.

<sup>c</sup>Energy change during the final SCF cycle.

<sup>d</sup>The undistorted geometry is given in Table 3 as the entry "Hartree-Fock (this work)."

specific for tetrahedral molecules with  $C_{2V}$  symmetry and includes options for isotopic substitution and SEFC computation. A single-precision FORTRAN IV program (UBP) was written for the PDP-10 time-sharing computer to carry out the fitting of the Urey-Bradley potential model to a set of FC's for a tetrahedral  $C_{2V}$  molecule.

Synthesis of  $CH_2F_2$ ; synthesis and IR spectrum analysis of  $CHDF_2$  and  $CD_2F_2$

Difluoromethane. -- Under nitrogen, 7.5 g (0.0314 moles) of mercuric fluoride (Ozark-Mahoning, 98.5%) was placed in a 50 ml round-bottomed flask. To this was added 5 g (0.0187 moles) of methylene iodide dissolved in 15 g of carbon tetrachloride. The flask was equipped with a reflux condenser topped with a T-joint which carried a slow flow of dry nitrogen from the condenser to a trap cooled in liquid nitrogen. The outlet of the trap was attached to a calcium chloride drying tube. The reaction mixture was heated under reflux with magnetic stirring in a  $100^\circ$  oil bath for two hours, and the product was collected as a white solid in the trap. The cold trap was connected to the top of an inverted wide-diameter burette filled with mineral oil and suspended so that its mouth was beneath the surface of an oil reservoir. The trap was evacuated, then warmed slowly until a slight positive gas pressure developed, at which time the burette was opened. In this way, 67 ml of gas were collected, corresponding to about 2.5 mmoles at standard temperature and pressure (13% yield based on  $CH_2I_2$  used). The product was then

condensed into an NMR tube (or, for the deuterated compounds, was allowed to escape into an evacuated vapor-phase IR cell), and the low-temperature NMR showed no proton- or fluorine-containing impurities.

Difluoromethane-d<sub>2</sub>. -- The above procedure was repeated using CD<sub>2</sub>I<sub>2</sub> in place of CH<sub>2</sub>I<sub>2</sub>. The deuterated diiodomethane was obtained via an H-D exchange reaction on CH<sub>2</sub>I<sub>2</sub> according to the method of Winstein et al. (34). Deuteration is not quantitative in this reaction, and the vapor-phase IR of the CD<sub>2</sub>F<sub>2</sub> product thus showed the presence of a modest amount of CHDF<sub>2</sub>.

Difluoromethane-d. -- Dichloromethane-d, obtained from the reduction of deuteriochloroform with tri-n-butyltin hydride (35), was treated with sodium iodide in refluxing 2-butanone according to the method of Perkin and Scarborough (36) to give diiodomethane-d. This was treated with HgF<sub>2</sub> as above, and the vapor-phase IR of the product showed virtually no CD<sub>2</sub>F<sub>2</sub> or CH<sub>2</sub>F<sub>2</sub> impurity.

All vapor-phase IR spectra were run on the Perkin-Elmer 225 Grating Infrared Spectrometer using a cell with 6 mm KBr windows and a path length of 4 cm. A slow scan speed was used to give maximum resolution. The gas pressure was measured only approximately upon filling the cell, and was initially about 100 mm Hg for each of the deuterated difluoromethanes. Subsequent spectra were taken after reducing the cell pressure by a factor of about ten. Some air was present in the cell due to a slight leak, so an air spectrum was run to help in the identification of impurities from this

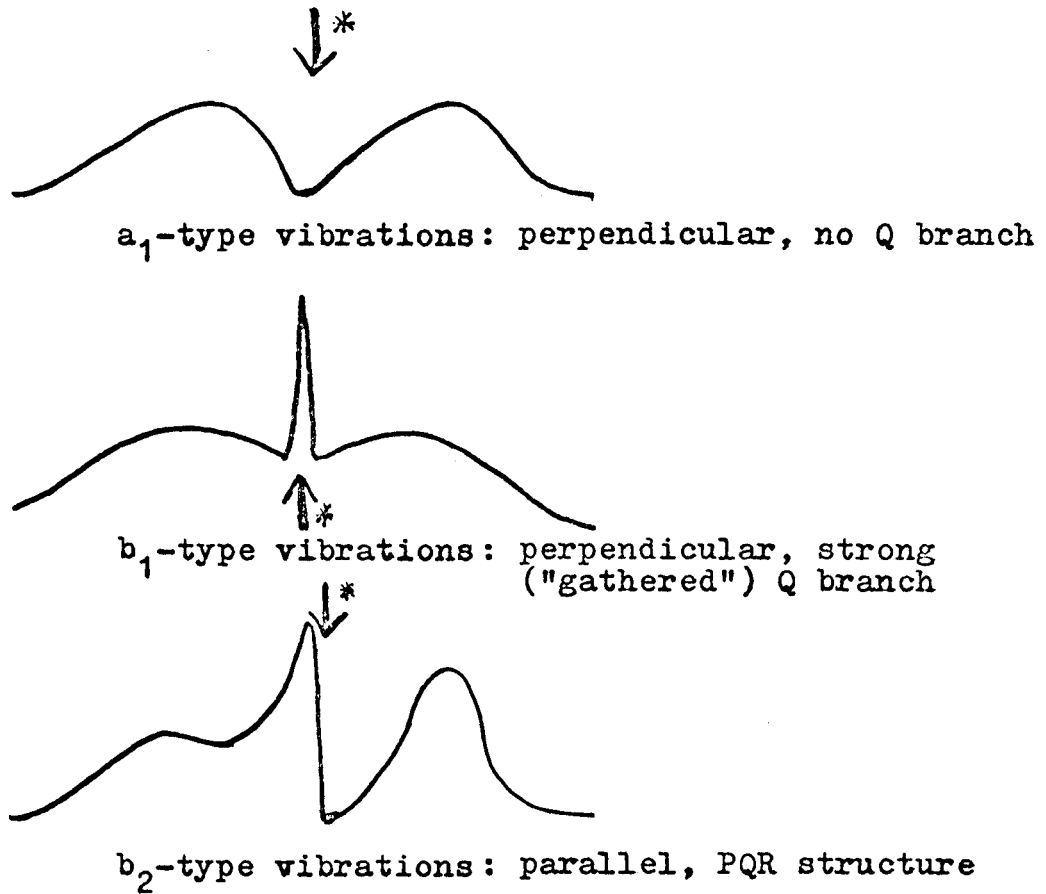
source. Little rotational fine structure was apparent in the bands because of pressure broadening, but this was actually an asset because the band envelopes could be easily seen.

In the spectrum of  $\text{CD}_2\text{F}_2$ , only seven of the nine vibrations were potentially observable, because the  $a_2$  mode is IR-inactive while the lowest  $a_1$  band undoubtedly fell below the cutoff of the cell. Stewart and Nielsen (37) have pointed out that the difluoromethane molecule is nearly a symmetric top (about the F-F axis), and thus the bands of the three IR-active symmetry types have three distinctive band envelopes. The same is true for  $\text{CD}_2\text{F}_2$ , so we may obtain not only the frequency but also the symmetry of each vibration band. Figure 8 shows the general shape we expect for each of the symmetry types, and all three were found in the spectrum. In assigning the following peaks, the apparent band centers were used to define the observed frequencies, because without the rotational fine structure, combination rules (37) could not be used. Thus, we estimate an accuracy of about  $\pm 3 \text{ cm}^{-1}$  in the assignments. The following spectral regions contain peaks not attributable to  $\text{CHDF}_2$  or air impurities.

#### 4.0-5.0 $\mu$ region (Figure 9)

Two strong peaks occur in this region, one of symmetry  $b_1$  at  $2284 \text{ cm}^{-1}$  and one of symmetry  $a_1$  at  $2128 \text{ cm}^{-1}$ . A smaller  $a_1$ -type peak at about  $2348 \text{ cm}^{-1}$  is an air impurity, while a small well-formed  $b_1$  peak at  $2030 \text{ cm}^{-1}$  seems too weak to be a fundamental, and qualitatively one expects to find only two peaks (symmetric and anti-symmetric C-D stretching) in this region.

Figure 8. Expected band envelopes for the three IR-active symmetry types of vibrations of  $\text{CD}_2\text{F}_2$ .



\*The arrow indicates the approximate band center.

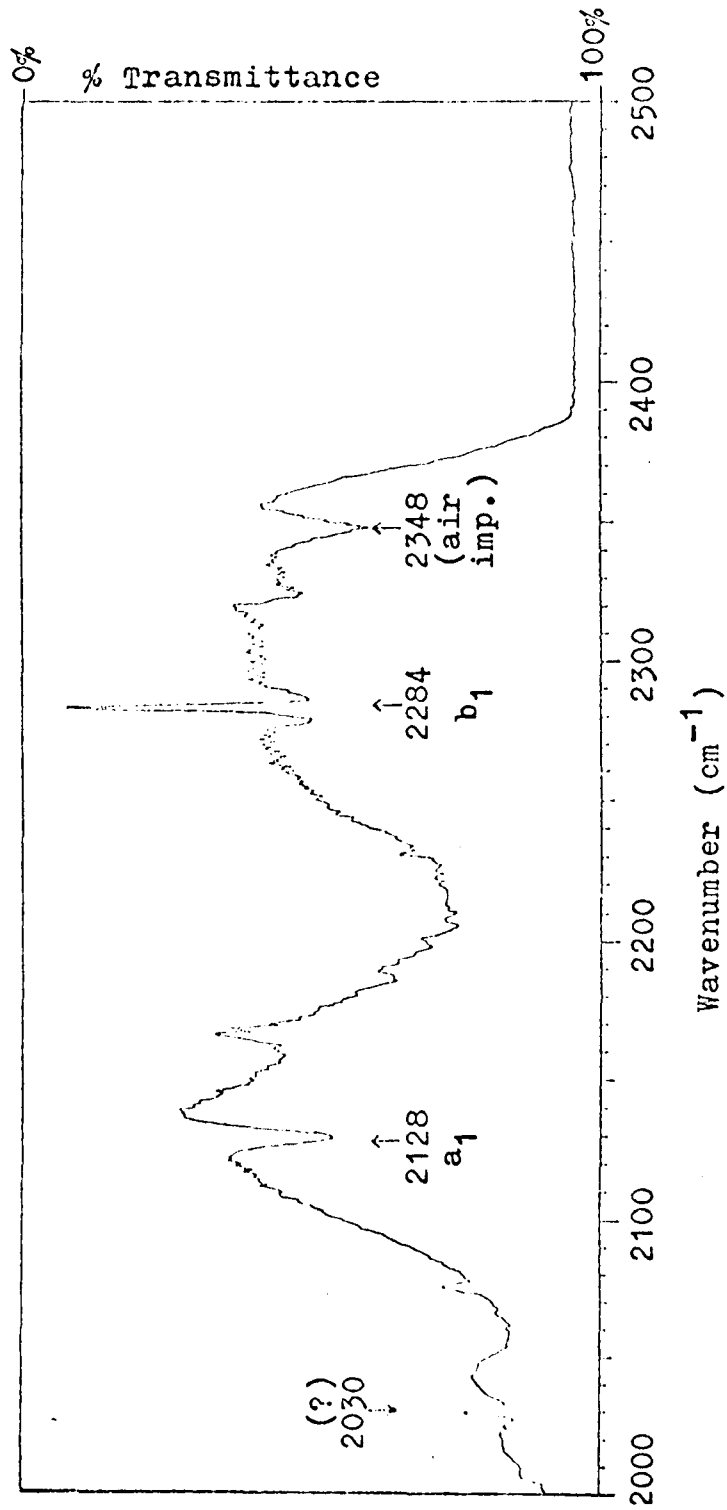


Figure 9. The 4.0-5.0  $\mu$  region of the vapor-phase IR spectrum of difluoromethane-d<sub>2</sub>.

### 8.0-10.0 $\mu$ region (Figure 10)

Four very strong peaks occur in this region, three of  $b_2$  symmetry at 1159, 1103 and 1003  $\text{cm}^{-1}$  and one of  $a_1$  symmetry at 1032  $\text{cm}^{-1}$ . The latter is somewhat obscured by the 1003 peak, but it shows the strong central depression surrounded by two "shoulders" characteristic of  $a_1$  peaks. The 1103 peak was later identified as belonging to  $\text{CHDF}_2$  and is, in fact, the strongest peak in the spectrum of that molecule.

### 10.0-11.0 $\mu$ region (Figure 11)

There is one fairly strong peak in this range with a maximum at 963  $\text{cm}^{-1}$ , but its envelope does not seem to correspond to any of the "standard" types. It has a single strong maximum and is thus probably a b-type peak. The molecule can, by symmetry, have only two  $b_1$  and two  $b_2$  fundamentals, and both of the  $b_2$  bands are elsewhere and quite strong. We have thus tentatively assigned this as a  $b_1$ -type peak.

The above assignments are summarized in Table 7. The only potentially observable peak not found was predicted to lie at 1174  $\text{cm}^{-1}$  by us, 1254  $\text{cm}^{-1}$  by Meister et al. (19). Stewart and Nielsen (37) failed to observe the analogous peak in the  $\text{CH}_2\text{F}_2$  spectrum and concluded that it was weak. We believe this to be true in our case, too, and if our prediction for this frequency is correct, then even a moderately strong peak would be overshadowed by the intense  $b_2$  peak at 1159  $\text{cm}^{-1}$ .

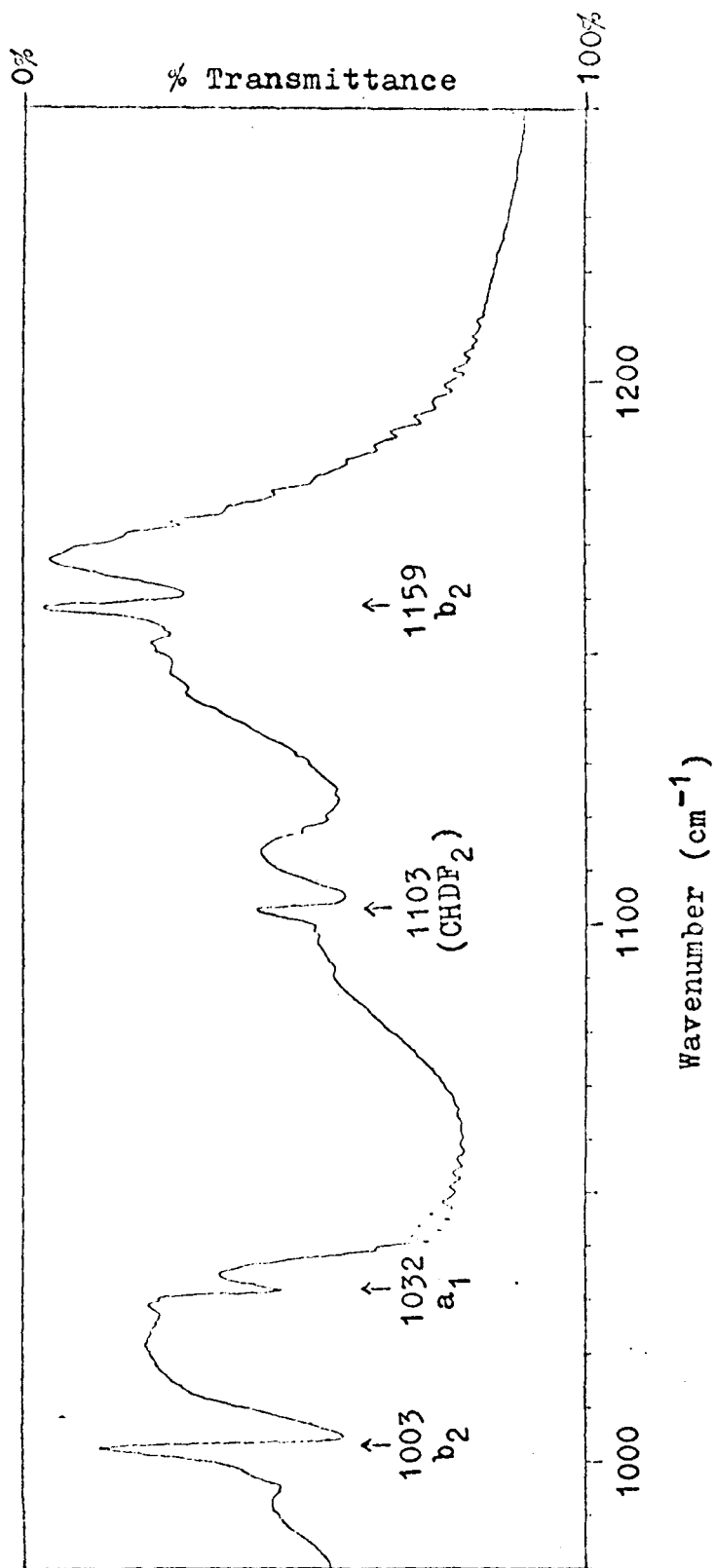


Figure 10. The 8.0-10.0  $\mu$  region of the vapor-phase IR spectrum of difluoromethane-d<sub>2</sub>.

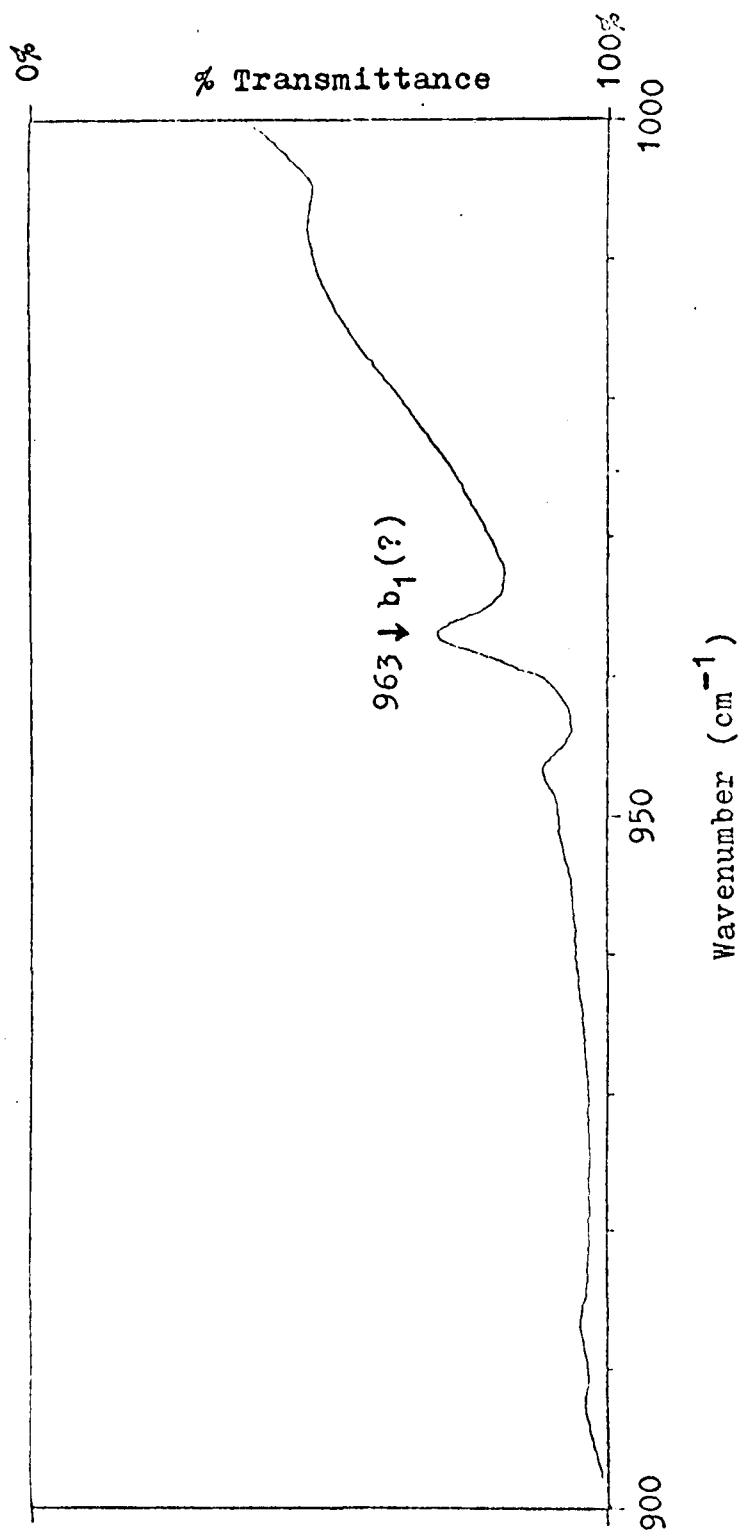


Figure 11. The 10.0-11.0  $\mu$  region of the vapor-phase IR spectrum of difluoromethane-d<sub>2</sub>.

The CHDF<sub>2</sub> spectrum is somewhat more difficult to analyze. Replacing one of the protons on CH<sub>2</sub>F<sub>2</sub> by a deuterium destroys the nearly symmetric rotor qualities of the spectrum. The molecule still has two nearly equal moments of inertia, but the dipole moment changes produced by the normal vibrations no longer lie along the principal axes of inertia, which is a requirement for the characteristic band envelopes (38). The three a'' modes are pure "parallel" vibrations analogous to the b<sub>2</sub>-type bands in CD<sub>2</sub>F<sub>2</sub>, but the a' vibrations have no special symmetry with respect to the "unique" (i. e., F-F) axis and thus should have envelopes which are combinations of the three shown in Figure 8. The following spectral regions contain peaks not attributable to air impurities.

3.0-4.0 μ region (Figure 12)

This region contains only one strong peak and the band envelope resembles the b<sub>1</sub> contour of Figure 8. Thus, this is an a' peak, and its maximum is at 2987 cm<sup>-1</sup>.

4.0-5.0 μ region (Figure 13)

Two peaks occur in this region, one of which is also seen in the air spectrum. The other appears to be a hybrid of the a<sub>1</sub> and b<sub>1</sub> envelopes in Figure 8 with a small central peak at 2230 cm<sup>-1</sup>.

We assign this as an a' band.

7.0-8.0 μ region (Figure 14)

Only one peak, resembling the b<sub>1</sub> type in Figure 8, occurs here. It is an a' peak, and its maximum occurs at 1367 cm<sup>-1</sup>.

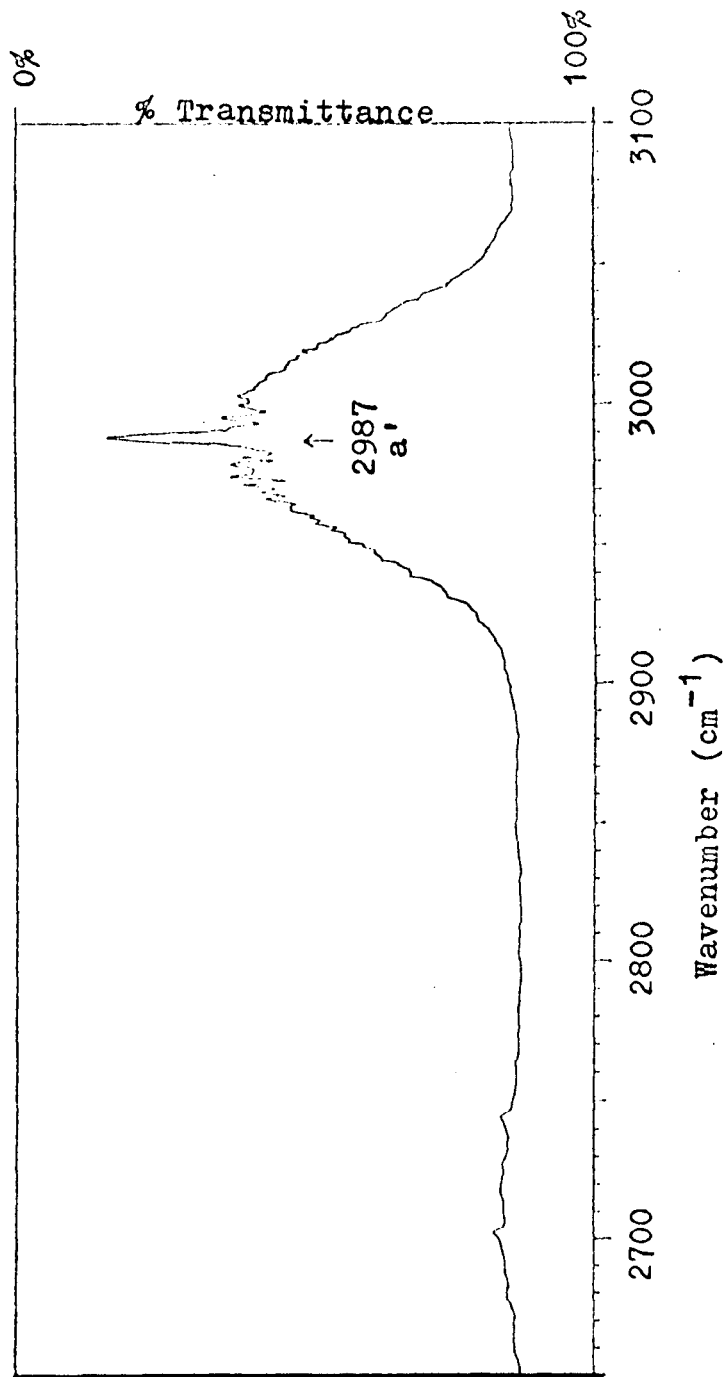


Figure 12. The 3.0-4.0  $\mu$  region of the vapor-phase IR spectrum of difluoromethane-d<sub>2</sub>.

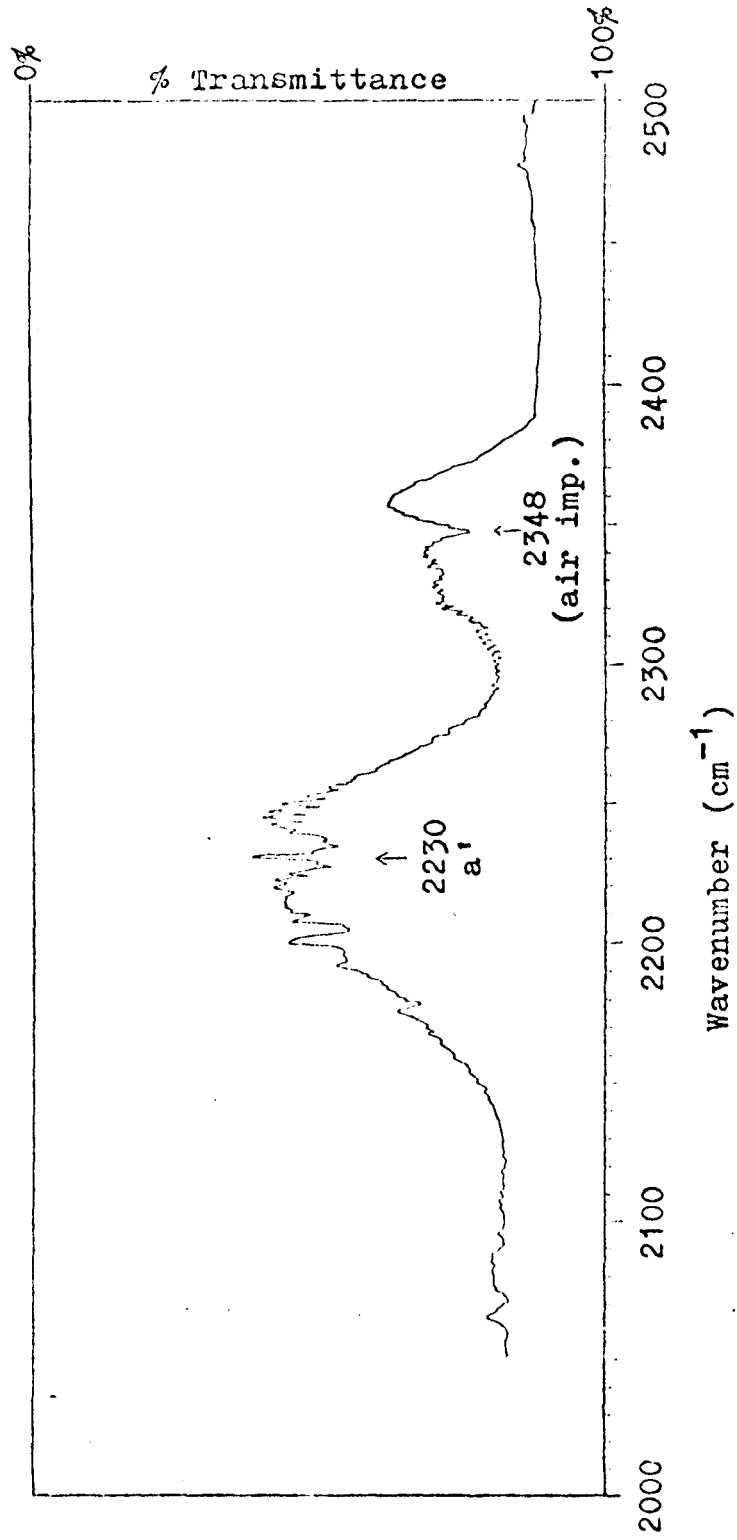


Figure 13. The 4.0-5.0  $\mu$  region of the vapor-phase IR spectrum of difluoromethane-d<sub>2</sub>.

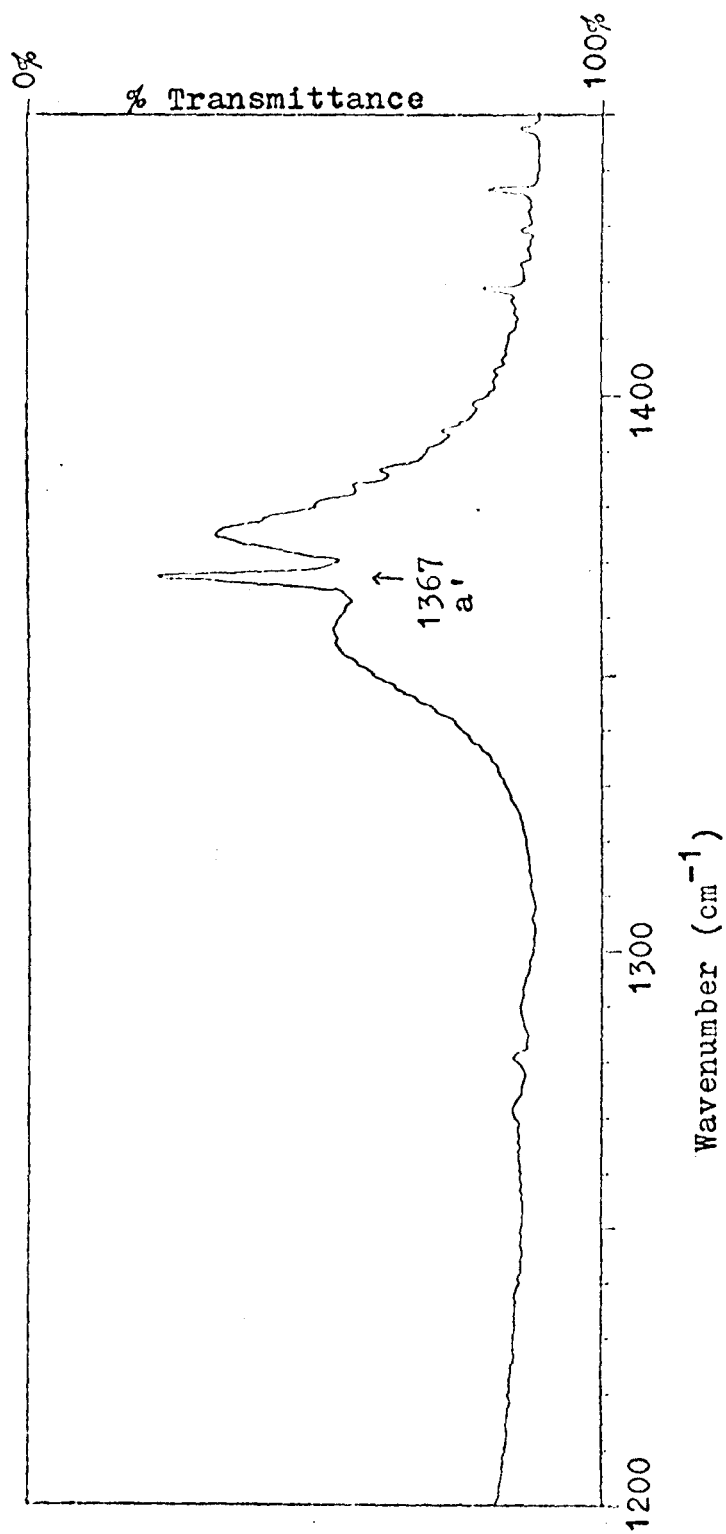


Figure 14. The 7.0-8.0  $\mu$  region of the vapor-phase IR spectrum of difluoromethane-d.

8.0-10.0  $\mu$  region (Figure 15)

The most prominent feature of this region is the very strong  $a''$ -type peak at  $1103\text{ cm}^{-1}$ . A smaller  $a'$  peak appears at  $1030\text{ cm}^{-1}$ . The area around  $1000\text{ cm}^{-1}$  contains the exceptionally clear rotational structure of the band at  $991\text{ cm}^{-1}$  (see below).

10.0-11.0  $\mu$  region (Figure 16)

The above-mentioned band at  $991\text{ cm}^{-1}$ , of  $a'$  symmetry, appears here and some of the rotational structure shows up vaguely in the region  $970\text{-}980\text{ cm}^{-1}$  on the shoulder of a larger  $a''$  band centered at  $943\text{ cm}^{-1}$ .

The above assignments are summarized in Table 6. Only two fundamentals were not found, one of which is predicted to fall below the cell cutoff and the other of which is predicted to fall close to, and is probably obscured by, the strong peak at  $1367\text{ cm}^{-1}$ .

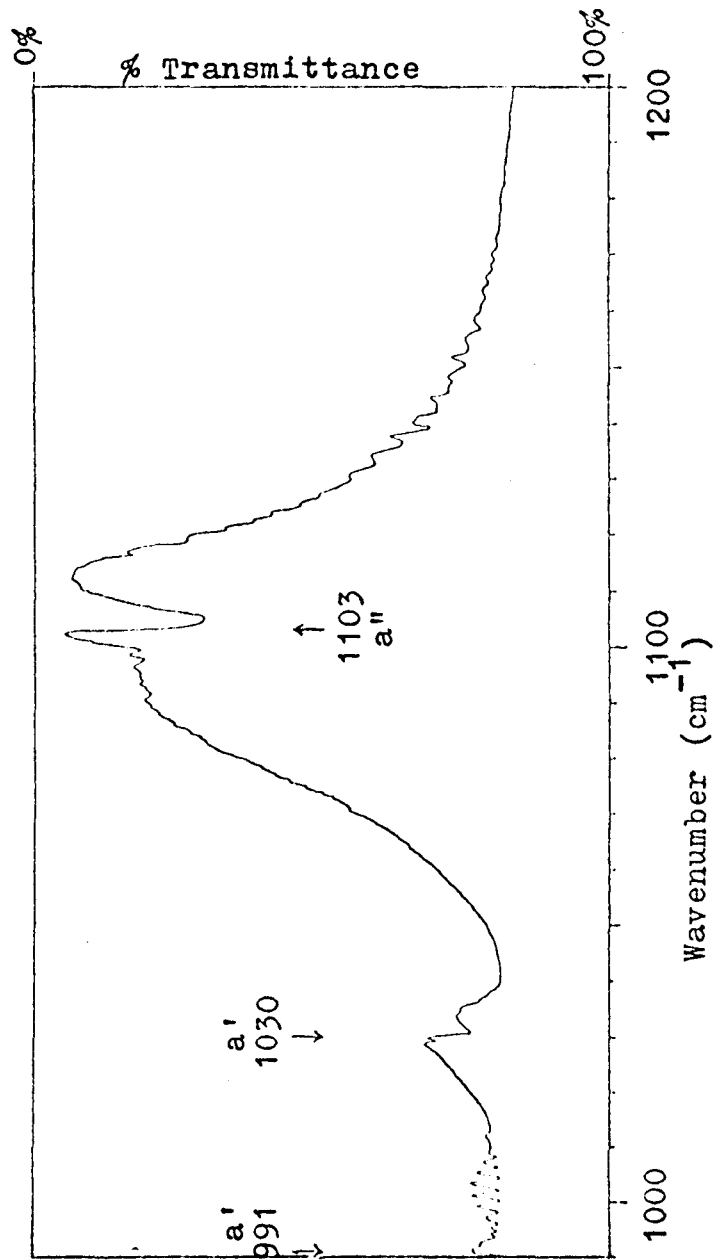


Figure 15. The 8.0-10.0  $\mu$  region of the vapor-phase IR spectrum of difluoromethane-d.

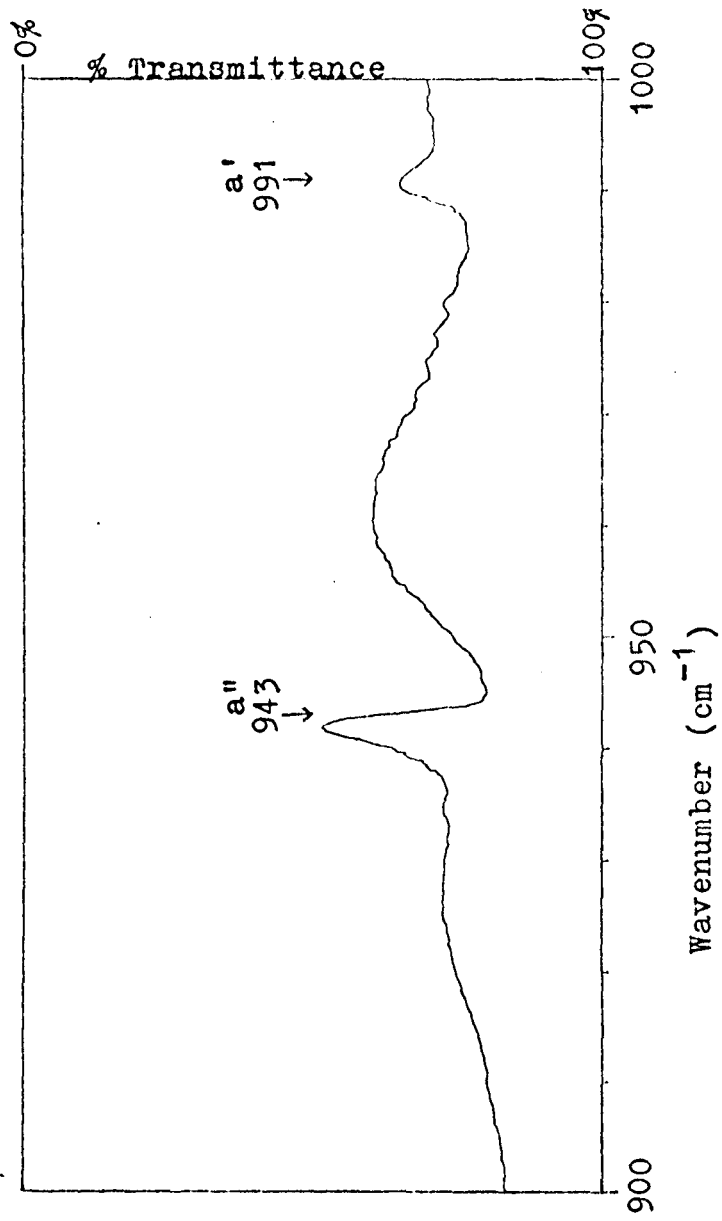


Figure 16. The 10.0-11.0  $\mu$  region of the vapor-phase IR spectrum of difluoromethane-d<sub>2</sub>.

## G. References

- <sup>1</sup> M. L. Unland, J. H. Letcher, I. Absar and J. R. van Wazer, J. Chem. Soc. (A), 1328 (1971).
- <sup>2</sup> C. R. Brundle, M. B. Robin and H. Basch, J. Chem. Phys., 53, 2196 (1970).
- <sup>3</sup> M. D. Newton, W. A. Lathan, W. J. Hehre and J. A. Pople, ibid., 52, 4064 (1970).
- <sup>4</sup> J. A. Pople and G. A. Segal, ibid., 44, 3289 (1966).
- <sup>5</sup> C. C. J. Roothaan, Rev. Mod. Phys., 23, 69 (1951).
- <sup>6</sup> (a) H. C. Urey and C. A. Bradley, Jr., Phys. Rev., 38, 1969 (1931); (b) T. Shimanouchi, Pure Appl. Chem., 7, 131 (1963).
- <sup>7</sup> (a) R. G. Body, D. S. McClure and E. Clementi, J. Chem. Phys., 49, 4916 (1968); (b) E. Menna, R. Moccia and L. Randaccio, Theoret. Chim. Acta, 4, 408 (1960); (c) M. Allavena and S. Bratož, J. Chim. Phys., 60, 1199 (1963); (d) S. Bratož and M. Allavena, J. Chem. Phys., 37, 2138 (1962); (e) D. M. Bishop and M. Randič, ibid., 44, 2480 (1966).
- <sup>8</sup> By this we mean that no full normal-coordinate analysis of the vibration spectra of difluoromethane and its deuterated analogs has appeared. A force constant set derived in a rather unreliable fashion is given in Reference 19 and will be discussed in the text.
- <sup>9</sup> R. M. Pitzer and D. P. Merrifield, J. Chem. Phys., 52, 4782 (1970).
- <sup>10</sup> P. A. Dobosh, Program CNINDO, program 142 of the Quantum Chemistry Program Exchange, Chemistry Department, Room 204, Indiana University, Bloomington, Indiana 47401.
- <sup>11</sup> J. A. Pople, D. L. Beveridge and P. A. Dobosh, J. Chem. Phys., 47, 2026 (1967).
- <sup>12</sup> M. S. Gordon and J. A. Pople, ibid., 49, 4643 (1968).

- <sup>13</sup> M.-K. Lo and W. H. Flygare, J. Molec. Spectry., 25, 365 (1968).
- <sup>14</sup> E. Hirota, T. Tanaka, A. Sakakibara, Y. Ohashi and Y. Morino, ibid., 34, 222 (1970).
- <sup>15</sup> W. H. Shaffer and R. C. Herman, J. Chem. Phys., 12, 494 (1944).
- <sup>16</sup> See, for example, E. B. Wilson, J. C. Delius and P. C. Cross "Molecular Vibrations," McGraw-Hill Book Company, Inc., New York, N. Y., 1955, pp. 347-349.
- <sup>17</sup> P. M. Morse, Phys. Rev., 34, 57 (1929).
- <sup>18</sup> G. A. Segal, J. Chem. Phys., 47, 1876 (1967).
- <sup>19</sup> A. G. Meister, J. M. Dowling and A. J. Bielecki, ibid., 25, 941 (1956).
- <sup>20</sup> J. Tyson, H. H. Claassen<sup>a</sup> and H. Kim, ibid., 54, 3142 (1971).
- <sup>21</sup> D. M. Dennison, Rev. Mod. Phys., 12, 175 (1940).
- <sup>22</sup> J. Aldous and I. M. Mills, Spectrochimica Acta, 18, 1073 (1962).
- <sup>23</sup> J. L. Duncan and I. M. Mills, ibid., 20, 523 (1964).
- <sup>24</sup> For example, see Reference 16, pp. 169-182.
- <sup>25</sup> We simply define the vector of "errors" by  $v_i = F_i - (F_0)_i$  and expand the square of its length,  $v^T v$ , as a quadratic function of the  $f_i$ . Setting the derivatives of this function with respect to each  $f_i$  to zero leads directly to equation (XXIX).
- <sup>26</sup> T. Shimanouchi, I. Nakagawa, J. Hiraishi and M. Ishii, J. Mol. Spectry., 19, 78 (1966).
- <sup>27</sup> See, e.g., J. Aldous and I. M. Mills, Spectrochimica Acta, 19, 1567 (1963).
- <sup>28</sup> Aside from routine computer-dependent modifications, the "labels" and "integrals" sections are essentially unchanged. The SCF section was rewritten by W. J. Hunt.

- <sup>29</sup> Originated at New York University, Washington Square, New York, N. Y.
- <sup>30</sup> B. N. Taylor, W. H. Parker and D. N. Langenberg, Rev. Mod. Phys., 41, 375 (1969).
- <sup>31</sup> D. R. Whitman and C. J. Hornback, J. Chem. Phys., 51, 398 (1969).
- <sup>32</sup> S. Huzinaga, ibid., 42, 1293 (1965).
- <sup>33</sup> T. H. Dunning, Jr., ibid., 53, 2823 (1970).
- <sup>34</sup> S. Winstein, E. C. Friedrich, R. Baker and Y.-I. Lin, Tet. Supp. No. 8, 621 (1966). Only one exchange was carried out rather than the two suggested by these authors.
- <sup>35</sup> The analogous reduction of chloroform is reported by D. Seyferth, H. Yamazaki and D. L. Alleston, J. Org. Chem., 28, 703 (1963).
- <sup>36</sup> Aside from the difference in pressure and solvent, our preparation was taken from W. H. Perkin, Jr. and H. A. Scarborough, J. Chem. Soc., 119, 1400 (1921).
- <sup>37</sup> H. B. Stewart and H. H. Nielsen, Phys. Rev., 75, 640 (1949).
- <sup>38</sup> G. Herzberg, "Infrared and Raman Spectra of Polyatomic Molecules," D. van Nostrand Company, Inc., New York, N. Y., 1945, pp. 460-484.
- <sup>39</sup> T. H. Dunning, R. M. Pitzer and S. Aung, BMI-ICG Report No. 73, (Battelle Memorial Institute, 505 King Avenue, Columbus, Ohio 43201).
- <sup>40</sup> W. C. Ermler and C. W. Kern, J. Chem. Phys., 55, 4851 (1971).

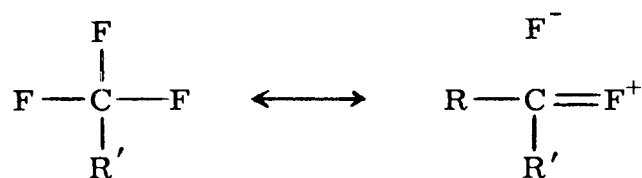
## Chapter 2

## THE ELECTRONIC STRUCTURE OF DIFLUOROMETHANE

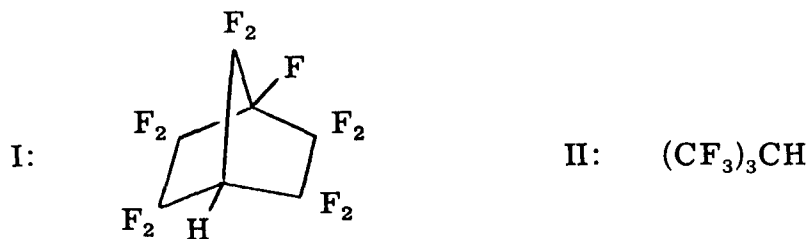
A. Introduction

In the first chapter, we investigated the potential energy surface of the difluoromethane molecule. Although the molecular energy is an important result of any theoretical calculation, there is a great deal of other information contained in the wavefunction. If such information is properly extracted, we can gain some insight into the general electronic structure of the molecule, and in this chapter, we undertake such an analysis in an effort to learn about the bonding in difluoromethane and about the orbital changes which take place as the molecule is distorted.

The anomalous nature of the C-F bond has long been recognized, and Sheppard and Sharts (1) have recently presented a good review and discussion of its unusual features. One of the most controversial points has been the possibility of "double bond-no bond" resonance in saturated polyfluoro compounds as shown below.



Such resonance was originally proposed by Brockway (2) to explain the marked shortening of the C–F bond in the series  $\text{CH}_3\text{F}$ ,  $\text{CH}_2\text{F}_2$ ,  $\text{CHF}_3$ ,  $\text{CF}_4$ . The currently accepted C–F bond lengths are 1.385, 1.358, 1.332 and 1.317 Å (3), respectively, and the total shortening through the series amounts to nearly 0.07 Å, a significant quantity. Pauling (4) supports such a view, though Peters (5) has given an alternative explanation based on hybridization changes of the central carbon. In Peters' view, the bonding orbitals on carbon take on an increased s character as the number of strongly electron-withdrawing fluorines is increased, which rationalizes the shortening of the bonds but not their simultaneous strengthening (1). Indeed, one would expect a weakening of the C–F bonds due to the decreased overlap of the carbon and fluorine orbitals. Streitwieser (6) has challenged the view that double bond–no bond resonance is important in determining the relative stabilities of polyfluoro anions (7), presenting as evidence the fact that compound I has slightly higher kinetic acidity



than compound II. The bridgehead in I should destabilize the doubly bonded resonance structure and should thus lead to a much lower acidity if the proposed resonance is an important stabilizing factor.

Both Hine (8) and Lucken (9), however, present evidence that this kind of resonance is important not only in fluorocarbons but also in nitrogen- and oxygen-containing molecules. Hine (8) has even estimated the stability resulting from this source, obtaining a value of about 3.2 kcal/mole for each double bond–no bond resonance structure involving fluorines.

One purpose of this study, then, is to gain a greater understanding of the theoretical aspects of C–F bonding in difluoromethane. An important question to consider, however, is whether we can reasonably expect to find evidence for double bond–no bond hyperconjugation within the framework of Hartree-Fock theory. The valence-bond (VB) description of resonance interactions (10) involves a configuration interaction (CI) analysis using formally bonded structures as the individual configurations. The Hartree-Fock approach (11) considers only one configuration with optimized (molecular) orbitals. Delocalization of these orbitals can describe resonance effects, as for example in the pi-electron system of benzene (12), but it is possible that certain types of resonance would need additional Hartree-Fock configurations for proper description. There are two bits of evidence which suggest that some type of unusual C–F bonding is indeed present in the Hartree-Fock description of fluorocarbons. First, Newton et al. (13) have carried out geometry optimizations on a variety of small organic molecules using the Hartree-Fock method with a minimum ("STO-3G") basis set.

They found that, in the series of fluorinated methanes, the experimental trend in C-F bond lengths could be duplicated theoretically, albeit to a much smaller extent, with a theoretical shortening of about  $0.02\text{\AA}$  through the series as compared to the experimental value of  $0.07\text{\AA}$ . The failure to duplicate the trend quantitatively may be due to the absence of CI terms or to the small size and relative inflexibility of the basis set. Using a basis of about the same size but with greater flexibility, we have found (see Chapter 1) a C-F bond length about  $0.004\text{\AA}$  shorter than theirs, suggesting that a better basis set would improve the trend in calculated distances. In any event, the Hartree-Fock calculations mimic the C-F bond shortening which originally led to the double bond-no bond resonance hypothesis. Secondly, Unland *et al.* (14) have analyzed the canonical Hartree-Fock MO's of  $\text{CH}_2\text{F}_2$  using Mulliken population analysis (15) and have found that the two orbitals antisymmetric with respect to the F-C-F plane combine to give a positive contribution to the C-F overlap populations. Because these orbitals cannot be involved in the C-F sigma bonds, this result suggests a pi-pi bonding interaction of some sort between the fluorines and the carbon.

There has been a great deal of interest recently in the use of localized orbitals (16) and bond-function models (17) as theoretical tools. They can aid greatly the interpretation of electronic wavefunctions by providing descriptions which are in accord with the usual chemical concepts of bonds, lone pairs, etc. Also, the use of bond-function models is an economical alternative to the full ab initio study

of molecular electronics, because the number of variables needed to define the wavefunction for such a model is relatively small. In fact, if transferability is assumed for similar bonds in different molecules, an entire molecular wavefunction could be generated by taking functions from appropriate reference cases. Such methods have already been used successfully to calculate the rotation barriers in some small hydrocarbons (17a, 17b), and they may eventually provide a means of greatly extending the range of molecules which can be investigated theoretically. The question of how bond functions change as molecules are distorted from their equilibrium geometries is an interesting one, and is particularly important in the generalization of the bond-function approach, but it has received relatively little attention. Therefore, the second purpose of the current study has been the investigation of the orbital changes in difluoromethane as the F-C-F angle is grossly distorted.

## B. Localized Hartree-Fock Orbitals

The closed-shell Hartree-Fock SCF-MO method (11), though fairly accurate, has the drawback that the canonical molecular orbitals are generally distributed over the entire molecule. This somewhat obscures the qualitative interpretation of the wavefunction, because these delocalized orbitals do not correspond to the intuitive concepts of bonding, lone and core pairs of electrons, and it also makes difficult the comparison of wavefunctions of chemically related molecules whose symmetries differ.

Fortunately, there is a way around this problem. The orbitals which are solutions of the Hartree-Fock equations are not unique in their description of the total antisymmetric wavefunction, and in fact, any non-singular transformation of these canonical orbitals yields a new set which describes, to within a normalization constant, the same total wavefunction (11). It is possible, then, that the canonical orbitals might be "untangled" (i. e., localized) through such a transformation to give a set of orbitals conforming more closely to the intuitive models. The interpretation of the wavefunction is greatly simplified if the transformation is chosen to retain the orthonormality of the orbitals, and although other types of transformations are possible, they are usually not considered.

Currently, the most widely used criterion for localization is the one suggested by Lennard-Jones and Pople (16a) and implemented by Pitzer (16d) and by Edmiston and Ruedenberg (16b). It involves the minimization of the total electrostatic repulsion between the transformed orbitals,

which effectively places them "as far apart" as possible. This is equivalent to maximizing the total self-repulsion of the orbitals, making them as "compact" as possible, and to minimizing the "odd" part of the Hartree-Fock energy, the sum of the two-electron exchange terms between the various orbitals. Edmiston and Ruedenberg (16b, 18) have discussed this criterion at some length and have presented a general iterative procedure for finding the localizing transformation. Newton and co-workers (16c) have reviewed and reported a variety of studies based on this criterion, and have found it to provide a good, unbiased method for analyzing Hartree-Fock wavefunctions. In addition, they have defined two useful concepts which yield information about the nature of the localized orbitals, the first of which gives a measure of the "strength" of localization and the second of which gives a measure of the departure of the localized orbitals from pure one-, two- or three-centeredness. We will discuss these concepts a bit later, but first we will describe the various localization schemes currently available, including our own.

The iterative procedure of Edmiston and Ruedenberg (16b, 18) is one of successive two-by-two transformations of the Hartree-Fock orbitals, each of which increases the sum of the orbital self-repulsions as much as possible. At each stage, the new set of orbitals is formed by "mixing" just two of the old orbitals. If  $\{\lambda_k\}$  represents the new set and  $\{\phi_k\}$  represents the old, then

$$\begin{aligned}
 \lambda_{\mathbf{k}} &= \phi_{\mathbf{k}} & \mathbf{k} &\neq \mathbf{i}, \mathbf{j} \\
 \lambda_{\mathbf{i}} &= \phi_{\mathbf{i}} \cos(\theta) + \phi_{\mathbf{j}} \sin(\theta) \\
 \lambda_{\mathbf{j}} &= -\phi_{\mathbf{i}} \sin(\theta) + \phi_{\mathbf{j}} \cos(\theta)
 \end{aligned}
 \tag{I}$$

This is a two-by-two "rotation" of orbitals  $\phi_{\mathbf{i}}$  and  $\phi_{\mathbf{j}}$  by an angle  $\theta$ . Now, in general, the sum of the self-repulsions, given by

$$J(\lambda) = \sum_{\mathbf{k}=1}^n \iint \lambda_{\mathbf{k}}^2(1) \lambda_{\mathbf{k}}^2(2) / r_{12} \, d\tau_1 \, d\tau_2
 \tag{II}$$

(n is the number of Hartree-Fock orbitals and each  $\lambda_{\mathbf{k}}$  is assumed to be real)

will change during this rotation. It is possible to calculate analytically the optimum  $\theta$  for any particular  $\mathbf{i}$  and  $\mathbf{j}$  as long as the set of two-electron integrals for the  $\{\phi_{\mathbf{k}}\}$  is known, and the values of  $\mathbf{i}$  and  $\mathbf{j}$  which yield the greatest increase in  $J$  can be found. The above transformation is then performed on the orbitals and on the set of two-electron integrals, and this transformed set is used as the "old" set in the subsequent cycle. Convergence is achieved when no rotation produces an increase in  $J(\lambda)$  of more than a present threshold value, taken as  $10^{-15}$  a. u. in our application.

When this method was applied to the orbitals of the difluoromethane molecule in its Hartree-Fock equilibrium geometry (see Table 1 of Chapter 1), the convergence was disappointingly slow. After about 100 cycles involving several different orbital pairs,

the program (19) settled into a pattern of slightly intermixing the lone pair orbitals on each fluorine, the net result of these transformations being a slow rotation of the lone pairs about the C-F axis. Such a rotation necessarily involves three orbitals at a time, and the slow convergence was apparently a result of the fact that a general three-by-three transformation is not easily expressible as the product of a small number of two-by-two rotations. In all, 600 cycles were completed before we began the search for a more efficient method.

Two localization schemes have been suggested (20, 21) in which the restriction to two-by-two rotations is lifted. Edmiston and Ruedenberg (20) have presented a method in which the transformation matrix  $\underline{O}$ , which relates the  $\lambda$ 's to the  $\phi$ 's as follows

$$\lambda_i = \sum_{j=1}^n O_{ji} \phi_j \quad (\text{III})$$

is given the form

$$\underline{O} = \text{"exp}(-\epsilon \underline{A}\text{"} = 1 + \epsilon \underline{A} + (\epsilon^2/2!) \underline{A}^2 + (\epsilon^3/3!) \underline{A}^3 + \dots \quad (\text{IV})$$

where  $\underline{A}$  is a skew-symmetric matrix chosen so that the change in  $J(\lambda)$  with respect to an infinitesimal  $\epsilon$  is a maximum. This effectively locates the path of steepest ascent in the space of variables which define the orthogonal matrix  $\underline{O}$ , and it can be shown that

$$A_{ji} = -A_{ij} = [\phi_i \phi_i | \phi_i \phi_j] - [\phi_j \phi_j | \phi_j \phi_i]. \quad (V)$$

Here, we use the abbreviation  $[\phi_a \phi_b | \phi_c \phi_d]$  to represent the integral

$$\int_1 \int_2 \phi_a(1) \phi_b(1) \phi_c(2) \phi_d(2) / r_{12} d\tau_1 d\tau_2$$

(all  $\phi$ 's are assumed to be real)

Once  $\underline{A}$  is evaluated,  $\underline{Q}$  may be calculated for any particular value of  $\epsilon$  using (IV), and  $J(\lambda)$  may thus be found. Numerical variation of  $\epsilon$  leads eventually to the highest  $J(\lambda)$  along the path. At this point, the  $\lambda$ 's are formed using (III), the two-electron integrals are transformed to correspond to these new orbitals, and if convergence has not been attained, a new steepest-ascent path is found starting from the  $\lambda$ 's. Taylor (21) has improved upon this method by deriving expressions for the curvature of  $J(\lambda)$  along the steepest-ascent path. If  $J$  is assumed to vary parabolically as a function of  $\epsilon$ , a value for the optimum  $\epsilon$  may be predicted from the slope and curvature along the path, and thus the numerical search for this optimum value is bypassed. These methods have the advantage that they involve all orbitals simultaneously and may thus be well suited to cases in which the "two-by-two" method converges slowly.

We have taken a somewhat different tack (22) which partially accounts for the quadratic behavior of  $J(\lambda)$  with respect to all transformations, not just those along the path of steepest ascent. At the maximum, the gradient of  $J(\lambda)$  with respect to any

transformation must be zero, which leads to the  $n(n-1)/2$  conditions:

$$[\lambda_i \lambda_j | \lambda_j \lambda_j] - [\lambda_j \lambda_i | \lambda_i \lambda_i] = 0 \quad \text{all } j > i \quad (\text{VI})$$

a result which was originally derived by Edmiston and Ruedenberg (16b, 18). Now suppose we have a set of nearly localized orbitals  $\{\phi_k\}$ . Equation (VI) will not quite be true, and so we seek to carry out a slight transformation upon the orbitals so that it will be true, at least to first order. Let us define the matrix of "errors",  $\underline{X}^\phi$ , by

$$\underline{X}_{ji}^\phi = [\phi_j \phi_i | \phi_i \phi_i] - [\phi_i \phi_j | \phi_j \phi_j] \quad (\text{VII})$$

and carry out a slight transformation ( $\underline{Q}$ ) upon the  $\phi$ 's as in equation (III), the purpose being to reduce these errors to zero. Now,  $\underline{Q}$  is supposed to be nearly unity

$$\underline{Q} = \underline{1} + \underline{A} \quad (\underline{A} \text{ small}) \quad (\text{VIII})$$

and if we require that  $\underline{Q}$  be orthogonal only to first order, we may take  $\underline{A}$  to be skew-symmetric (23). Thus, we effectively isolate the  $n(n-1)/2$  degrees of freedom of  $\underline{Q}$  in the upper triangle of  $\underline{A}$ . For a general, small  $\underline{A}$ , the error matrix for the  $\lambda$ 's may be expanded to first order in the elements of  $\underline{A}$  to give

$$\begin{aligned}
\mathbf{X}_{ji}^\lambda &= [\lambda_j \lambda_i | \lambda_i \lambda_i] - [\lambda_i \lambda_j | \lambda_j \lambda_j] \quad (\text{IX}) \\
&\cong \mathbf{X}_{ji}^\phi + \sum_q \sum_{p>q} A_{pq} \frac{\partial}{\partial A_{pq}} \left( [\lambda_j \lambda_i | \lambda_i \lambda_i] - [\lambda_i \lambda_j | \lambda_j \lambda_j] \right) \\
&\cong \mathbf{X}_{ji}^\phi + \sum_q \sum_{p>q} A_{pq} \left\{ \left[ \left( \frac{\partial \lambda_j}{\partial A_{pq}} \right) \phi_i | \phi_i \phi_i \right] + \left[ \phi_j \left( \frac{\partial \lambda_i}{\partial A_{pq}} \right) | \phi_i \phi_i \right] \right. \\
&\quad \left. + 2 \left[ \phi_j \phi_i | \left( \frac{\partial \lambda_i}{\partial A_{pq}} \right) \phi_i \right] - \left[ \left( \frac{\partial \lambda_i}{\partial A_{pq}} \right) \phi_j | \phi_j \phi_j \right] \right. \\
&\quad \left. - \left[ \phi_i \left( \frac{\partial \lambda_j}{\partial A_{pq}} \right) | \phi_j \phi_j \right] - 2 \left[ \phi_i \phi_j | \left( \frac{\partial \lambda_j}{\partial A_{pq}} \right) \phi_j \right] \right\}
\end{aligned}$$

But, from (III) we have

$$\frac{\partial \lambda_i}{\partial A_{pq}} = \sum_j \phi_j \partial O_{ji} / \partial A_{pq} \quad (\text{X})$$

and using equation (VIII) and the fact that  $\underline{A}$  is skew-symmetric, we may obtain

$$\partial O_{ji} / \partial A_{pq} = \delta_{jp} \delta_{iq} - \delta_{jq} \delta_{pi} \quad (\text{XI})$$

Substituting (XI) into (X) and summing over j, we get

$$\frac{\partial \lambda_i}{\partial A_{pq}} = \delta_{iq} \phi_p - \delta_{ip} \phi_q \quad (\text{XII})$$

Using this, we may rewrite (IX) as

$$\mathbf{X}_{ji}^\lambda \cong \mathbf{X}_{ji}^\phi + \sum_q \sum_{p>q} A_{pq} B_{pq,ji} \quad (\text{XIII})$$

where

$$B_{pq,ji} = \delta_{ip}Y_{jq,i} - \delta_{jp}Y_{iq,j} + \delta_{jq}Y_{ip,j} - \delta_{iq}Y_{jp,i} \quad (\text{XIV})$$

in which

$$Y_{ab,c} = [\phi_a\phi_a|\phi_a\phi_b] - [\phi_a\phi_b|\phi_c\phi_c] - 2[\phi_a\phi_c|\phi_b\phi_c] \quad (\text{XV})$$

Thus, we may evaluate the supermatrix  $\underline{B}$  directly from the set of two-electron integrals over the  $\phi$ 's. Now, we wish to find the matrix  $\underline{A}$  which will cause the skew-symmetric  $\underline{X}^\lambda$  matrix to vanish.

Setting the left-hand side of (XIII) to zero for all unique elements  $\underline{X}_{ji}^\lambda$ , we obtain  $n(n-1)/2$  equations for the  $n(n-1)/2$  unique  $\underline{A}$  elements:

$$\sum_q \sum_{p>q} A_{pq} B_{pq,ji} \cong -X_{ji}^\phi \quad \text{all } (j, i) \text{ with } j > i \quad (\text{XVI})$$

Both  $\underline{B}$  and  $\underline{X}^\phi$  are defined by the two-electron integrals over the  $\phi$ 's, and thus we may solve the linear equations (XVI) for the desired  $\underline{A}$  values. To simplify the solution, we consider  $(j, i)$  with  $j > i$  to be a single index, say  $k$ , and  $(p, q)$  with  $p > q$  to be a second index, say  $l$ . Now (XVI) can be written in a much more familiar form; a simple matrix equation. We have

$$\sum_l A_l B_{l,k} \cong -X_k^\phi \quad \text{all } k \quad (\text{XVII})$$

or, considering  $\underline{B}$  to be a simple "matrix" and  $\underline{A}$  to be a "vector", we have, in matrix form

$$\underline{\hat{B}}^T \underline{A} \cong -\underline{X}\phi \quad (\text{XVIII})$$

which we may solve straightforwardly for the "vector"  $\underline{A}$ , obtaining

$$\underline{A} \cong -(\underline{\hat{B}}^T)^{-1} \underline{X}\phi \quad (\text{XIX})$$

The values in the "vector"  $\underline{A}$  thus obtained define the  $\underline{A}$  matrix, and thus we may compute the transformation matrix  $\underline{Q}$  using equation (VIII). Because  $\underline{A}$  is not vanishingly small,  $\underline{Q}$  will not be a truly orthogonal matrix, but we can rectify this by symmetrically orthogonalizing the columns of  $\underline{Q}$  (24). Then,  $\underline{Q}$  can be used to form the new localized orbitals  $\lambda_k$  using (III). These should constitute a better guess than the  $\phi$ 's for the actual localized orbitals, and may be used as the starting point for another cycle of refinement.

The above constitutes a pseudo-second-order approach to the localization problem, since it deals with the first-order changes in the first-order conditions of equation (VI). After we had implemented the method, we learned of the work of Newton et al. (16c) and noted the close relationship between our supermatrix  $\underline{B}$  and the supermatrix of theirs which gives the second derivatives of  $J(\lambda)$  with respect to the  $n(n-1)/2$  unique orthogonal transformations. Their supermatrix has the same form as ours, except that the term  $Y_{ab,c}$  of equation (XV) is defined by

$$\begin{aligned} Y_{ab,c} = Y_{ba,c} = & [\phi_a \phi_b | \phi_b \phi_b] + [\phi_b \phi_a | \phi_a \phi_a] \\ & - 2[\phi_a \phi_b | \phi_c \phi_c] - 4[\phi_a \phi_c | \phi_b \phi_c] \end{aligned} \quad (\text{XX})$$

At the maximum, the first two terms on the right-hand side are equivalent via (VI), which yields an expression identical to ours except for a factor of two. They have not used  $\underline{\underline{B}}$  in the localization procedure, but they find that its eigenvalues provide a measure of the "strength" of localization [i. e., the sensitivity of  $J(\lambda)$  toward various orbital mixings] and can be used to verify that the localized orbitals correspond to a true local maximum in  $J(\lambda)$ . It is possible to derive a truly second-order approach to localization in much the same way as we have derived our method. In this case, the  $\underline{\underline{Q}}$  matrix is written as

$$\underline{\underline{Q}} = \underline{\underline{1}} + \underline{\underline{A}} + \frac{1}{2}\underline{\underline{A}}^2 \quad (\underline{\underline{A}} \text{ is small and skew-symmetric}) \quad (\text{XXI})$$

which makes it orthogonal through second order in the elements of  $\underline{\underline{A}}$ . Expanding  $J(\lambda)$  through second order and solving for the local quadratic extremum gives equations nearly identical to ours, the only difference being in the definition of  $Y_{ab,c}$  (equation XV). The term

$$[\phi_a \phi_a | \phi_a \phi_b]$$

simply needs to be replaced by

$$\frac{1}{2}([\phi_a \phi_a | \phi_a \phi_b] + [\phi_b \phi_b | \phi_b \phi_a]).$$

This makes our supermatrix  $\underline{\underline{B}}$  proportional to the second-derivative matrix of Newton and co-workers (16c).

Only four cycles of pseudo-second-order (PSO) localization were needed to obtain the final localized orbitals for difluoromethane, starting from the partially localized orbitals obtained after 600 two-by-two rotations. Each cycle of the PSO method is considerably more costly than a two-by-two rotation, because the full set of two-electron integrals must be transformed each time in the former, while the latter alters only a small subset of them. With our case, involving thirteen orbitals, we found a cost factor of about forty between the two, but in view of the fact that the PSO method converged so rapidly, we feel that an overall savings was realized.

The localized molecular orbitals (LMO's) thus obtained were readily identifiable as core, bonding and lone pair orbitals. The core orbitals are somewhat less compact than the canonical cores, but are still concentrated in small regions about the C and F nuclei.

The two symmetrically related C-F bonds are, as expected, quite polar, and the fluorine contribution contains little s character. Figure 1 shows a plot of the amplitude, in the F-C-F plane, of one of these bonding orbitals. We may divide each such orbital into a carbon hybrid, composed of the contributions from the carbon AO's, and a similarly defined fluorine hybrid, but we must keep in mind that hybrids derived from doubly occupied LMO's may not be as meaningful as, nor comparable to, hybrids obtained in the usual way from singly occupied valence-bond orbitals. The hybrids show 74% and 85% p-character for carbon and fluorine, respectively, based on a population analysis (15) over the pertinent AO's. These values

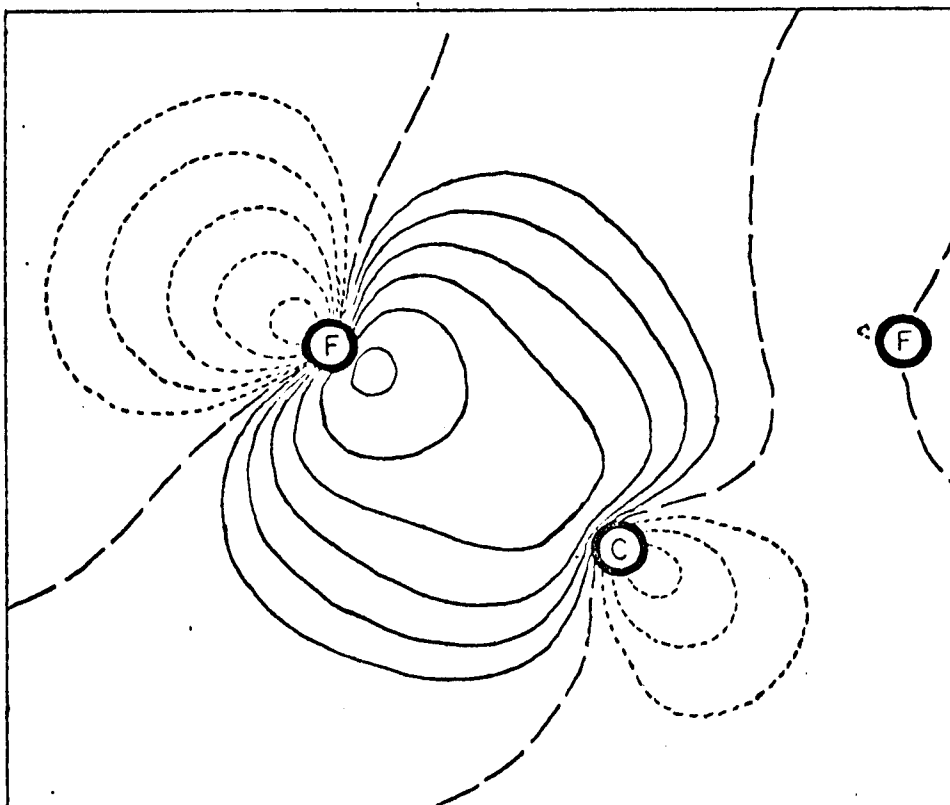


Figure 1. Orbital amplitude plot, in the F-C-F plane, of one of the two C-F bonding LMO's in difluoromethane (Hartree-Fock equilibrium geometry). The dotted, dashed and solid lines are negative, zero and positive contours, respectively. The contour closest to the node represents an absolute value of 0.05 a.u., and the ratio between successive contours is 1.7.

correspond to  $sp^{2.8}$  and  $sp^{5.7}$  hybridization, respectively. The "direction" of each hybrid is difficult to define precisely because of the nature of our basis set. For the C hybrids, the coefficients of the inner (i. e., smaller) p orbitals indicate an angle between the carbon hybrids of the two C-F bonds of about  $101^\circ$ , while for the outer p orbitals, the value is roughly  $94^\circ$ . Both are substantially below the actual F-C-F angle of  $109^\circ$ , a result which supports the view (25) that fluorine induces extra p-character in the C hybrids, thus reducing the inter-hybrid angle below its natural tetrahedral value. These C hybrids show a bending which cannot be described in terms of simple hybridization parameters, but we may define an "average" hybrid direction by grouping together the inner and outer p orbitals of each type (x, y and z) and carrying out a population analysis (15) over these groups. We thus obtain gross x, y and z populations reduced to a minimum basis level. By taking the square roots of these and appending the appropriate signs, we generate minimum basis coefficients which yield the correct populations and which may be used to define the average hybrid direction. In this manner, we obtain an average angle between the carbon hybrids of  $99.4^\circ$ . Each fluorine hybrid points in a direction which is only about  $1^\circ$  away from the pertinent C-F axis so that the two fluorine hybrids intersect with an angle of  $111.2^\circ$ . The inner and outer p-contributions are quite similar in this case, giving angles of  $111.6^\circ$  and  $111.0^\circ$ , respectively. If each bonding orbital is expressed as a linear combination of normalized hybrids, the fluorine coefficient is

nearly 2.2 times as large as the carbon coefficient, which points up the polar nature of the bond.

The carbon hybrids of the two symmetrically related C-H bonding orbitals contain 57% p-character, corresponding to hybridization of  $sp^{1.3}$ . The average angle between the carbon hybrids of the two C-H bonds is  $117.8^\circ$ , with inner and outer p contributions of  $119.0^\circ$  and  $115.8^\circ$ , respectively. The coefficient of the normalized carbon hybrid is about 35% larger than the coefficient of the normalized hydrogen hybrid in the bond, indicating the presence of a slight polarity in the direction  $C^-H^+$ . Figure 2 shows an orbital-amplitude plot of one of the C-H bonds in the H-C-H plane.

It is interesting to note that the overall carbon hybridization is not at all consistent with the usual relationships (26). For example, the average angle of nearly  $120^\circ$  between the C hybrids of the C-H bonds is consistent with roughly  $sp^2$  hybridization, but we found it to be  $sp^{1.3}$ . Similarly, for the C-F bonds the angle suggests about  $sp^5$  hybridization, but we obtained  $sp^{2.8}$ . The equations relating angles to hybridization (26) are derived from the assumption that all hybrids on a given center are orthogonal, though, and this is where the discrepancy arises; the fact that the localized molecular orbitals must be orthogonal does not imply that the individual hybrids must be. All we can really say about the bonding orbitals, aside from the above-mentioned bond polarities, is that the carbon contribution to the C-F bond contains substantially more p-character than its contribution to the C-H bond.

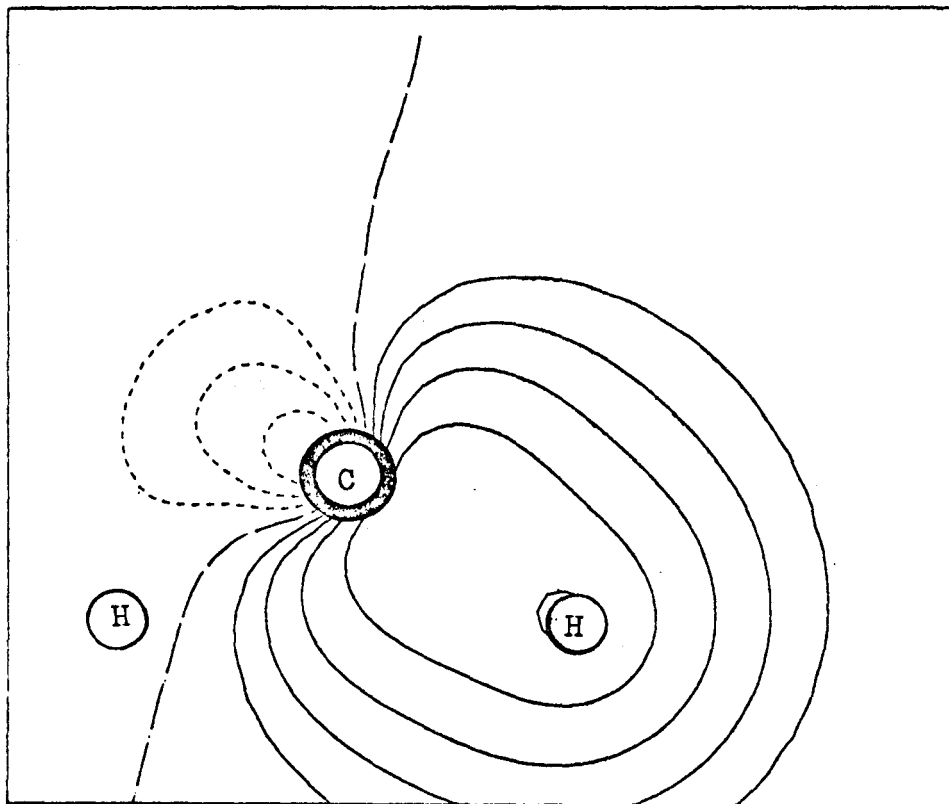


Figure 2. Orbital amplitude plot, in the H-C-H plane, of one of the two C-H bonding LMO's. See Figure 1 for contour values.

There are, in addition to the bonding and core orbitals, six lone pair orbitals. Each fluorine carries three, and the two sets are related by a reflection through the H-C-H plane. The lone pairs are distributed much as are the hydrogens on the terminal carbons in propane; they are staggered with respect to the bonding orbitals on the neighboring carbon. Figure 3 shows an orbital amplitude plot of one of the two lone pairs lying in the F-C-F plane. The most interesting feature of this plot is the marked "smearing" of the orbital toward carbon, an effect which is also seen in Figure 4, which is a plot of one of the other four pairs in the pertinent F-C-H plane. A similar effect has been noted by Newton *et al.*(27) in the oxygen lone pairs of formaldehyde, and we will discuss this delocalization shortly.

As to the gross structure of these pairs, we find that the fluorine contribution in each case contains 69%-70% p-character, corresponding to  $sp^{2.3-2.4}$  hybridization. The average angle between hybrids on a given fluorine is  $113.6^\circ \pm 0.70^\circ$ , which is consistent with  $sp^{2.5}$  hybridization. In this case, the angles are well-defined, because the inner and outer p contributions point in almost exactly the same directions. The angle between the lone pairs and the fluorine hybrid of the C-F bond is  $105.10^\circ \pm 0.1^\circ$ , which agrees well with the prediction of  $105^\circ$  based on  $sp^{2.5}$  hybridization of the lone pairs. The fluorine hybrid of the C-F bond is similarly predicted to have  $sp^{5.8}$  hybridization, which agrees well with the value of  $sp^{5.7}$  which we obtained above. We conclude that the usual hybridization concepts (26) apply quite well to the fluorines.

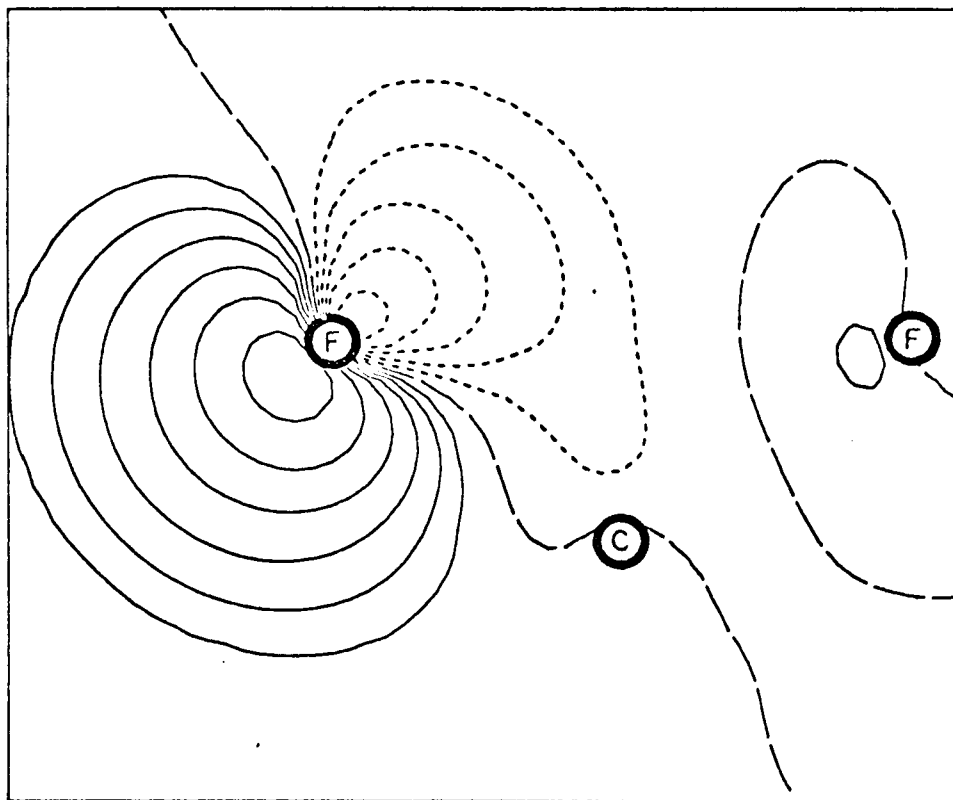


Figure 3. Orbital amplitude plot, in the F-C-F plane, of one of the two fluorine lone pair LMO's which lie in that plane. See Figure 1 for contour values.

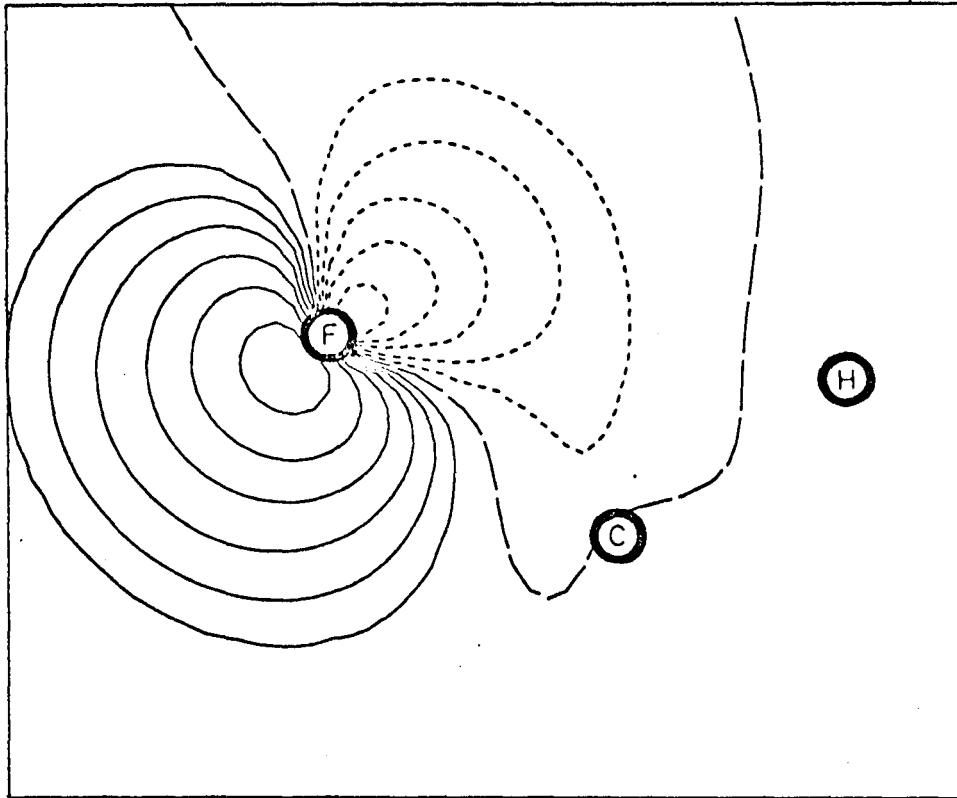


Figure 4. Orbital amplitude plot, in one of the four F-C-H planes, of the fluorine lone pair LMO lying in that plane. There are three other such pairs, symmetrically related to this one. See Figure 1 for contour values.

As noted above, all of the lone pairs show an apparent delocalization toward carbon in what appears to be a slightly bonding interaction. Examining Figure 3, we see that, in addition to this bonding, the delocalization introduces some electron density onto the other fluorine and some antibonding character into the other C-F bond, which gives it all the earmarks of the double bond-no bond resonance structure discussed in the introduction. Figure 4 shows a similar situation for the lone pairs in the F-C-H planes, although the nodal structure is somewhat different and the amount of charge-transfer to hydrogen is less than the analogous charge-transfer to fluorine in Figure 3. We would like to study these effects in more quantitative detail, but there is a notable lack of tools with which to do so. We discuss our approach to this problem below.

There are two major problems in the quantitative analysis of delocalization effects. First, we must consider the very definition of delocalization, which is quite evasive because it is not possible to identify uniquely those portions of an orbital which "belong" to a particular atom. Most current theoretical calculations use atom-centered basis functions, and it has become customary to dissect the orbitals into atomic contributions using the MO expansion coefficients. Such a dissection may lose its meaning, though, if each AO basis is very complete, if one-centered expansion methods are used, or if functions other than atom-centered ones are used. In spite of this, the method has proven quite useful, particularly in connection with Mulliken population analysis (15), and we shall rely upon it, keeping

in mind that our results can be, at best, only semi-quantitative. The second problem involves the use of LMO's. Because these must be mutually orthogonal, a certain amount of natural delocalization must be present, and it is not possible at present to separate such "orthogonality delocalization" from "real delocalization", assuming the latter exists.

Newton and co-workers (16c) have dealt with the problem of delocalization using a simple truncation procedure. Bond functions are derived from the LMO's by simply setting to zero those coefficients which do not "belong". Once an LMO has been identified as, say, an A-B bond, the corresponding bond function is obtained by retaining only those AO coefficients pertaining to A- or B-centered basis functions. Nonbonding orbitals and three-centered bonds may be treated analogously. Using such bond functions, which they call TLMO's (for truncated LMO's), they have defined a parameter, the percent delocalization, to measure the extent to which an LMO and its corresponding TLMO differ. If  $\phi$  represents an LMO and  $\phi^T$  represents the corresponding TLMO, both normalized, then

$$\text{percent delocalization} = \left[ \frac{1}{2} \int (\phi - \phi^T)^2 d\tau \right]^{\frac{1}{2}} \times 100\%. \quad (\text{XXII})$$

Carrying out the integration and letting S be the overlap of  $\phi$  with  $\phi^T$ , we obtain

$$\text{percent delocalization} = 100\% \times (1 - S)^{\frac{1}{2}}. \quad (\text{XXIII})$$

We have calculated these values for our LMO's in difluoromethane, obtaining the following:

F core .....	0.9%	C-H bond .....	12.6%
C core .....	3.2%	F lone pair .....	7.3%
C-F bond .....	6.5%		

which are generally consistent with the results of Newton and co-workers (16c). They find typical values of 10% for C-H bonds in methyl or methylene groups, about 4% for C-X sigma bonds where X is a first-row heteroatom, about 4.5% for carbon cores and about 1% for heteroatom cores. The lone pair delocalization appears usually low when compared to the values for O (13%) and N (19%) lone pairs in H<sub>2</sub>CO and HCN, but we note that these are unsaturated systems with substantially shorter C-X bonds, so we might expect generally greater delocalization effects for them. Using Newton's delocalization criterion, we must conclude that the fluorine lone pairs in difluoromethane are somewhat delocalized, though the effect is by no means a large one.

Newton's criterion, though, may be criticized on several counts. First, the method does not attempt to account for delocalization resulting from orthogonality, which, we have found, can be quite substantial. To show this, we have symmetrically orthogonalized (28) the TLMO's to give a set of orbitals resembling the LMO's, and presumably containing about the same amount of "orthogonality delocalization". We then truncated these approximate LMO's just as

we did the actual ones, and computed the resulting delocalization percentages, obtaining

F core	.....	0.3%	C-H bond	.....	7.4%
C core	.....	1.1%	F lone pair	.....	3.2%
C-F bond	.....	4.2%			

Comparing these to the previous values, we find that, in all cases, a substantial fraction of the original delocalization could arise from orthogonality. Thus, if we are interested in "real" delocalization, whatever it might be, then the parameter defined by Newton does not seem to be particularly useful.

The only reliable way we can see to surmount this problem would be to develop a localization scheme which lifts the orthogonality restriction. Short of this, we may take a more approximate approach in which we make the following three assumptions: a) There exists a well-defined and meaningful set of non-orthogonal, localized Hartree-Fock orbitals (NLO's); b) These NLO's, when symmetrically orthogonalized (28), yield the LMO's; and c) The overlap matrix for the NLO's is approximately the same as that for the TLMO's. If  $\{\lambda_k\}$  is the set of NLO's and  $\{\phi_k\}$  is the set of LMO's, then the second assumption leads to

$$\lambda_i = \sum_j (\tilde{S}^{\frac{1}{2}})_{ij} \phi_j \quad (\text{XXIV})$$

where  $\tilde{S}^{\frac{1}{2}}$  is the symmetric "square root" (29) of  $\tilde{S}$ , the matrix of

overlaps between the NLO's. The third assumption allows us to evaluate  $S_{ij}$  at least approximately, and thus to obtain approximate NLO's. The NLO's thus obtained bear the same relationship to the LMO's as the TLMO's bear to their symmetrically orthogonalized counterparts, and the NLO's represent orbitals which are, at least partially, corrected for orthogonality delocalization. We may truncate these to give TNLO's, and compute the percent delocalization of the TNLO's relative to the NLO's using (XXIII). We have done this, obtaining

F core	.....	0.6%	C-H bond	.....	6.0%
C core	.....	2.3%	F lone pair	.....	6.9%, 6.3%
C-F bond	.....	2.8%			

where the higher value for the lone pairs corresponds to the orbital in the F-C-F plane. These values, which hopefully express mostly real delocalization, are seen to be generally lower than the analogous values for the LMO's, and they indicate that the lone pairs are the most highly delocalized of the orbitals. Interestingly, the lone pairs which lie in the F-C-F plane are substantially more delocalized than the out-of-plane pairs.

A second criticism which may be applied to Newton's delocalization criterion, as well as to the one we have given above, is that they refer to overlap quantities rather than energy quantities. The delocalization energy of a single-determinant MO wavefunction can be straightforwardly defined as the energy increase which results

from replacing the actual MO's by orbitals which are localized in some fashion. In simple Hückel theory (30), for example, the localized orbitals for a hydrocarbon pi system are considered to be simple ethylenic bonds between neighboring carbons. For more general types of wavefunctions, a good definition of "localized" is needed, and it seems reasonable to rely upon some form of bond-function model. Newton et al. (16c) find that replacing LMO's by TLMO's increases the energy of a variety of small molecules by 30-100 mh (we use the symbol mh, "milli-Hartree", to represent  $10^{-3}$  a. u., which is about 0.6 kcal/mole). We obtain 121.5 mh for the delocalization energy of difluoromethane, defined in this way. If, instead, we replace the NLO's by their truncated counterparts, the energy increase is only 99.7 mh, indicating that the TNLO's are better bond functions than the TLMO's. This seems reasonable because, to obtain the approximate Hartree-Fock orbitals, the bond functions must be orthogonalized; the TNLO's partially account for this while the TLMO's do not.

A logical way to extend the above method is to consider the energy increase which results from replacing each individual orbital by its localized counterpart, a process which gives the delocalization energies (DE's) for these orbitals. If we are using TLMO's as the localized functions, the DE for an orbital is obtained by calculating the energy of a wavefunction in which only that orbital is truncated and subtracting from it the Hartree-Fock energy. If we are using TNLO's, we go through the same process, but replace an NLO by its

TNLO. Generally, the sum of the individual DE's will not quite match the total DE because of the nonlinearity of the orthonormalization procedure which precedes the energy evaluation, and for meaningful DE's, this error should be small. Table 1 gives the DE's we have obtained for the orbitals in difluoromethane, based on both TLMO and TNLO bond functions. In view of the fact that the latter show a smaller overall DE, better DE additivity and more reasonable description of the C core, we will concentrate mainly on them, though our conclusions apply fairly well to the TLMO values, too.

Examining the TNLO values in Table 1, we find that the lone pairs account for about 80% of the total DE of the molecule, and that they have by far the highest individual DE's. The total stabilization from this source amounts to about 80 mh (50 kcal/mole), or about 25 kcal/mole for each C-F bond. We note that the DE of the lone pairs which lie in the F-C-F plane is greater by about 4 mh (2.5 kcal/mole) than the DE for the out-of-plane pairs, and that this value is not sensitive to the nature of the bond-function model. This is a very interesting result, implying that delocalization is more efficient (from an energy standpoint) when a fluorine lone pair opposes a C-F bond than when it opposes a C-H bond. We may view this extra stability as a fluorine-fluorine interaction of sorts, and counting 2.5 kcal/mole for each in-plane pair, we calculate a total F-F stabilization of about 5 kcal/mole. In a study of the thermodynamic stabilities of the fluorinated methanes, Hine (8) has estimated that each such interaction is "worth" 6.5 kcal/mole, which is in

Table 1. Delocalization Energies (in mH) for the Localized Orbitals of Difluoromethane.

<u>Orbital</u>	<u>Number</u>	<u>Delocalization energy (mh)</u>			
		<u>From TLMO's</u>		<u>From TNLO's</u>	
		<u>Per orbital</u>	<u>Sum over related orbitals</u>	<u>Per orbital</u>	<u>Sum over related orbitals</u>
All	13	-	121.55 <sup>a</sup>	-	99.68 <sup>a</sup>
F core	2	0.79	1.58	0.79	1.58
C core	1	10.37	10.37	6.27	6.27
C-F bond	2	2.45	4.90	0.62	1.24
C-H bond	2	7.23	14.46	5.22	10.44
F lone pair in F-C-F plane	2	17.27	34.54	16.03	32.06
F lone pair out of plane	4	13.28	<u>53.12</u>	11.94	<u>47.76</u>
			sum = 118.97 <sup>b</sup>		sum = 99.35 <sup>b</sup>
			error = 2.58 <sup>c</sup>		error = 0.33 <sup>c</sup>

<sup>a</sup>Actual total DE.

<sup>b</sup>Sum of individual orbital DE's.

<sup>c</sup>Non-additivity error, the difference of the above.

surprisingly (and perhaps fortuitously) good agreement with our theoretical value.

Thus, if we consider the delocalization percentages and DE's for the TNLO's, we conclude that the fluorine lone pairs are substantially delocalized in difluoromethane, that this delocalization represents a marked stabilization of the molecule and that the effect is most pronounced for the pairs which lie in the F-C-F plane. These conclusions, though, may be criticized on the grounds that the TNLO concept is a new one which has not been tested on other molecules, so we have no guidelines by which we can judge the reliability or our results. We believe that these results represent real effects, but that it would be wise to look at the problem from a different, and somewhat more soundly established viewpoint, that of Mulliken population analysis (15).

Table 2 gives the overlap populations (OP's) and gross populations (GP's) for each of the six different types of LMO's, for certain groups of orbitals, and for the total Hartree-Fock wavefunction. In Table 3 are the analogous populations for the symmetrically orthogonalized TNLO's which show only orthogonality delocalization because the original non-orthogonal functions are fully localized. We have included these so that we may see the general pattern of populations which results from such delocalization, a pattern which is the same whether we start from TNLO's or TLMO's.

**Table 2.** Gross and Overlap Populations for LMO's and Groups of LMO's in Difluoromethane (Hartree-Fock Equilibrium Geometry).

Orbital or Group	Overlap populations <sup>a</sup>										Gross populations <sup>a</sup>					
	C-F1	C-F2	C-H1	C-H2	F-F	H-H	F1H1	F1H2	F2H1	F2H2	H1	H2	F1	F2	C	
F1 core	0	0	0	0	0	0	0	0	0	0	0	0	0	2000	0	0
C core	-2	-2	-1	-1	0	0	0	0	0	0	0	0	0	0	0	1999
C-F1 bond	530	-12	-6	-6	-9	2	-14	-14	1	1	-5	-5	1499	-3	514	
C-H1 bond	-56	-56	854	-58	1	-35	-22	4	-22	4	860	-23	-16	-16	1195	
Lone pair on F1, trans to C-F2 bond	51	-31	-1	-1	-8	1	-6	-6	-2	-2	-1	-1	1963	0	40	
Lone pair on F1, trans to C-H2 bond	13	-6	-3	-27	-3	-6	-11	-8	2	-3	-2	3	1984	0	16	
Core group	-3	-3	-1	-1	0	0	0	0	0	0	0	0	2000	2000	1999	
Bond group	406	406	783	783	-14	-68	-31	-31	-31	-31	826	826	1464	1464	3420	
Lone pairs	36	36	-62	-62	-27	-23	-29	-29	-29	-29	0	0	5929	5929	142	
All LMO's	439	439	721	721	-41	-91	-60	-60	-60	-60	826	826	9393	9393	5561	

<sup>a</sup>In units of  $10^{-3}$  electrons.

Table 3. Gross and Overlap Populations for the Symmetrically Orthogonalized TNLO's, and Groups thereof, in Difluoromethane (Hartree-Fock Equilibrium Geometry).

Orbital or group	Overlap populations <sup>a</sup>										Gross populations <sup>a</sup>					
	C-F1	C-F2	C-H1	C-H2	F-F	H-H	F1H1	F1H2	F2H1	F2H2	H1	H2	F1	F2	C	
F1 core	0	0	0	0	0	0	0	0	0	0	0	0	0	2000	0	0
C core	-1	-1	-1	-1	0	0	0	0	0	0	0	0	0	0	0	2001
C-F1 bond	509	-9	-2	-2	-7	1	-9	-9	0	0	-2	-2	1498	-3	510	
C-H1 bond	-36	-36	813	-20	0	-15	-13	1	-13	1	825	-9	-10	-10	1205	
Lone pair on F1, <u>trans</u> to C-F2 bond	-16	0	1	1	-2	0	-1	-1	0	0	0	0	2006	0	-6	
Lone pair on F1, <u>trans</u> to C-H2 bond	-19	0	1	0	-1	0	-2	-1	0	0	0	0	2007	0	-7	
Core group	-2	-2	-1	-1	0	0	0	0	0	0	0	0	2000	2000	2001	
Bond group	429	429	789	789	-13	-30	-21	-21	-21	-21	811	811	1474	1474	3430	
Lone pairs	-54	-54	4	4	-5	0	-4	-4	-4	-4	0	0	6020	6020	-40	
All TNLO's	374	374	792	792	-18	-30	-25	-25	-25	-25	811	811	9494	9494	5391	

<sup>a</sup>In units of  $10^{-3}$  electrons.

First, we note that the cores show virtually quantitative GP's on their respective centers. The carbon core shows a very slight negative contribution to the OP's of the directly bonded atom pairs, an effect which is duplicated by the bond-function model.

The bonding LMO's show a regular pattern of populations which is present in the TNLO model as well: The atoms included in the bond, of course, have a large positive OP; each atom which is not in the bond shows a negative OP with each atom in the bond; and the OP between two atoms which are not in the bond is positive. This pattern is a logical result of the orthogonality restriction. To illustrate this, we consider an idealized system of three C-H bonds in a plane, each of which is completely localized. These bonds, shown schematically in Figure 5a, will have a slight positive mutual overlap because of the positive amplitudes on the hydrogens. Upon symmetric orthogonalization, each bond will have subtracted from it a small amount of each other bond, as shown in Figure 5b. We see that the result is a pattern of bonding and antibonding character which agrees with the noted population pattern in difluoromethane. Both the LMO's and the TNLO model show that the sum of the GP's for the atoms in a bond is greater than 2.0, which can be traced to the fact that most of the OP's to other atoms are negative. This tends to induce negative GP's upon these nonbonded atoms, and to compensate for this, the bonded atoms must contain an excess of electrons. Based on the population analysis, then, we find nothing particularly unusual about the C-F or C-H bonding LMO's; the populations may be understood

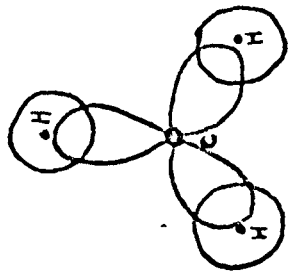
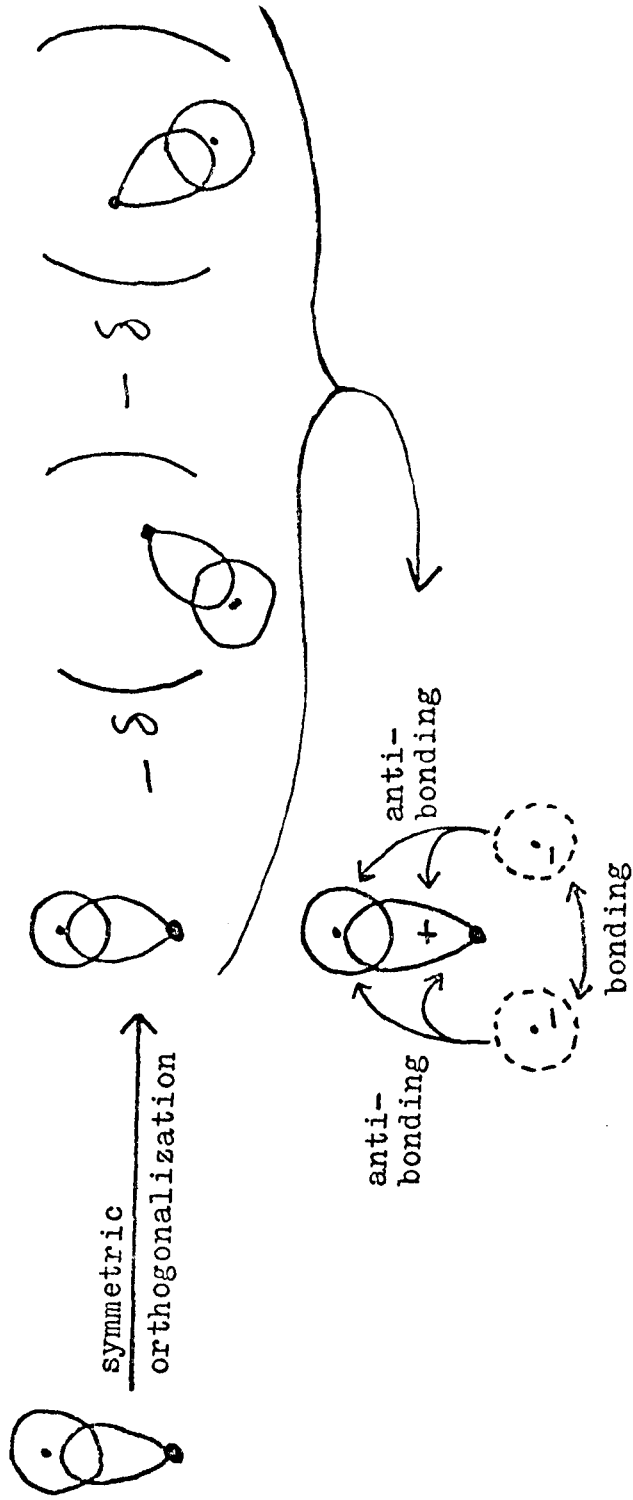


Figure 5. Schematic illustration of the effects of symmetric orthogonalization on bonding orbitals.

5 (a). Three fully localized C-H bonds in a plane



5 (b). Effect of symmetric orthogonalization on one C-H bond

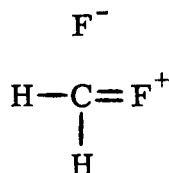
on the basis of orthogonality restrictions alone.

The situation is quite different for the lone pairs, though. We note that the GP on fluorine for each type of lone pair LMO is less than 2.0, with most of the remaining population residing on the carbon. This is in contrast to the TNLO model, which shows exactly the opposite behavior. The lone pair LMO's contribute a positive OP to the adjacent C-F bond and a negative OP to the bond which is trans to the pair. The remaining OP's do not seem to show a consistent pattern, though we note that the major interactions are negative ones between the fluorine carrying the pair and atoms which are not bonded to that fluorine. The TNLO model shows that each lone pair contributes a negative OP to the adjacent C-F bond, and virtually no OP's to any other interactions. Thus, the lone pair LMO's do not give a pattern of populations which can be understood on the basis of orthogonality restrictions, and we take this as evidence that they possess "real" delocalization. Finally, we note that the lone pair LMO's which lie in the F-C-F plane contribute more C-F bonding character, and give a greater charge-transfer to carbon, than the out-of-plane pairs do, which leads us once again to the conclusion that delocalization is most efficient when the lone pair opposes a C-F bond.

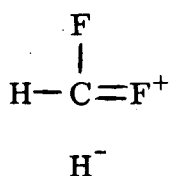
In order to see the overall effects of the lone pairs more clearly, we have partitioned the thirteen orbitals into three groups, one containing the three cores, one containing the four bonding orbitals, and the last containing the six lone pairs. Table 2 shows

that the effect of the LMO lone pair group on the GP's is a transfer of 0.14 electrons from the two fluorines to the carbon, while its effect on the OP's is a 9% "strengthening" of the C-F bonds, an 8% "weakening" of the C-H bonds, and a fairly large antibonding contribution to all other interactions. Table 3 shows that the lone pair group in the TNLO model gives almost exactly the opposite effects, so that although the bond groups of the two models show a good parallel, the total populations for the TNLO wavefunction agree rather poorly with the LMO values.

Thus we have looked at the "fine structure" of the localized orbitals in difluoromethane from three different viewpoints. Our percent delocalization criterion suggested that substantial lone pair delocalization is present, the DE's indicated that it is energetically significant, and the population analysis pointed out that it is responsible for a charge-transfer to carbon, an increase in the C-F overlap population and a decrease in the C-H overlap population. Together with the visual evidence of Figures 3 and 4, these results constitute what we believe to be a strong argument that our Hartree-Fock wavefunction contains features which cannot be adequately described by a single valence-bond configuration. At this point we can say little about the nature of the VB resonance structures which would be needed to describe these features, but it seems likely that inclusion of structures such as



and structures such as



would capture the main effects. The latter would be necessary to account for the delocalization of the lone pairs which are trans to the C-H bonds.

We turn now to the question of how the LMO's of difluoromethane change as the F-C-F angle is altered. We consider two cases in addition to the equilibrium geometry; those in which the F-C-F angle is increased and decreased by 30° from its equilibrium value. For conciseness, we will refer to the three geometries as the +30°, 0° and -30° cases, indicating the distortion of the F-C-F angle. The localizations for the +30° and -30° cases were carried out as described previously for the 0° case. Several hundred two-by-two transformations were completed to obtain an approximate localization, and these were followed by a few PSO cycles to complete the process. Again, the LMO's could readily be identified as bonds, lone pairs and cores. The cores are virtually the same in the +30° and -30° cases as they were for the 0° one, and they will not be

discussed further. The remaining LMO's will be examined in somewhat less detail than we have previously considered because we are interested only in the overall orbital changes which result from the F-C-F angle variation.

The greatest single change appears in the  $-30^\circ$  case, where we find that the sets of lone pairs on the two fluorines are no longer related by a reflection through the H-C-H plane. Rather, the pairs on one fluorine, which we arbitrarily call  $F_2$ , are rotated by  $60^\circ$  about the C-F axis so that they eclipse the bonds to the adjacent carbon. Thus, the lone pairs exhibit a "cogwheel" effect which is understandable because the electrostatic repulsion between the lone pairs above and below the F-C-F plane would be quite large if one set was not rotated. Of course, this does not mean that the molecular wavefunction has lost symmetry, only that this unsymmetrical description of it has a lower total inter-orbital repulsion than any symmetrical description. In the  $+30^\circ$  case, the lone pairs have the same symmetry and "staggered" orientation that we found in the  $0^\circ$  case.

Table 4 summarizes the most important features of the LMO hybrids in the three cases. As before, we consider an A-B bond to be composed primarily of two hybrids. The A hybrid is the contribution to the bonding LMO from all A-centered basis functions and the B hybrid is similarly defined using the B-centered basis functions. In the case of lone pairs, only one hybrid is present, and it is defined in an analogous manner. For the purpose of discussion, it is useful

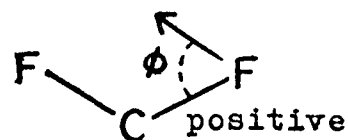
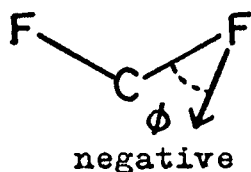
Table 4. Geometry variation of Difluoromethane:  
Hybrid Analysis of LMO's.

Parameter <sup>a</sup>	Value		
	+30° case	0° case	-30° case <sup>b</sup>
$\theta_{C^*F, C^*F}$	90.9°	99.5°	105.6°
$\theta_{C^*F, C^*F}^{\text{inner}}$	106.8°	101.4°	98.2°
$\theta_{C^*F, C^*F}^{\text{outer}}$	47.8°	93.6°	123.7°
$\theta_{C^*H, C^*H}$	117.1°	117.7°	118.2°
$\theta_{C^*H, C^*H}^{\text{inner}}$	119.1°	118.0°	119.6°
$\theta_{C^*H, C^*H}^{\text{outer}}$	114.0°	115.8°	115.9°
$\theta_{LP-o, LP-o}$	115.0°	114.3°	113.3° (112.7°)
$\theta_{LP-i, LP-o}$	113.1°	113.0°	114.5° (114.7°)
$\theta_{LP-o, CF^*}$	105.2°	105.1°	103.3° (105.7°)
$\theta_{LP-i, CF^*}$	103.8°	105.3°	106.4° (102.0°)
$\phi$	9.0°	1.2°	-8.1° (-9.3°)
$n_{C^*F}$	2.39	2.82	2.90 ( 2.91 )
$n_{C^*H}$	1.46	1.34	1.31
$n_{CF^*}$	5.66	5.70	6.28 ( 6.14 )
$n_{LP-i}$	2.39	2.35	2.53 ( 2.03 )
$n_{LP-o}$	2.24	2.25	2.14 ( 2.41 )

<sup>a</sup>See text for a description of the parameters.

<sup>b</sup>The values in parentheses are those unique to F<sub>2</sub>, whose lone pairs eclipse the carbon bonds. All other values involving fluorine refer to F<sub>1</sub>, which has the normal staggered configuration.

to "name" the hybrids. The carbon and fluorine hybrids of a C-F bond are symbolized by  $C^*F$  and  $CF^*$ , respectively, the carbon hybrid of a C-H bond is given the symbol  $C^*H$ , while  $LP-i$  and  $LP-o$  stand for lone pairs which are in and out of the F-C-F plane, respectively. The symbol  $\theta_{AB}$  in Table 4 represents the angle between two different hybrids A and B which reside upon the same atom. If  $\theta_{AB}$  does not carry a superscript, it refers to the angle between the average directions (as defined previously in terms of populations) of A and B, but if a superscript appears, the angle is determined by the relative coefficients of the inner p-type AO's (superscript = inner) or by the relative coefficients of the outer p-type AO's (superscript = outer). This distinction is important only in the hybrids  $C^*F$  and  $C^*H$  in which a fair amount of "hybrid bending" takes place. The amount of p-character in a hybrid A is given by  $n_A$ , which stands for the "x" in " $sp^x$ ". Finally, the angle  $\phi$  measures the degree to which the average direction of the F hybrid departs from the C-F axis. The sign of  $\phi$  is illustrated below:



Now, with our terminology defined, we may examine the values in Table 4. We note, first of all, that the H-C-H fragment of the molecule remains remarkably constant as the F-C-F angle is changed. There is only about a  $1^\circ$  change in  $\theta_{\text{C}^*\text{H}, \text{C}^*\text{H}}$  over the whole range, while the hybridization of C\*H varies from  $\text{sp}^{1.5}$  (+30° case) to  $\text{sp}^{1.3}$  (-30° case). We expect carbon to rehybridize in some way to maintain high overlap with the fluorine, but we find that the hybrid C\*H does not reflect this. A second point we notice is that the fluorines tend to react as relatively rigid units: The angles between lone pair hybrids are, in all cases, within  $1.3^\circ$  of  $114^\circ$ , while the angle between the hybrid CF\* and the lone pairs remains within about  $2^\circ$  of  $104^\circ$ ; the lone pair hybridizations are only modestly variable, ranging from  $\text{sp}^{2.03}$  (67% p-character) to  $\text{sp}^{2.53}$  (72% p-character), while the hybridization of CF\* is quite constant (the extremes of  $\text{sp}^{5.7}$  and  $\text{sp}^{6.3}$  correspond, respectively, to 85% and 86% p-character). The fluorine units tend to "rock" as the F-C-F angle is changed, so that the CF\* hybrid does not remain pointed toward carbon. The deviation ( $\phi$ ) is substantial, about  $9^\circ$  for each distorted case,\* which means that the CF\* hybrids on the two fluorines intersect in an angle which ranges from  $158^\circ$  (+30° case) to  $62^\circ$  (-30° case).

---

\* We note that, because  $\phi$  is measured from the C-F axis, and because this axis varies in direction by  $15^\circ$  in each distorted case, the direction of CF\* changes by  $9^\circ + 15^\circ = 24^\circ$  for each case.

Not surprisingly, the C hybrids show the greatest effects of the angle bending. At the extremes,  $\theta_{C^*F, C^*F}$  differs by  $+6^\circ$  ( $-30^\circ$  case) and  $-9^\circ$  ( $+30^\circ$  case) from its equilibrium value, rather small changes when we consider that the F-C-F angle covers a  $60^\circ$  range. Most importantly, though, we note that the  $\theta_{C^*F, C^*F}$  changes are in the 'wrong' direction. We would expect, on the basis of orbital following (31), that the inter-hybrid angle  $\theta_{C^*F, C^*F}$  would parallel the F-C-F angle, but it decreases as the F-C-F angle increases and vice versa. Examining the inner and outer contributions to this angle, we see that  $\theta_{C^*F, C^*F}^{\text{inner}}$  does follow the F-C-F angle to a slight extent, but that  $\theta_{C^*F, C^*F}^{\text{outer}}$  strongly opposes this trend. We recall, of course, that the carbon contribution to the C-F bond is small, so these hybridization changes do not have as large an effect as they would in a more homopolar bond, and we also recall that the very definition of hybridization is somewhat clouded by the nature of our basis set; nonetheless, we must conclude that as the F-C-F angle in difluoromethane is distorted, there is no evidence for orbital following on the part of carbon. Rather, the fluorine atoms "pivot" to maintain high bonding overlaps with the relatively static C\*F hybrids.

We may verify these effects visually by examining Figure 6, which shows the orbital amplitude plots of one C-F bonding LMO for the three geometries we have treated. The plots are nearly super-imposable near the carbon "end" of the bond, while the fluorine "end" undergoes a rotation which is almost solely responsible for the bond

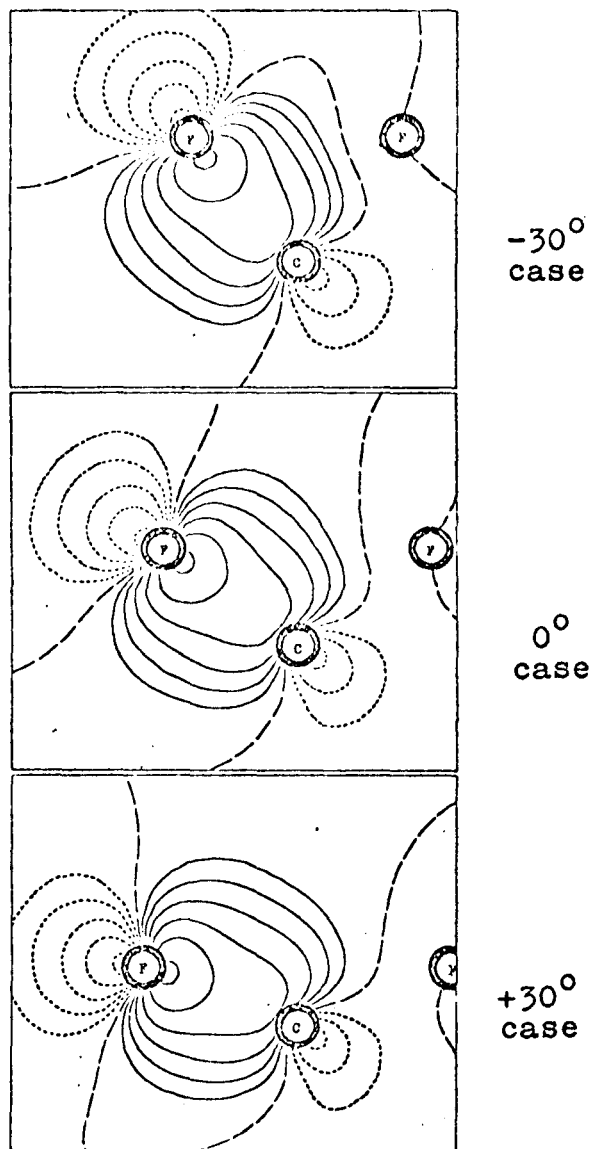


Figure 6. Orbital amplitude plots of the C-F bonding LMO for the equilibrium and two distorted geometries of difluoromethane. The plots are in the F-C-F plane. For contour values, see Figure 1.

bending.

There is the possibility that part of the noted effect is due to the orthogonality restriction rather than to "real" changes in the LMO's. To test this, we have carried out the hybrid analysis of the NLO's (see equation XXIV), which are partially corrected for orthogonality delocalization. Table 5 gives the results, and we see that the conclusions drawn above apply equally well here.

Table 5. Geometry Variation of Difluoromethane:  
Hybrid analysis of NLO's.

Parameter <sup>a</sup>	Value		
	+30° case	0° case	-30° case <sup>b</sup>
$\theta_{C^*F, C^*F}$	96.6°	104.0°	106.9°
$\theta_{C^*F, C^*F}^{\text{inner}}$	111.8°	104.6°	97.8°
$\theta_{C^*F, C^*F}^{\text{outer}}$	53.4°	101.8°	130.0°
$\theta_{C^*H, C^*H}$	112.6°	112.6°	113.6°
$\theta_{C^*H, C^*H}^{\text{inner}}$	115.0°	114.3°	115.4°
$\theta_{C^*H, C^*H}^{\text{outer}}$	109.3°	110.0°	110.9°
$\theta_{LP-o, LP-o}$	115.8°	115.0°	112.7° (113.1°)
$\theta_{LP-o, LP-i}$	113.3°	113.2°	115.5° (115.2°)
$\theta_{LP-o, CF^*}$	104.5°	104.3°	101.5° (106.2°)
$\theta_{LP-i, CF^*}$	103.8°	105.5°	107.8° (99.0°)
$\phi$	9.2°	1.6°	-7.7° (-6.4°)
$n_{C^*F}$	1.14	1.39	1.52 ( 1.53 )
$n_{C^*H}$	1.02	0.92	0.88
$n_{CF^*}$	4.40	4.39	4.56 ( 4.47 )
$n_{LP-i}$	2.16	2.09	2.34 ( 1.80 )
$n_{LP-o}$	2.02	2.00	1.89 ( 2.16 )

<sup>a</sup>See text for a description of the parameters.

<sup>b</sup>The values in parentheses are those unique to  $F_2$ , whose lone pairs eclipse the carbon bonds. All other values involving fluorine refer to  $F_1$ , which has the normal staggered configuration.

### C. Approximate Generalized-Valence-Bond (GVB) Orbitals

In the previous section, we drew certain conclusions about the electronic structure of difluoromethane from an analysis of the localized Hartree-Fock (HF) orbitals. These conclusions rest upon the assumption that the LMO's are meaningful, but even though they provide a description of this and other molecules which is intuitively correct, we must realize that they are not unique in their representation of the total wavefunction. The localization criterion does not relate to any physical observable, and we must thus question whether an analysis of LMO's can ever lead to "real" conclusions. In order to develop a criterion which is physically meaningful, we must consider the relationship between the HF method and other, more general techniques.

The Generalized Valence-Bond (GVB) method, recently developed by Goddard and co-workers (32), provides us with the necessary generality. In contrast to the HF method, in which each electron pair is described as a doubly-occupied (molecular) orbital of the form

$$\psi_{\text{pair}}^{\text{HF}}(i, j) = \phi(i) \phi(j) [\alpha(i) \beta(j) - \beta(i) \alpha(j)] \quad (\text{XXV})$$

the GVB approach assumes each pair to be a valence-bond type of singlet pairfunction:

$$\psi_{\text{pair}}^{\text{GVB}}(i, j) = [\chi_a(i) \chi_b(j) + \chi_b(i) \chi_a(j)] \times [\alpha(i) \beta(j) - \beta(i) \alpha(j)] \quad (\text{XXVI})$$

In either method, the 2N-electron closed-shell wavefunction is taken to be the normalized, antisymmetrized product of N pairfunctions, with the assumption that the orbitals of each pair are orthogonal to the orbitals of every other pair (this is a constraint in the GVB method but not in the HF approach), and in either case, the orbitals of all pairs are variationally optimized. We see that setting  $\chi_a = \chi_b$  in (XXVI) gives the GVB pairfunction the same form as the HF one in (XXV), and thus the GVB method may be viewed as an extension of the HF technique. The optimum GVB pairfunctions turn out to be localized bonding pairs, core pairs and lone pairs, so the GVB method, in addition to giving energies lower than HF, gives an intuitively pleasing description of molecular electronics. We should emphasize, though, that this localization is not a result of any arbitrary scheme; it is a result of the variational principle.

Hurley et al. (33) have shown that a pairfunction of the type in equation (XXVI) may be written as a two-electron CI wavefunction whose component configurations are doubly-occupied, orthogonal orbitals called natural orbitals (NO's):

$$\psi_{\text{pair}}^{\text{GVB}}(i, j) = [c_1 \phi(i) \phi(j) + c_2 \phi'(i) \phi'(j)] \times [\alpha(i) \beta(j) - \beta(i) \alpha(j)] \quad (\text{XXVII})$$

where

$$\begin{aligned}
 \phi &= \text{first natural orbital} \\
 &= (\chi_a + \chi_b)/(2 + 2S)^{\frac{1}{2}} \quad (S = \langle \chi_a | \chi_b \rangle, \text{ assumed} \\
 &\quad \text{positive}) \\
 \phi' &= \text{second natural orbital} \\
 &= (\chi_a - \chi_b)/(2 - 2S)^{\frac{1}{2}} \\
 c_1 &= (S + 1)/(2 + 2S^2)^{\frac{1}{2}} \\
 c_2 &= (S - 1)/(2 + 2S^2)^{\frac{1}{2}} \\
 \langle \phi | \phi' \rangle &= 0 \\
 c_1^2 + c_2^2 &= 1
 \end{aligned} \tag{XXVIII}$$

With the GVB wavefunction expressed in terms of NO's, it is possible to derive equations (32a) for self-consistently optimizing the orbitals and CI coefficients. These are roughly analogous to the HF equations, except that each NO has a different hamiltonian, and of course, HF involves no CI coefficients.

Now, in the event that all pairs in the molecule are strongly overlapping ( $S$  close to unity), we see from (XXVIII) that  $c_1$  will be much larger than  $c_2$  for each pair, and thus the set of first NO's will dominate the total wavefunction. We expect this to be the case for typical molecules near the equilibrium geometry, and in view of the fact that the Hartree-Fock configuration is the major contributor to general CI wavefunctions in such cases (32b, 34), it is reasonable to assume that the set of first NO's will correspond closely to a set of transformed HF orbitals. But these first NO's, like the GVB orbitals

which define them, are localized into bonds, cores and lone pairs, and it should be possible to relate them to localized Hartree-Fock orbitals, orbitals with the conceptual advantages of the LMO's but which are defined by a physically meaningful criterion.

We see from the above that it should not be a severe restriction to constrain the set of first NO's to span the Hartree-Fock space of functions. This constraint, together with the normal GVB assumption, forms the basis for what we will call the Hartree-Fock projected GVB (PGVB) method. The optimum first NO's in the PGVB wavefunction are naturally localized molecular orbitals (NLMO's). They should be good approximations to the corresponding GVB NO's, and within the PGVB context, they have a well-defined physical meaning.

In principle, then, we see that meaningful localized HF orbitals can be defined. There are several practical difficulties which render the exact NLMO's in difluoromethane unattainable for the present, but we have developed an approximate approach which we describe below. The most serious problem relates to the fact that, in any GVB-like method, each NO has its own hamiltonian (32a), so for a  $2N$  electron system,  $2N$  separate hamiltonians must be generated and diagonalized. In the HF method, only one is needed, and because hamiltonian formation and diagonalization is the most time-consuming part of such SCF calculations, a full GVB (or PGVB) solution would require about  $2N$  times as much work as the corresponding HF calculation. Difluoromethane has 26 electrons,

so it is clear that a complete treatment using GVB or PGVB techniques would be far too costly. We may simplify the problem somewhat by neglecting the three core pairs (35), but we are still left with 20 valence electrons, too many for a full analysis. To surmount this problem, we have developed a method of optimizing just one PGVB pair at a time, and we have assumed that the orbitals thus obtained are quite similar to those which would result from a more complete treatment. The accuracy of this assumption is difficult to assess because no direct comparison of full versus partial GVB calculations has appeared in the literature. Goddard and co-workers (37) have used the working assumption that one can concentrate on only a few pairs, leaving the others doubly occupied in the HF sense, and they have obtained reasonable results for a variety of molecules. We have certain results for difluoromethane which suggest that our assumption is a good one, at least for bonding orbitals, and we shall discuss these a bit later.

We now develop the PGVB method for splitting one pair, starting from the Hartree-Fock solution. We begin by writing our wavefunction in the form

$$\psi = A[(c_1 \phi_1 \bar{\phi}_1 + c_2 \phi_1' \bar{\phi}_1') \phi_2 \bar{\phi}_2 \phi_3 \bar{\phi}_3 \cdots \phi_N \bar{\phi}_N] \quad (\text{XXIX})$$

We assume that the  $\phi$ 's together with  $\phi_1'$  form an orthonormal set, and we use  $A$  to represent the normalized antisymmetrizer. We also indicate the spin associated with a particular orbital by an overscore,

"-" ( $\beta$  spin), or lack thereof ( $\alpha$  spin). The first pair in (XXIX) is split into a first NO ( $\phi_1$ ) and a second NO ( $\phi_1'$ ), while all other pairs ( $\phi_2, \phi_3, \dots, \phi_N$ ) are doubly occupied in the Hartree-Fock sense. The PGVB assumptions in this case are simply that  $\phi_1, \dots, \phi_N$  are related by an orthogonal transformation ( $\underline{T}$ ) to the canonical HF orbitals, which we call  $o_1, \dots, o_N$ , while  $\phi_1'$  can be written as a normalized linear combination of the canonical virtuals, which we call  $v_1, \dots, v_M$  ( $N + M =$  number of basis functions). That is,

$$\phi_i = \sum_{j=1}^N o_j T_{ji} \quad (i = 1, \dots, N; \underline{T} \text{ orthogonal})$$

and

$$\phi_1' = \sum_{j=1}^M b_j v_j \quad \left( \sum_{i=1}^M b_i^2 = 1 \right) \quad (\text{XXX})$$

In the subsequent development, it will not be necessary to consider the full  $\underline{T}$  matrix, and we find it convenient to express  $\phi_1$  as a normalized linear combination of the  $o_i$ 's without explicitly expanding  $\phi_2, \dots, \phi_N$ :

$$\phi_1 = \sum_{j=1}^N a_j o_j \quad \left( \sum_{i=1}^N a_i^2 = 1 \right) \quad (\text{XXXI})$$

Now, we rewrite  $\psi$  as

$$\begin{aligned} \psi &= c_1 A[\phi_1 \bar{\phi}_1 \phi_2 \bar{\phi}_2 \dots \phi_N \bar{\phi}_N] + c_2 A[\phi_1' \bar{\phi}_1' \phi_2 \bar{\phi}_2 \dots \phi_N \bar{\phi}_N] \\ &= c_1 \psi_1 + c_2 \psi_2 \end{aligned} \quad (\text{XXXII})$$

where  $\psi_1$  and  $\psi_2$  are two normalized, mutually orthogonal configurations. The energy of  $\psi$  may be evaluated in the usual way to give

$$\begin{aligned} E &= \langle \psi | \hat{\mathcal{H}} | \psi \rangle = (c_1^2 H_{11} + 2 c_1 c_2 H_{12} + c_2^2 H_{22}) / (c_1^2 + c_2^2) \\ &= H_{11} + [2 c_1 c_2 H_{12} + c_2^2 (H_{22} - H_{11})] / (c_1^2 + c_2^2) \\ &= H_{11} + (2 c_1 c_2 A + c_2^2 B) / (c_1^2 + c_2^2) \end{aligned} \quad (\text{XXXIII})$$

where

$$\begin{aligned} H_{11} &= \langle \psi_1 | \hat{\mathcal{H}} | \psi_1 \rangle \\ H_{22} &= \langle \psi_2 | \hat{\mathcal{H}} | \psi_2 \rangle \\ H_{12} &= \langle \psi_1 | \hat{\mathcal{H}} | \psi_2 \rangle = \langle \psi_2 | \hat{\mathcal{H}} | \psi_1 \rangle \end{aligned} \quad (\text{XXXIV})$$

and where

$$A = H_{12} \quad \text{and} \quad B = H_{22} - H_{11} \quad (\text{XXXV})$$

We have assumed here that  $\psi_1$ ,  $\psi_2$ ,  $c_1$  and  $c_2$  are all real quantities. Now,  $H_{11}$  is just the Hartree-Fock energy because the  $\phi$ 's are just transformed HF orbitals, and such transformations do not influence the total energy of the HF wavefunction ( $\psi_1$ ). Thus, we obtain for the CI energy lowering ( $\Delta E$ ) beyond the HF energy,

$$\Delta E = E - H_{11} = (2 c_1 c_2 A + c_2^2 B) / (c_1^2 + c_2^2) \quad (\text{XXXVI})$$

We now seek to eliminate  $c_1$  and  $c_2$  by minimizing  $\Delta E$  with respect to them. We have the two conditions

$$\partial\Delta E/\partial c_1 = 0 \quad \text{and} \quad \partial\Delta E/\partial c_2 = 0 \quad (\text{XXXVII})$$

which, using (XXXVI), yield two equations;

$$c_2A - c_1(\Delta E) = 0 \quad (\text{XXXVIII})$$

and

$$c_1A + c_2B - c_2(\Delta E) = 0$$

These may be written in matrix form as

$$\begin{pmatrix} -\Delta E & A \\ A & (B-\Delta E) \end{pmatrix} \begin{pmatrix} c_1 \\ c_2 \end{pmatrix} = \begin{pmatrix} 0 \\ 0 \end{pmatrix} \quad (\text{XXXIX})$$

which implies that, because  $c_1$  and  $c_2$  cannot both be zero, the determinant of the above matrix must be zero. Thus

$$(\Delta E)^2 - B(\Delta E) - A^2 = 0 \quad (\text{XL})$$

or

$$\Delta E = \frac{1}{2}B \pm \frac{1}{2}(B^2 + 4A^2)^{\frac{1}{2}} \quad (\text{XLI})$$

and so, taking the negative root to give the most negative value for  $\Delta E$ , we have

$$\Delta E = \frac{1}{2}B - \frac{1}{2}(B^2 + 4A^2)^{\frac{1}{2}} \quad (\text{XLII})$$

This is the basic energy expression from which we shall work.

It has the advantage that it does not involve the CI coefficients  $c_1$  and  $c_2$ , and the disadvantage that it is not a linear expression in A and B.

The latter adds only a slight amount of complexity to the optimization of  $\phi_1$  and  $\phi_1'$ .

Now, in order to optimize the two NO's, we must consider the derivative of  $\Delta E$  with respect to the expansion coefficients  $b_i$  ( $i = 1, \dots, M$ ) and  $a_i$  ( $i = 1, \dots, N$ ) of equations (XXX) and (XXXI). If  $X$  represents any variable upon which  $A$  and  $B$  depend, we have, from (XLII):

$$\begin{aligned}\partial \Delta E / \partial X &= \frac{1}{2} (\partial B / \partial X) - \frac{1}{4} (B^2 + 4A^2)^{-\frac{1}{2}} [2B(\partial B / \partial X) + 8A(\partial A / \partial X)] \\ &= k_1 (\partial B / \partial X) + k_2 (\partial A / \partial X)\end{aligned}\quad (\text{XLIII})$$

where it can be shown that

$$\begin{aligned}k_1 &= -\Delta E (B^2 + 4A^2)^{-\frac{1}{2}} = \Delta E / (2\Delta E - B) \\ k_2 &= -2A (B^2 + 4A^2)^{-\frac{1}{2}} = 2A / (2\Delta E - B)\end{aligned}\quad (\text{XLIV})$$

We shall use these equations in a moment, but while we are at this point, we will write down the formula for the second derivative of  $\Delta E$  with respect to two variables,  $X$  and  $Y$ , upon which  $A$  and  $B$  depend. We will require these in the subsequent discussion of the quadratically convergent approach to the PGVB solution. Differentiating (XLIII) with respect to  $Y$  gives a rather complicated expression which may be simplified by the substitution of various identities derived from (XLII) and (XLIV). There are several alternative forms for the simplified equation, and we have chosen the following:

$$\begin{aligned}
\partial^2(\Delta E)/\partial X \partial Y &= k_1(\partial^2 B/\partial X \partial Y) + k_2(\partial^2 A/\partial X \partial Y) \\
&+ k_3(\partial A/\partial Y)(\partial A/\partial X) \\
&+ k_4[(\partial A/\partial Y)(\partial \Delta E/\partial X) + (\partial \Delta E/\partial Y)(\partial A/\partial X)] \\
&+ k_5(\partial \Delta E/\partial Y)(\partial \Delta E/\partial X)
\end{aligned}$$

where  $k_1$  and  $k_2$  are as in (XLIV) and

$$k_3 = 2k_1/\Delta E, \quad k_4 = -A k_3/\Delta E \quad \text{and} \quad k_5 = -A k_4/\Delta E \quad (\text{XLVI})$$

Now, in order to evaluate the derivatives of  $\Delta E$  with respect to the expansion coefficients of (XXX) and (XXXI), we must consider the explicit form of the quantities  $A$  and  $B$ . Using the properties of the antisymmetrizer  $A$  (37), it can be shown that

$$A = \langle \phi_1 \bar{\phi}_1 \phi_2 \bar{\phi}_2 \phi_3 \bar{\phi}_3 \cdots | \hat{\mathcal{C}} | P(\phi_1' \bar{\phi}_1' \phi_2 \bar{\phi}_2 \phi_3 \bar{\phi}_3 \cdots) \rangle \quad (\text{XLVII})$$

where  $P = [(2N)!]^{1/2} A$  is the "ordinary" (unnormalized) anti-symmetrizer. We note that because the hamiltonian contains, at most, two-electron operators, any permutation in  $P$  other than the interchange of  $\phi_1'$  and  $\bar{\phi}_1'$  will give a term which does not contribute to  $A$ . Indeed, any such permutation will leave more than two orbitals in the right-hand side of the integral orthogonal to their left-hand side counterparts, and we will thus always be able to separate out a term which is zero due to this orthogonality. Furthermore, the  $(\phi_1', \bar{\phi}_1')$  interchange gives zero due to spin orthogonality. Thus, only the "unit" permutation in  $P$  needs be considered. Because of the

orthogonality of  $\phi_1$  and  $\phi_1'$ , only the operator in  $\hat{\mathcal{K}}$  which couples electrons 1 and 2 will give a nonzero contribution, and this term is simply  $1/r_{12}$ . Thus we have

$$\begin{aligned}
 A &= \langle \phi_1 \bar{\phi}_1 | 1/r_{12} | \phi_1' \bar{\phi}_1' \rangle \langle \phi_2 | \phi_2 \rangle \langle \bar{\phi}_2 | \bar{\phi}_2 \rangle \langle \phi_3 | \phi_3 \rangle \langle \bar{\phi}_3 | \bar{\phi}_3 \rangle \cdots \\
 &= \langle \phi_1 \phi_1 | 1/r_{12} | \phi_1' \phi_1' \rangle \langle \alpha | \alpha \rangle \langle \beta | \beta \rangle (1)(1)(1)(1) \cdots \\
 &= \langle \phi_1 \phi_1 | 1/r_{12} | \phi_1' \phi_1' \rangle \quad \quad \quad \text{(XLVIII)} \\
 &= \iint \phi_1^*(1) \phi_1^*(2) \phi_1'(1) \phi_1'(2) / r_{12} \, d\tau_1 \, d\tau_2
 \end{aligned}$$

This is similar to the exchange integral

$$\mathbf{K}_{\phi_1 \phi_1'} = \text{"K}_{1,1'}" = \iint \phi_1^*(1) \phi_1(2) \phi_1'^*(1) \phi_1'(2) / r_{12} \, d\tau_1 \, d\tau_2 \quad \quad \quad \text{(XLIX)}$$

except for the position of the complex conjugation. But we have assumed that  $\phi_1$  and  $\phi_1'$  are real, and thus the two are identical, so we have

$$A = K_{1,1'} \quad \quad \quad \text{(L)}$$

The evaluation of the B term is somewhat more complex. It is the difference in energy of two Hartree-Fock-like wavefunctions which differ in only one orbital, the first. The energy  $H_{1,1}$  of  $\psi_1$  is given by

$$H_{1,1} = 2 \sum_{i=1}^N h_{ii} + \sum_{i=1}^N \sum_{j=1}^N (2J_{ij} - K_{ij}) \quad \quad \quad \text{(LI)}$$

where  $h_{ii}$  is the expectation value of the one-electron portion of  $\hat{\mathcal{H}}$  for  $\phi_i$  and where  $J_{ij}$  and  $K_{ij}$  are the usual coulomb and exchange integrals. The analogous expression for  $H_{22}$  contains many identical terms, the only differences occurring in the values which involve  $\phi'_1$ . Thus, the difference  $H_{22} - H_{11}$  will give cancellation for all terms not related to  $\phi_1$  and  $\phi'_1$ , and we obtain

$$B = H_{22} - H_{11} = 2h_{1'1'} - 2h_{11} + J_{1'1'} - J_{11} + 2 \sum_{i=2}^N [(2J_{1'i} - K_{1'i}) - (2J_{1i} - K_{1i})] \quad (\text{LII})$$

The summation runs from 2 to N, but by adding and subtracting the analogous term for  $i = 1$ , we may complete the range, obtaining

$$B = 2h_{1'1'} - 2h_{11} + J_{1'1} - J_{11} - 4J_{1'1} + 2K_{1'1} + 4J_{11} - 2K_{11} + 2 \sum_{i=1}^N (2J_{1'i} - K_{1'i} - 2J_{1i} + K_{1i}) \quad (\text{LIII})$$

or, combining like terms and recalling that  $J_{ii} = K_{ii}$ ,

$$B = 2h_{1'1'} - 2h_{11} + J_{1'1'} + J_{11} - 4J_{1'1} + 2K_{1'1} + 2 \sum_{i=1}^N (2J_{1'i} - K_{1'i} - 2J_{1i} + K_{1i}) \quad (\text{LIV})$$

We now make use of the identities

$$\begin{aligned}
h_{1'1'} &= \langle \phi_1' | \hat{h} | \phi_1' \rangle & h_{11} &= \langle \phi_1 | \hat{h} | \phi_1 \rangle \\
J_{1'1} &= \langle \phi_1' | \hat{J}_1 | \phi_1' \rangle & J_{11} &= \langle \phi_1 | \hat{J}_1 | \phi_1 \rangle \\
K_{1'1} &= \langle \phi_1' | \hat{K}_1 | \phi_1' \rangle & K_{11} &= \langle \phi_1 | \hat{K}_1 | \phi_1 \rangle
\end{aligned} \tag{LV}$$

where  $\hat{h}$  is the one-electron portion of  $\hat{\mathcal{K}}$  and where  $\hat{J}_1$  and  $\hat{K}_1$  are the coulomb and exchange operators for  $\phi_1$ . Substituting these into the expression for B and combining terms, we have

$$\begin{aligned}
B &= 2 \langle \phi_1' | \hat{h} + \sum_{i=1}^N (2\hat{J}_i - \hat{K}_i) | \phi_1' \rangle \\
&\quad - 2 \langle \phi_1 | \hat{h} + \sum_{i=1}^N (2\hat{J}_i - \hat{K}_i) | \phi_1 \rangle \\
&\quad + J_{11} + J_{1'1'} - 4J_{1'1} + 2K_{1'1}
\end{aligned} \tag{LVI}$$

But the operator within the brackets is simply the Hartree-Fock operator ( $\hat{F}$ ) defined by  $\phi_1, \dots, \phi_N$ . Thus,

$$B = 2F_{1'1'} - 2F_{11} + J_{11} + J_{1'1'} - 4J_{1'1} + 2K_{1'1} \tag{LVII}$$

The usefulness of this expression is apparent when we consider that it depends only on orbitals  $\phi_1$  and  $\phi_1'$ . If we had considered a more general form for the orbitals in the CI wavefunction of equation (XXIX), then B would contain terms depending upon  $\phi_2, \dots, \phi_N$ . These orbitals are included, above, but only in an implicit sense through the operator  $\hat{F}$ , which is invariant to transformations among  $\phi_1, \dots, \phi_N$ .

We are now in a position to derive the necessary conditions for optimum  $\phi_1$  and  $\phi'_1$ . We recall the expansions (XXX) and (XXXI):

$$\phi_1 = \sum_{i=1}^N a_i o_i \quad (\underline{a} \text{ normalized})$$

$$\phi'_1 = \sum_{i=1}^M b_i v_i \quad (\underline{b} \text{ normalized})$$

where the  $o_i$ 's are the canonical, occupied Hartree-Fock orbitals and the  $v_i$ 's are the canonical virtuals. The CI energy lowering depends upon  $\underline{a}$  and  $\underline{b}$  through  $\phi_1$  and  $\phi'_1$  and thus, the conditions necessary for a minimum  $\Delta E$  are:

$$\partial(\Delta E)/\partial a_i - 2\lambda_a a_i = 0 \quad i = 1, \dots, N \quad (\text{LVIII})$$

and 
$$\partial(\Delta E)/\partial b_i - 2\lambda_b b_i = 0 \quad i = 1, \dots, M$$

where the Lagrange multipliers  $\lambda_a$  and  $\lambda_b$  result from the two restrictions

$$R_a = \sum_{i=1}^N a_i^2 - 1 = 0 \quad (\text{LIX})$$

and 
$$R_b = \sum_{i=1}^M b_i^2 - 1 = 0$$

We have given, in equation (XLIII), the expression for the derivative of  $\Delta E$  in terms of A and B derivatives. We may expand (L) to give an expression for A which depends only on  $\underline{a}$ ,  $\underline{b}$  and integrals over the

$o_i$ 's and  $v_i$ 's, and differentiation of this expression gives

$$\begin{aligned}\partial A/\partial a_i &= 2 \sum_{j=1}^N \langle o_i | K_1' | o_j \rangle a_j = 2 \sum_{j=1}^M K_{ij}^{1', o} a_j = 2(\underline{\widehat{K}}^{1', o} \underline{a})_i \\ \partial A/\partial b_i &= 2 \sum_{j=1}^M \langle v_i | K_1 | v_j \rangle b_j = 2 \sum_{j=1}^M K_{ij}^{1, v} b_j = 2(\underline{\widehat{K}}^{1, v} \underline{b})_i\end{aligned}\tag{LX}$$

Here,  $\underline{\widehat{K}}^{1', o}$  is the exchange matrix for  $\phi_1'$  defined over the occupied orbitals and  $\underline{\widehat{K}}^{1, v}$  is the exchange matrix for  $\phi_1$  defined over the virtuals. We may similarly expand (LVII) and differentiate it, which gives, for the derivatives of B,

$$\begin{aligned}\partial B/\partial a_i &= (-4 \underline{\widehat{F}}^o \underline{a} + 4 \underline{\widehat{J}}^{1, o} \underline{a} - 8 \underline{\widehat{J}}^{1', o} \underline{a} + 4 \underline{\widehat{K}}^{1', o} \underline{a})_i \\ \partial B/\partial b_i &= (4 \underline{\widehat{F}}^v \underline{b} + 4 \underline{\widehat{J}}^{1', v} \underline{b} - 8 \underline{\widehat{J}}^{1, v} \underline{b} + 4 \underline{\widehat{K}}^{1, v} \underline{b})_i\end{aligned}\tag{LXI}$$

where each  $\underline{\widehat{J}}$  indicates a coulomb matrix for either  $\phi_1$  or  $\phi_1'$  (superscripts 1 and 1', respectively) defined over either the occupied or virtual orbitals (superscripts o and v, respectively). The  $\underline{\widehat{F}}^o$  matrix is the Hartree-Fock matrix defined over the occupied orbitals and  $\underline{\widehat{F}}^v$  is the same thing, but defined over the virtuals. These  $\underline{\widehat{F}}$  matrices are diagonal because we have used the canonical occupied and virtual Hartree-Fock orbitals as the bases for expanding  $\phi_1$  and  $\phi_1'$ .

We now have all the information needed to set up the matrix equations which must be satisfied if  $\phi_1$  and  $\phi_1'$  are optimum.

Combining (LX) and (LXI) with (XLIII) gives us the derivatives of  $\Delta E$  we need in (LXIII), which becomes:

$$\widehat{H}_a \underline{a} = 2\lambda_a \underline{a} \quad (\text{LXII})$$

$$\widehat{H}_b \underline{b} = 2\lambda_b \underline{b}$$

where

$$\widehat{H}_a = k_1(-4\widehat{F}^O + 4\widehat{J}^{1,O} - 8\widehat{J}^{1',O}) + (4k_1 + 2k_2)\widehat{K}^{1',O} \quad (\text{LXIII})$$

$$\widehat{H}_b = k_1(4\widehat{F}^V - 8\widehat{J}^{1,V} + 4\widehat{J}^{1',V}) + (4k_1 + 2k_2)\widehat{K}^{1,V}$$

In practice, we have found it convenient to divide both sides of equations (LXII) by  $4k_1$ , which gives us equations of the same form but with new hamiltonians  $\widehat{H}'_a$  and  $\widehat{H}'_b$  defined by

$$\widehat{H}'_a = (1/4k_1)\widehat{H}_a = -\widehat{F}^O + \widehat{J}^{1,O} - 2\widehat{J}^{1',O} + (1 + A/\Delta E)\widehat{K}^{1',O} \quad (\text{LXIV})$$

$$\widehat{H}'_b = (1/4k_1)\widehat{H}_b = \widehat{F}^V - 2\widehat{J}^{1,V} + \widehat{J}^{1',V} + (1 + A/\Delta E)\widehat{K}^{1,V}$$

where we have used the relation, derived from (XLIV), that  $k_2/2k_1 = A/\Delta E$ . Thus we see that the condition for an energy minimum is that  $\underline{a}$  and  $\underline{b}$  be eigenvectors of their respective hamiltonians.

These eigenvalue equations can be used in the usual way to define a method of solving for the optimum  $\underline{a}$  and  $\underline{b}$  self-consistently. We begin by choosing starting guesses for  $\underline{a}$  and  $\underline{b}$ , forming the two hamiltonians according to (LXIV) and diagonalizing them to obtain the eigenvectors. The eigenvector of  $\widehat{H}'_a$  which has the highest overlap

with a is chosen as the new guess for a, and a new b is similarly obtained. These eigenvectors have proven to be the ones with lowest eigenvalues in all cases we have considered. The new guesses for a and b are then used to generate new hamiltonians and the process is continued until the vectors do not change significantly from one cycle to the next, that is, until self-consistency is reached.

It is fortunate that this procedure does not always converge to the best  $\phi_1$  and  $\phi'_1$ . If this were the case, then the solution would always correspond to splitting the pair which gives the best CI energy lowering, which in most cases would be a core pair. We have found that, if the starting vectors are properly chosen, the method will converge upon a local minimum corresponding to the splitting of some other pair. Thus it is possible to use this method to investigate several pairs in the same molecule as long as starting guesses are used which are reasonable approximations to the local solutions.

The above method shows the linear convergence (38) typical of SCF methods based on this type of linear matrix equation. Convergence may be hastened by the use of various extrapolation techniques (39) but it can still be fairly slow. In order to speed the optimization of the orbitals, we have developed a quadratically convergent approach (40) which takes into account the second-order changes in the energy with respect to the  $a_i$ 's and  $b_i$ 's while applying the constraints to these variables to second order. The quadratic method is not only faster than the linear method, but also more informative, because it can distinguish between solutions which are true local minima and those which correspond to

maxima or "saddle-points". This is important because the linear equations could, in principle, converge to such non-minimum stationary points without any indication.

The first step involves obtaining the second derivatives of  $\Delta E$  with respect to the  $a_i$ 's and  $b_i$ 's. Examining equation (XLV), we see that to obtain these, we must evaluate the corresponding second derivatives of A and B, along with the first derivatives of A and  $\Delta E$ . These first-derivative terms have already been considered, above, and the second-derivative terms may be obtained by the expansion (L) and (LVII) as functions of  $\underline{a}$  and  $\underline{b}$  followed by differentiation of the resulting expressions. After quite a bit of involved manipulation, we obtain:

$$\begin{aligned} \partial^2(\Delta E)/\partial a_m \partial a_n &= (\underline{H}_a)_{mn} + 8k_1(\underline{K}^1, 0)_{mn} + k_3 p_m p_n \\ &+ k_4(p_m q_n + q_m p_n) + k_5 q_m q_n \\ \partial^2(\Delta E)/\partial b_m \partial b_n &= (\underline{H}_b)_{mn} + 8k_1(\underline{K}^1, v)_{mn} + k_3 r_m r_n \\ &+ k_4(r_m s_n + s_m r_n) + k_5 s_m s_n \end{aligned} \quad (\text{LXV})$$

$$\begin{aligned} \partial^2(\Delta E)/\partial a_m \partial b_n &= 4k_1[o_m \phi_1 | v_n \phi_1'] + (4k_1 + 2k_2)[o_m v_n | \phi_1 \phi_1'] \\ &+ (4k_1 + 2k_2)[o_m \phi_1' | v_n \phi_1] + k_3 p_m r_n \\ &+ k_4(p_m s_n + q_m r_n) + k_5 q_m s_n \end{aligned}$$

where, in the third expression, we have used the symbol for the two-

electron integrals defined following equation (V). All of the matrices above have been defined except  $\underline{\tilde{K}}^{1,0}$ , which is the exchange matrix for  $\phi_1$  defined over the occupied orbitals, and  $\underline{\tilde{K}}^{1,v}$ , the exchange matrix for  $\phi_1'$  defined over the virtuals. The vectors  $\underline{p}$ ,  $\underline{q}$ ,  $\underline{r}$  and  $\underline{s}$  are defined by

$$\begin{aligned} p_i &= \partial A / \partial a_i = (\underline{\tilde{K}}^{1,0} \underline{a})_i & q_i &= (\partial E) / \partial a_i = (\underline{H}_a \underline{a})_i \\ r_i &= \partial A / \partial b_i = (\underline{\tilde{K}}^{1,v} \underline{b})_i & s_i &= (\partial E) / \partial b_i = (\underline{H}_b \underline{b})_i \end{aligned} \quad (\text{LXVI})$$

and the values of  $k_1$  to  $k_5$  have been given in equations (XLIV) and (XLVI).

Now, the derivatives of equations (LXV) together with the vectors  $\underline{q}$  and  $\underline{s}$  give us a complete description of the local quadratic behavior of  $E$  about the "point" defined by  $\underline{a}$  and  $\underline{b}$ , the best current guesses for the coefficients of the first and second NO's. We could solve directly for the new "point" representing the local minimum (or other stationary point) of this quadratic function, thus obtaining new guesses for  $\underline{a}$  and  $\underline{b}$ . The solution is not that easy, though, because the variation of  $\underline{a}$  and  $\underline{b}$  cannot be perfectly general: they must both remain normalized according to the restrictions in equations (LIX), and the straightforward solution suggested above will not account for this restriction. We must thus isolate the actual degrees of freedom in  $\underline{a}$  and  $\underline{b}$ , and we must carry out the solution using these proper variables.

Various methods of isolating the proper variables may be used, and we have chosen the following. The restriction on a is

$$\sum_{i=1}^N a_i^2 = 1 \quad (\text{LXVII})$$

which means that any particular a element, say  $a_k$ , may be considered a dependent variable, related to the remaining a elements via

$$a_k^2 = 1 - \sum_{\substack{i=1 \\ (i \neq k)}}^N a_i^2 \quad (\text{LXVIII})$$

Thus, the proper variables are  $a_1, a_2, \dots, a_{k-1}, a_{k+1}, \dots, a_N$ , while  $a_k$  may be obtained (to within a sign - see below) from them. The elements of b may be similarly treated, leaving us with  $N+M-2$  proper variables in all. For definiteness, we shall take  $a_1$  and  $b_1$  as the dependent variables, though it does not matter which we pick and the equations below are easily generalized to other choices. We shall distinguish the set of proper variables from the improper set by giving the former the superscript "p". We have:

$$\begin{aligned} a_1 &= \pm \left[ 1 - \sum_{i=2}^N (a_i^p)^2 \right]^{\frac{1}{2}} & a_i &= a_i^p \quad (i = 2, \dots, N) \\ b_1 &= \pm \left[ 1 - \sum_{i=2}^M (b_i^p)^2 \right]^{\frac{1}{2}} & b_i &= b_i^p \quad (i = 2, \dots, M) \end{aligned} \quad (\text{LXIX})$$

We have considered  $\Delta E$  as a function of  $\underline{a}$  and  $\underline{b}$ , which in turn are functions of " $\underline{a}^p$ " and " $\underline{b}^p$ ". To obtain the needed derivatives with respect to these proper variables, we apply the usual techniques (41) of differential calculus relating to the differentiation of composite functions. We thus obtain

$$\begin{aligned} \partial(\Delta E)/\partial a_i^p &= \sum_{j=1}^N [\partial(\Delta E)/\partial a_j] (\partial a_j / \partial a_i^p) \\ &+ \sum_{j=1}^M [\partial(\Delta E)/\partial b_j] (\partial b_j / \partial a_i^p) \end{aligned} \quad (\text{LXX})$$

The second summation, above, vanishes because  $\underline{b}$  is independent of the  $a_i^p$ 's, and the first summation is simplified by the substitution of the expression, derived from (LXIX):

$$\partial a_j / \partial a_i^p = \begin{cases} \delta_{ij}, & j \neq 1 \\ -a_i/a_1, & j = 1 \end{cases} \quad (\text{LXXI})$$

We find, making this substitution,

$$\partial(\Delta E)/\partial a_i^p = \partial(\Delta E)/\partial a_i - (a_i/a_1) \partial(\Delta E)/\partial a_1 \quad (\text{LXXII})$$

Similarly, we may derive

$$\partial(\Delta E)/\partial b_i^p = \partial(\Delta E)/\partial b_i - (b_i/b_1) \partial(\Delta E)/\partial b_1 \quad (\text{LXXIII})$$

The above expressions for the proper first derivatives may be differentiated again using the same procedure. We will not give the

details, but the resulting formulas for the proper second derivatives are:

$$\begin{aligned}
\partial^2(\Delta E)/\partial a_i^p \partial a_j^p &= \partial^2(\Delta E)/\partial a_i \partial a_j - (a_j/a_1)[\partial^2(\Delta E)/\partial a_1 \partial a_i] \\
&\quad - (a_i/a_1)[\partial^2(\Delta E)/\partial a_1 \partial a_j] \\
&\quad + (a_i a_j/a_1^2)[\partial^2(\Delta E)/\partial a_1 \partial a_1] \\
&\quad - (a_i a_j/a_1^3 + \delta_{ij}/a_1^2)[\partial(\Delta E)/\partial a_1] \\
\partial^2(\Delta E)/\partial b_i^p \partial b_j^p &= \partial^2(\Delta E)/\partial b_i \partial b_j - (b_j/b_1)[\partial^2(\Delta E)/\partial b_i \partial b_1] \\
&\quad - (b_i/b_1)[\partial^2(\Delta E)/\partial b_j \partial b_1] \\
&\quad + (b_i b_j/b_1^2)[\partial^2(\Delta E)/\partial b_1 \partial b_1] \\
&\quad - (b_i b_j/b_1^3 + \delta_{ij}/b_1^2)[\partial(\Delta E)/\partial b_1] \\
\partial^2(\Delta E)/\partial a_i^p \partial b_j^p &= \partial^2(\Delta E)/\partial a_i \partial b_j - (b_j/b_1)[\partial^2(\Delta E)/\partial a_i \partial b_1] \\
&\quad - (a_i/a_1)[\partial^2(\Delta E)/\partial b_j \partial a_1] \\
&\quad + (a_i b_j/a_1 b_1)[\partial^2(\Delta E)/\partial a_1 \partial b_1]
\end{aligned} \tag{LXXIV}$$

Thus, we have everything we need to transform the improper first and second derivatives into proper ones.

Now let us suppose that the energy varies approximately as a quadratic function of the proper variables near the initial guess point:

$$\begin{aligned} \Delta E \cong \Delta E_0 + \sum_i (\Delta P_i) [\partial(\Delta E)/\partial P_i] \\ + \frac{1}{2} \sum_{i,j} (\Delta P_i)(\Delta P_j) [\partial^2(\Delta E)/\partial P_i \partial P_j] \end{aligned} \quad (\text{LXXV})$$

where  $\underline{P}$  is a single vector composed of all proper variables, that is where  $\underline{P} = (a_2^P, a_3^P, \dots, a_N^P, b_2^P, b_3^P, \dots, b_N^P)$ . This can be written in matrix form as

$$\Delta E \cong \Delta E_0 + (\Delta \underline{P})^T \underline{V} + \frac{1}{2} (\Delta \underline{P})^T \underline{D} (\Delta \underline{P}) \quad (\text{LXXVI})$$

where

$$\underline{V}_i = \partial(\Delta E)/\partial P_i \quad \text{and} \quad D_{ij} = \partial^2(\Delta E)/\partial P_i \partial P_j \quad (\text{LXXVII})$$

The vector  $\Delta \underline{P}$  which corresponds to the minimum (or other stationary point) of this quadratic function is simply

$$\Delta \underline{P} = -\underline{D}^{-1} \underline{V} \quad (\text{LXXVIII})$$

The derivatives in  $\underline{D}$  and  $\underline{V}$  have been considered, and can be computed once initial guesses for  $\underline{a}$  and  $\underline{b}$  have been made. Equation (LXXVIII) gives us the corrections which must be applied to the proper variables to correspond to the (approximate) local energy minimum. The corrected proper variables  $(a_2^{P'}, a_3^{P'}, \dots, a_N^{P'})$  and  $(b_2^{P'}, b_3^{P'}, \dots, b_M^{P'})$  can then be used to evaluate the new improper variables using (LXIX). The only difficulty here is the choice of sign for  $a_1$  and  $b_1$ . Now, as long as  $a_1$  and  $b_1$  are originally fairly large, while the correction vector  $\Delta \underline{P}$  is fairly small, then we

expect, on the basis of continuity, that the new  $a_1$  and  $b_1$  will carry the same signs as the old values. In practice, we have insured this by choosing the largest element of  $\underline{a}$  and of  $\underline{b}$  as the dependent variables, while limiting the length of  $\underline{\Delta P}$  to some small value (currently 0.25). If the actual length is greater than this,  $\underline{\Delta P}$  is scaled down by an appropriate amount.

The eigenvalues of  $\underline{D}$  at the point of convergence indicate the curvature of the energy surface in various orthogonal "directions" in the space of proper variables. If they are all positive, then a true local minimum has been reached, while one or more negative values indicates that convergence has occurred upon a saddle-point. If all are negative, a maximum has been found.

So far, we have discussed the one-pair PGVB method for a rather restricted sort of wavefunction, one in which all other orbitals are doubly occupied. We now consider the generalization of these results to other types of wavefunctions. Instead of taking, as our starting point, the closed-shell Hartree-Fock solution, let us consider a wavefunction of the form

$$\psi_1 = A[o_1 \bar{o}_1 o_2 \bar{o}_2 \cdots o_n \bar{o}_n f(o_{n+1}, \bar{o}_{n+1}, \cdots, o_N, \bar{o}_N)] \quad (\text{LXXIX})$$

where  $o_1, o_2, \cdots, o_n$  represent the doubly-occupied "first shell" orbitals which may be transformed among themselves without altering  $\psi_1$ . The function  $f$  depends upon the spin state or other characteristic of  $\psi_1$ , but it is assumed that  $o_{n+1}, o_{n+2}, \cdots, o_N$  cannot

be mixed with  $o_1, o_2, \dots, o_n$  without changing the total wavefunction. It is also assumed that the former are orthogonal to the latter. We wish to split one of the doubly-occupied orbitals, say  $o_1$ , into a GVB-like pair, and to retain the simplifications involved in the closed-shell PGVB method, we must require that  $o_{n+1}, \dots, o_N$  remain frozen, that the first natural orbital be a normalized linear combination of the first-shell orbitals and that the second natural orbital be a normalized linear combination of the "virtinals", that is a set of functions orthogonal to  $o_1$  through  $o_N$ . The first assumption implies that we may treat the non-doubly-occupied orbitals as a fixed "core" which has a particular core energy and which adds a fixed-field term to the one-electron operator of the doubly-occupied orbitals and virtinals. We may carry out the PGVB analysis exactly as before, the only modification being that the one-electron portion,  $\hat{h}$ , of the hamiltonian for these orbitals is replaced by

$$\hat{h}' = \hat{h} + \hat{h}(o_{n+1}) + \hat{h}(o_{n+2}) + \dots + \hat{h}(o_N) \quad (\text{LXXX})$$

where  $\hat{h}(o_i)$  is the field term due to  $o_i$ . To consider a concrete example, let us suppose that the wavefunction of (LXXIX) represents an open-shell Hartree-Fock solution of spin state  $2S+1$ , in which  $o_{n+1}, \dots, o_{n+S}$  are singly-occupied orbitals which all have the same spin. In this case, each singly-occupied orbital  $o_i$  adds a term of  $\hat{J}_i - \hat{K}_i$  to  $h'$  (42), so we have

$$\begin{aligned} \hat{h}' = & \hat{h} + \hat{J}_{n+1} + \hat{J}_{n+2} + \cdots + \hat{J}_{n+S} \\ & - \hat{K}_{n+1} - \hat{K}_{n+2} - \cdots - \hat{K}_{n+S} \end{aligned} \quad (\text{LXXXI})$$

Another important case is the one in which the last  $(N-n)/2$  pairs are split into first and second NO's. In this case we may write

$$\begin{aligned} f(o_{n+1}, \bar{o}_{n+1}, \cdots, o_N, \bar{o}_N) = & (c_{n+1} o_{n+1} \bar{o}_{n+1} + c_{n+2} o_{n+2} \bar{o}_{n+2}) \\ & \times (c_{n+3} o_{n+3} \bar{o}_{n+3} + c_{n+4} o_{n+4} \bar{o}_{n+4}) \\ & \times (c_{N-1} o_{N-1} \bar{o}_{N-1} + c_N o_N \bar{o}_N) \end{aligned}$$

and it can be shown (43) that

$$\hat{h}' = \hat{h} + \sum_{i=n+1}^N c_i^2 (2\hat{J}_i - \hat{K}_i) \quad (\text{LXXXIII})$$

Thus, if we want to investigate several pairs simultaneously within a particular molecule, we may split the first pair using the PGVB technique outlined above, modify  $\hat{h}$  according to (LXXXIII) and split a second pair in this new field while fixing the first and holding it orthogonal to the second. This procedure has the drawback that it does not allow the first PGVB pair to readjust as the second is split, so the pairs thus obtained are only approximate PGVB solutions.

We have written a FORTRAN IV program to carry out the calculations necessary for this approximate PGVB method. It uses, as its starting point, a converged HF solution, and it has options for

"freezing" any canonical orbitals and for splitting a number of pairs sequentially as described in the above paragraph. The first option is useful when, for example, open-shell or core orbitals are to be excluded from the PGVB solution orbitals. The second option can be used to test the effect of splitting one pair upon the solution of another, and as will be discussed below, it provides the only means of obtaining reasonable lone pairs in difluoromethane.

We now discuss the results we have obtained for  $\text{CH}_2\text{F}_2$ . The appropriate HF calculations have been described in the first chapter, which includes a description of the double-zeta basis set we have used. The starting guesses for the first and second NO's were derived, in most cases, from either the LMO's or from closely related PGVB solutions, and in all cases, sufficient SCF iterations were undertaken so that the sum of the squares of the changes in the elements of the a and b vectors was less than  $10^{-8}$  from one cycle to the next (this leads to energy convergence well beyond the sixth decimal place). Unless otherwise noted, the quadratic PGVB method was used, and the solutions correspond to the splitting of a single orbital from the HF solution to give a true local minimum in  $\Delta E$ .

We consider first our HF equilibrium geometry of difluoromethane (see Chapter 1). The purposes here are two: First, we wish to gain a more detailed picture of the electronic structure of the molecule by examining the VB-like orbitals (hereafter called "the VB

orbitals"\*) which make up each pair; second, we hope to obtain an approximate set of naturally localized MO's (NLMO's) to assist us in the interpretation of the HF wavefunction just as the LMO's did.

Initially, the core pairs were considered. Splitting energies of -12.2 and -12.5 mh were obtained for C and F, respectively. The first NO for the carbon core pair gives an overlap of 0.97 with the canonical carbon core, while the analogous value for fluorine is 0.95. The VB orbitals for each pair overlap strongly ( $S = .98$  for fluorine, .97 for carbon), indicating that each core may be viewed as basically a doubly-occupied orbital.

The C-F bonding orbital was the next to be considered, and in this case, a direct comparison between the GVB and PGVB methods was made. The PGVB solution gives a CI energy lowering of 24.1 mh, the greatest of any pair in the molecule. The converged PGVB vectors were used as the starting point for a full, one-pair GVB calculation which was done with the CIT GVB program written by Drs. W. J. Hunt and P. J. Hay. The GVB solution gives an energy which is 24.6 mh below the HF value, only 0.5 mh lower than the PGVB energy. Thus, constraining the first NO of this pair to be a linear combination of HF orbitals increases the molecular energy by only 0.5 mh, a small amount indeed. The first and second PGVB

---

\* We note that this term, "VB orbitals", is usually reserved for purely atom-centered VB orbitals, not variationally optimized GVB or PGVB orbitals. We use the term here for conciseness.

NO's both show overlaps of 0.9998 with their GVB counterparts, while the full, many-electron wavefunctions have an overlap of 0.99973. Thus, it is clear that the PGVB method is a very good approximation to the GVB technique in this case, and we should point out that the former requires about 1/3 as much time per cycle of refinement.

We have also tested the assumption that the core pairs can be neglected in the splitting of the C-F pair. We have carried out a PGVB calculation in which the canonical HF cores (which we found, above, to be quite similar to the PGVB cores) were "frozen", that is, not allowed to participate in the description of the first NO. We find that the CI energy lowering and NO coefficients differ negligibly from those in the unfrozen case. In view of the fact that neglecting the cores simplifies the calculations slightly, we have frozen the cores in all subsequent calculations.

Figure 7 shows the orbital amplitude plots of the first NO of the C-F bond pair (cores frozen) and, for comparison, the corresponding LMO. The two are qualitatively similar, though we note that the LMO contains less p-character on both bonded atoms, and a lower amplitude on the non-bonded fluorine. The NO may be analyzed in terms of C and F hybrids just as the LMO was (see section B). The F hybrid contains 98.6% p-character and is directed only 0.2° away from the C-F axis, pointing slightly to the inside of the F-C-F triangle. The analogous hybrid of the LMO has only 85.1% p-character, deviating in the same direction, but by about 1°, from the C-F axis.

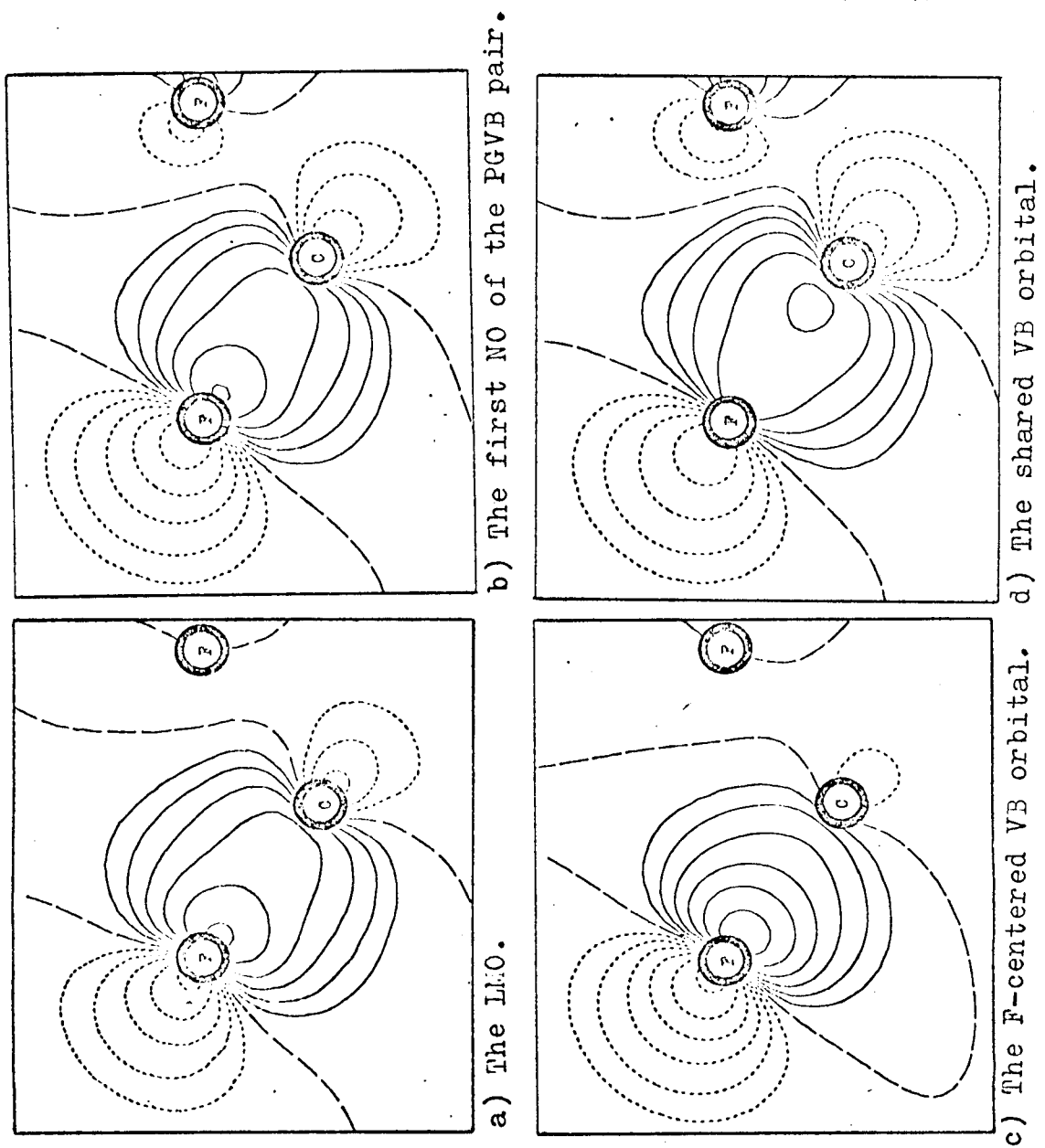


**Figure 7.**  
 The C-F bonding  
 pair in difluoro-  
 methane (eq. geom.).  
 See Figure 1 for  
 contour values.

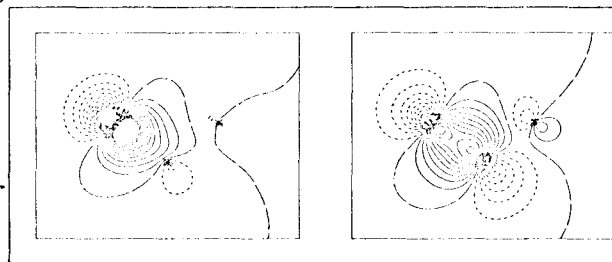
The C hybrid of the NO has 85.1% p-character ( $sp^{5.72}$ ) as compared to the LMO value of 73.8% ( $sp^{2.82}$ ). If we construct another NO (for the other C-F bond) by simply reflecting this one through the H-C-H plane, then we find that the average angle between the C hybrids of the two is  $95.6^\circ$  (inner and outer contributions of  $98.1^\circ$  and  $88.2^\circ$ ). This is somewhat less than the corresponding LMO value of  $99.5^\circ$  (inner and outer contributions of  $101.4^\circ$  and  $93.6^\circ$ ) which, in turn, is smaller than the actual F-C-F angle ( $109.0^\circ$ ).

The structure of the C-F bonding pair may be seen in more detail if we look at the VB orbitals which contribute to it, plots of which are included in Figure 7. One of these is essentially a pure p orbital on fluorine (95.7% p-character) which deviates, in its average direction, by only  $0.3^\circ$  from the C-F axis. The other is shared almost equally by the two atoms. The F hybrid of this shared pair has 99.7% p-character and lies right along the C-F axis, while the C hybrid has 77.6% p-character ( $sp^{3.46}$ ) and gives an average angle of  $97.4^\circ$  (inner and outer contributions of  $99.3^\circ$  and  $91.4^\circ$ ) between itself and a symmetrically related hybrid for the other C-F bond.

Figure 8 shows the GVB orbital amplitude plots for one of the two C-F bond pairs in  $CF_2$  (singlet ground state, geometry nearly optimum) obtained by Dunning (44) using a high-quality double-zeta basis set. Only the two C-F bonds and the non-bonding C pair were split in this calculation. We note a marked similarity between these GVB orbitals and the ones we have obtained for the C-F bond in  $CH_2F_2$ .

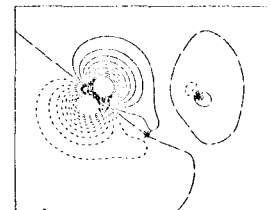
Figure 8.

GVB orbitals for one of the two C-F bonding pairs in difluorocarbene (singlet ground state, nearly optimum geometry) obtained by Dunning (44) using a high-quality double-zeta basis. The dotted, dashed and solid lines represent negative, zero and positive contours, respectively. The interval between contours is 0.05 a.u.

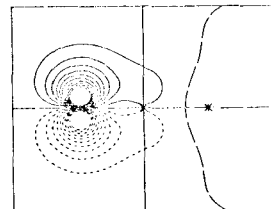
Figure 11.

The doubly-occupied (unsplit) lone pairs for one fluorine in difluorocarbene (singlet ground state, nearly optimum geometry) obtained by Dunning (44). See figure 8 for contour values.

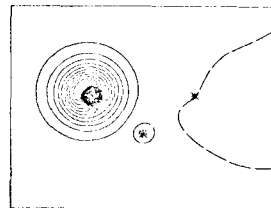
a) The 2p pair which lies in the F-C-F plane.



b) The 2p pair perpendicular to the F-C-F plane.



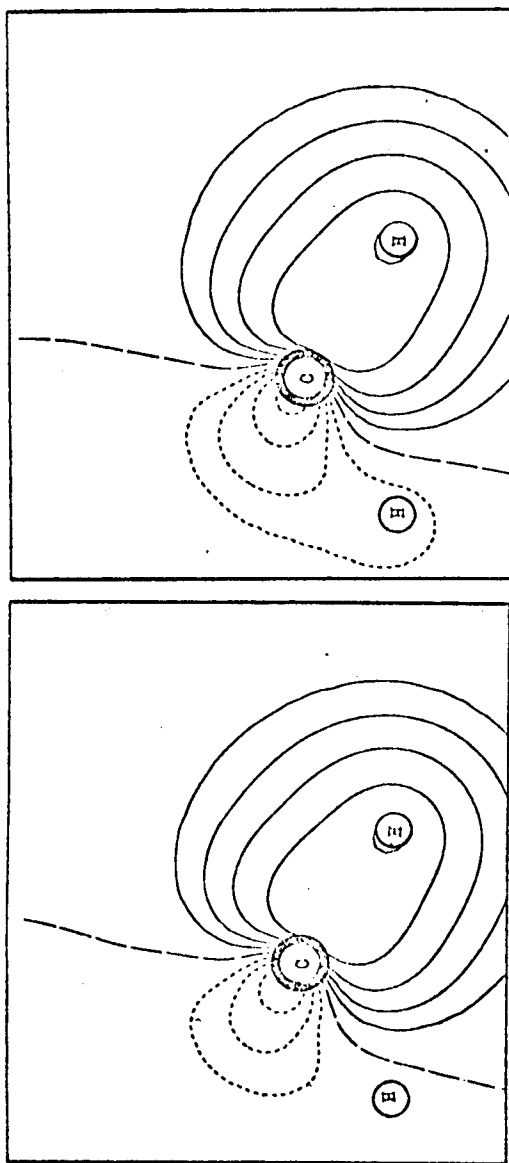
c) The 2s-like pair, plotted in the F-C-F plane.



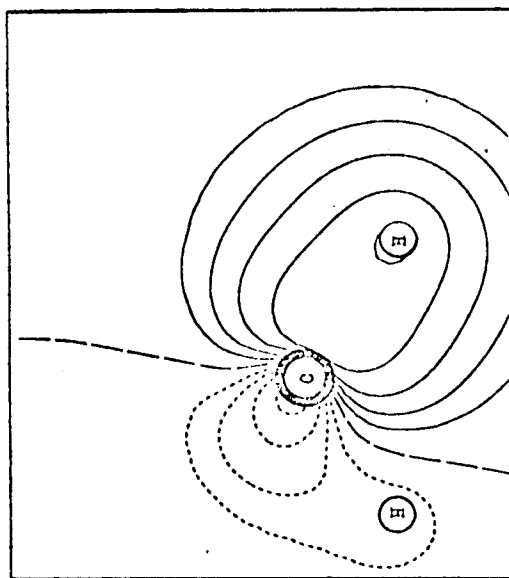
The C-H bonding orbital of CH<sub>2</sub>F<sub>2</sub> was the next to be considered. It gives a splitting energy of -16.4 mh. To test the assumption that the splitting of one valence pair does not greatly influence the splitting of other valence pairs, we have carried out a PGVB calculation in which the C-H bond pair was split in the field of the above C-F pair, and we find in this case that the C-H splitting energy increases by only 0.8 mh to -15.7 mh. The orbitals are quite similar in the two cases, giving overlaps of 0.995 between corresponding first NO's, 0.994 between corresponding second NO's. The C-H pairfunctions from the two cases show a two-electron overlap of 0.990. Thus, the assumption appears to be a good one.

Considering the unconstrained C-H solution, Figure 9 shows the first NO of the pair in comparison with the corresponding LMO. The two appear to be quite similar, but again the LMO shows less p-character on the carbon. The C hybrid of the NO has 66.3% p-character ( $sp^{1.97}$ ) as compared to the LMO value of 57.2% ( $sp^{1.34}$ ). The average angle between this hybrid and the C hybrid of "the other" C-H bond's first NO is 123.7° (inner and outer contributions of 124.8° and 122.0°), a few degrees larger than the analogous LMO value of 117.7° (inner and outer contributions of 119.0° and 115.8°), which in turn is larger than the actual H-C-H angle (112.2°).

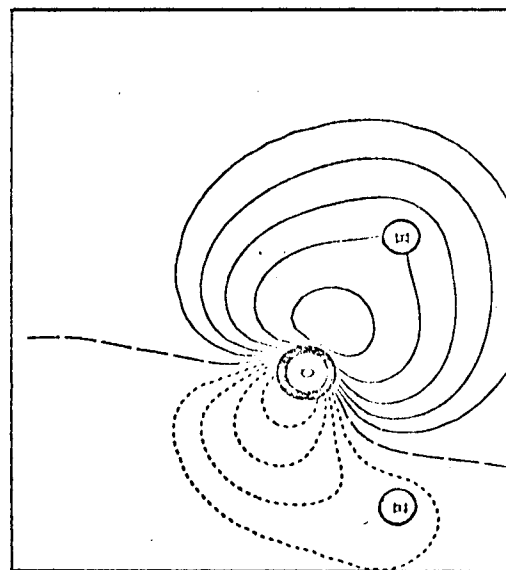
Figure 9 also shows the GVB orbitals which make up the C-H pair. One of these is essentially a hydrogen 1s function with a small contribution from the carbon. The other is nearly a pure C-centered lobe, the C hybrid of which contains 60.7% p-character ( $sp^{1.55}$ ).



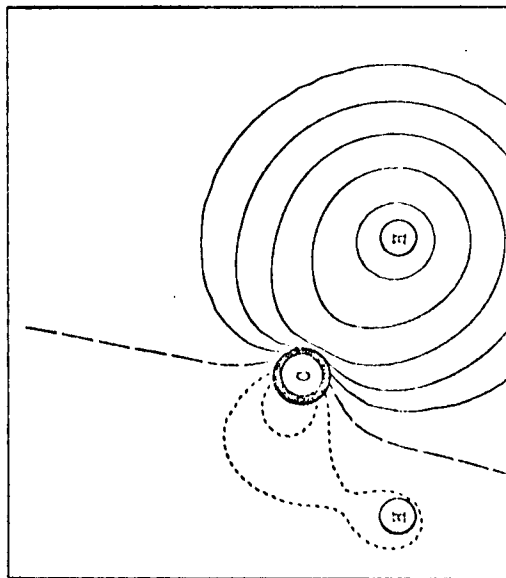
a) The IAO.



b) The first NO of the PGVB pair.



c) The C-centered VB orbital.



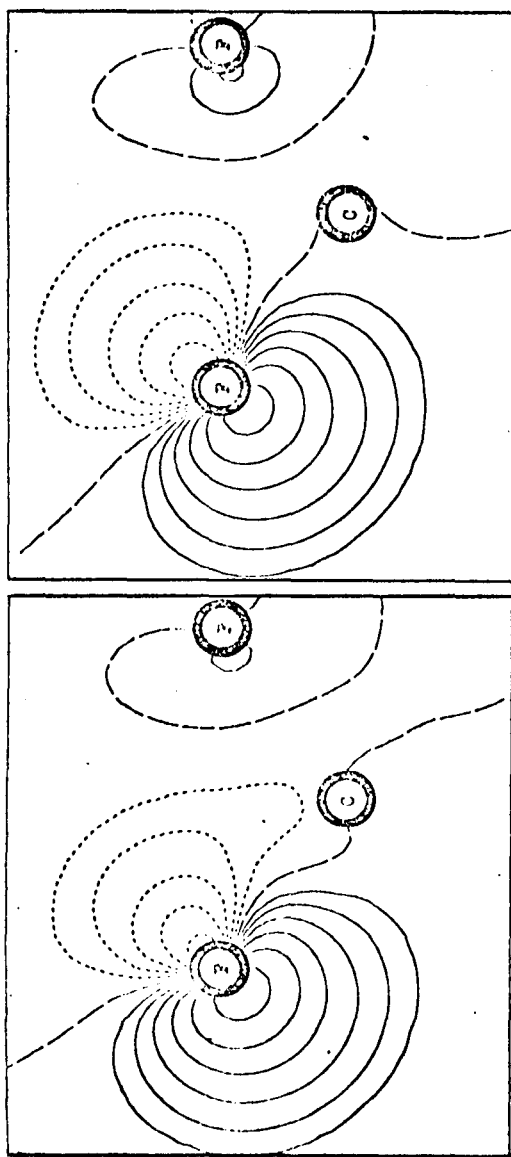
d) The H-centered VB orbital.

Figure 9.  
The C-H bonding  
pair in difluoro-  
methane (eq. geom.).  
See Figure 1 for  
contour values.

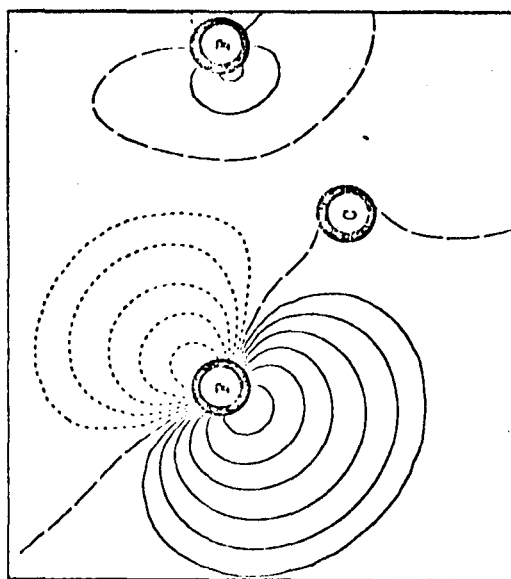
This hybrid gives an average angle of  $123.0^\circ$  (inner and outer contributions of  $123.6^\circ$  and  $121.6^\circ$ ) between itself and a symmetrically related hybrid for the other C-H bond.

The lone pair which lies in the F-C-F plane was investigated next. Initial attempts to obtain this pair using the linear PGVB method failed because apparently there is no local minimum in  $\Delta E$  corresponding to this pair. Upon each SCF cycle, the pair rotated a little further toward the C-F axis and acquired a bit more C-F bonding character until finally it became a C-F bonding pair. It seems that the C-F pair has such a large splitting energy that it overshadows other local features of the  $\Delta E$  variation, and the lone pairs are thus not directly obtainable. The quadratic PGVB method does yield a solution, but this corresponds to a saddle-point solution (one negative eigenvalue in the D matrix of LXXVII), and the physical meaning of such a solution is difficult to assess. It was found necessary, then, to hold the lone pair orthogonal to the C-F bond pair (which it "wants" to become) by splitting the former in the field of the latter. This process yields a reasonable lone pair with a splitting energy of -11.1 mh, 1.3 mh below the splitting energy of a 2p lone pair on an isolated fluorine atom with the same basis set.

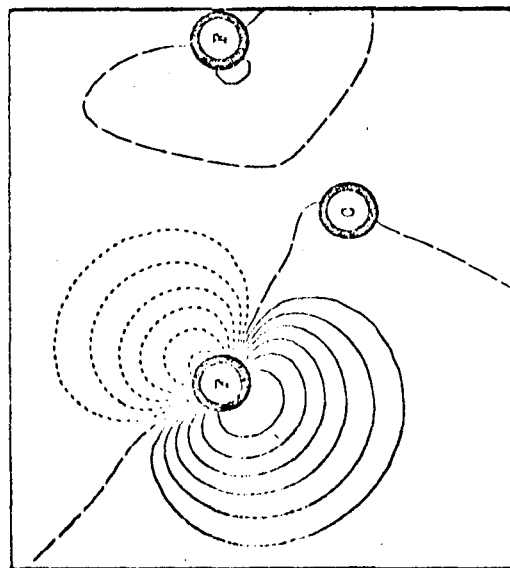
Figure 10 shows the orbital amplitude plot, in the F-C-F plane, of the first NO of this pair, together with the corresponding LMO for comparison. We see that the NO is nearly a pure p orbital on fluorine which does show a slight bit of "smearing" toward carbon, though this effect is more pronounced in the LMO. We see also that



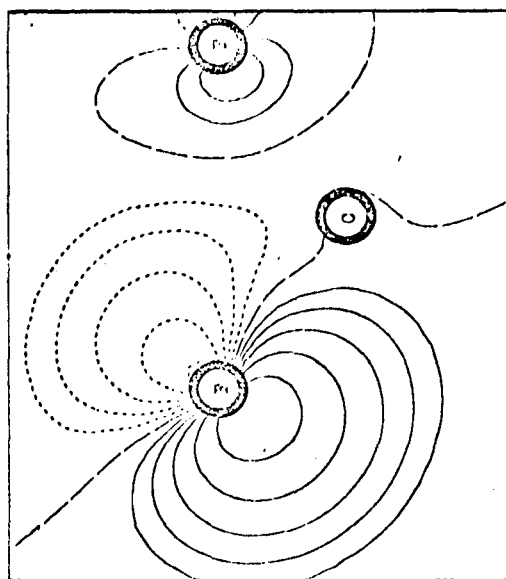
a) The LMO.



b) The first NO of the PGVB pair.



c) The smaller VB orbital.



d) The larger VB orbital.

Figure 10.  
The F lone pair of difluoromethane which lies in the F-C-F plane (eq. geom.). See Figure 1 for contour values.

the NO shows a greater admixture of "C-F<sub>other</sub>" anti-bonding character than the LMO does. A population analysis of the F hybrid of the NO gives a hybridization of  $sp^{5.7}$  (85.2% p-character) and an average angle with the C-F axis of  $94.5^\circ$  as compared to the LMO values of  $sp^{2.35}$  (70.2% p-character) and  $111.8^\circ$ . Here, as in all lone pairs which we will consider, the VB orbitals which make up the pair are quite similar in hybridization and direction to the NO, but one is smaller (greater contribution from the inner orbitals of the double-zeta set) and one is larger (greater contribution from the outer orbitals) than the NO. Figure 10 includes plots of these, and we see that the outer GVB orbital appears to be delocalized in a bonding fashion toward carbon. Goddard and co-workers (45) have observed a similar but more pronounced lone-pair delocalization in the  ${}^2\pi$  and  ${}^4\Sigma^-$  states of the C-F molecule. Dunning (44) has found, in the above-mentioned calculations on the singlet state of  $CF_2$ , a delocalization of the (unsplit) lone-pair orbitals which lie in the F-C-F plane and which correspond to our solution for  $CH_2F_2$ . Figure 11 shows a plot of one of these  $CF_2$  lone-pair orbitals, and we see that again the effect is more pronounced than in  $CH_2F_2$ .

The search for the lone pairs which are out of the F-C-F plane met with the same sort of difficulties that the in-plane solution did. In this case, freezing the C-F bond pair was not sufficient because the out-of-plane pair "wants" to become not only the C-F bond but also the in-plane pair (both of which have more negative splitting energies). Thus, to obtain a solution corresponding to a

local minimum, it was necessary to freeze both of these other pairs. The first NO of this pair contains a great deal of p-character (82.5%, corresponding to  $sp^{4.75}$  hybridization) and is nearly perpendicular to the C-F axis (average angle =  $84.7^\circ$ ) and the F-C-F plane (average angle =  $78.0^\circ$ ). This solution is, however, difficult to accept as a reasonable one. To see this, we recall that the first NO's for the C-F bond pair and in-plane lone pair are both, as far as fluorine is concerned, nearly pure p orbitals. Based on the usual hybridization arguments, which we found to apply rather well to the F-centered LMO's (see section B), we thus have roughly one 2s and one 2p orbital "left over" to describe the first NO's of the remaining two lone pairs. Now, the F-C-F plane is a symmetry element for the molecule, and we expect the exact, fully split PGVB wavefunction to describe each fluorine as having some well-defined symmetry with respect to this plane. The "left over" orbitals may be combined in two ways to yield such symmetry: a) one pure 2p orbital perpendicular to the F-C-F plane and one 2s orbital in the plane; or b) two sp-hybridized lobes extending to either side of the plane. However, the first NO of the pair we are considering corresponds to neither of these two cases: It is far from sp hybridization and, in fact, gives an overlap of -.60 with a similar orbital reflected through the F-C-F plane; neither is it a pure out-of-plane 2p orbital. It most closely resembles the latter, though, so we decided that it was most realistic to search for a lone pair which was antisymmetric with respect to the F-C-F plane. The solution might not correspond to a true local minimum in

$\Delta E$ , but the resulting set of lone pairs would have the right symmetry, and would have the same general structure as the F lone pairs found by Goddard and co-workers (45) in the CF molecule. As will be discussed below, this lone-pair structure is, in fact, not appropriate for  $\text{CH}_2\text{F}_2$ . Possibility b), above, is actually better than a), but the necessity for considering a) first will become apparent.

Thus, we considered next the 2p-like lone pair perpendicular to the F-C-F plane. The pair was split in the field of the C-F bond pair and in-plane lone pair, with starting guesses derived from the above out-of-plane solution. The quadratic PGVB method rapidly converged upon a saddle-point solution, which is as expected because the splitting energy of this pair (-10.3 mh) is slightly higher than that of the "best" out-of-plane solution discussed above (-10.8 mh). Figure 12 shows the amplitude plot for the first NO of this pair in the plane which contains the C-F axis and is perpendicular to the F-C-F plane. We see that it is almost exactly a pure fluorine 2p orbital which shows little bonding delocalization toward carbon. Also shown are the VB orbitals which make up the pair, and we see that here, in contrast to the in-plane pair, the outer VB orbital does not show any of this C-F bonding delocalization. Figure 11b shows the analogous (unsplit) pair in  $\text{CF}_2$ , where we see a substantial amount of such delocalization.

The only remaining lone pair is the 2s-like one. Starting guesses for the first and second NO's were derived from the plus and minus linear combinations of the outer two s-type AO's on fluorine.

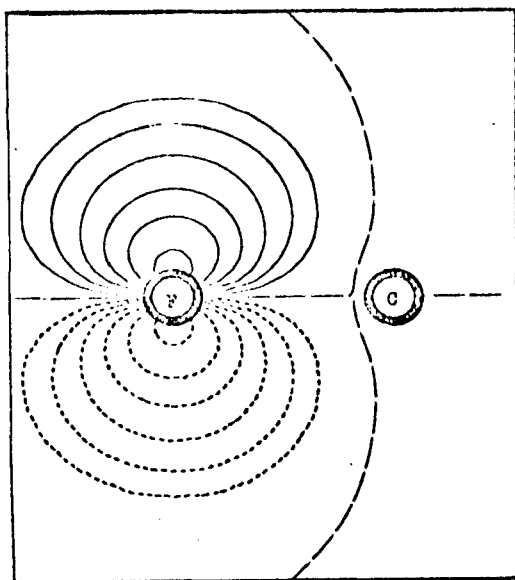
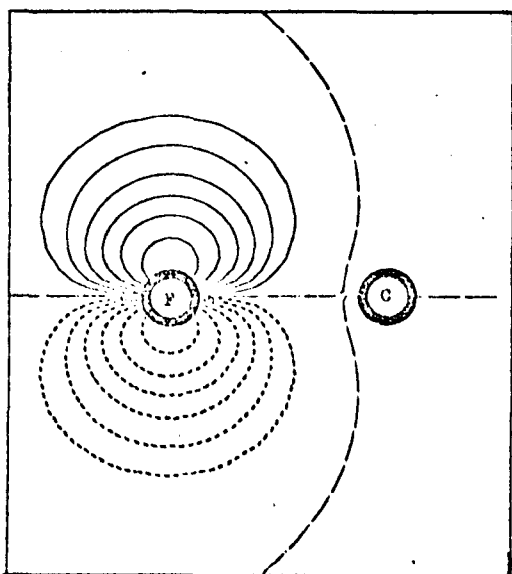
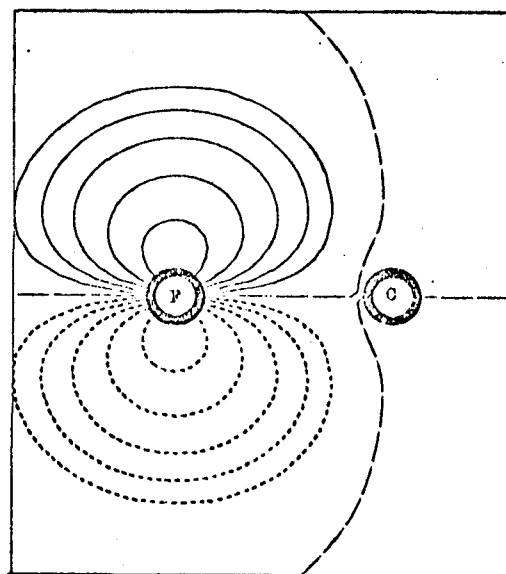


Figure 12.  
The F lone pair in difluoromethane which is perpendicular to the F-C-F plane (eq. geom.). See Figure 1 for contour values.

a) The first NO of the PGVB pair.



b) The smaller VB orbital.

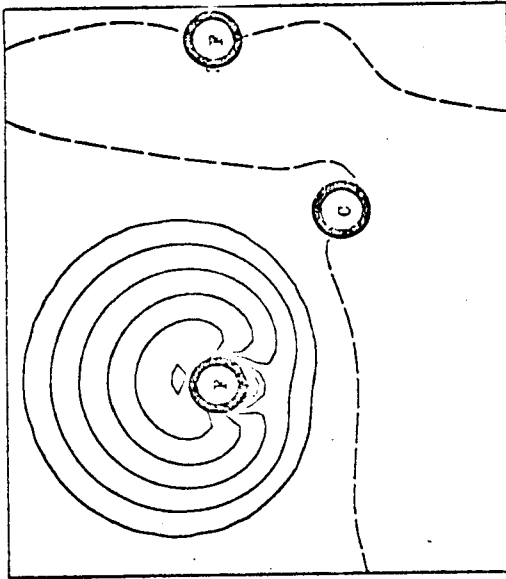


c) The larger VB orbital.

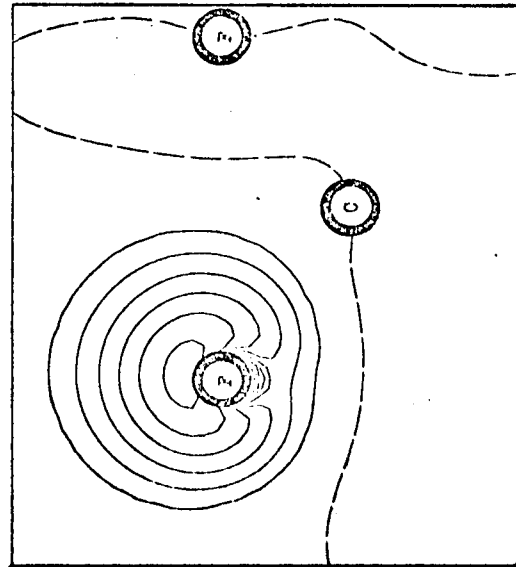
This pair was split in the fields of the C-F bond pair, in-plane lone pair and 2p-like lone pair so that the final set of four pairfunctions would be mutually orthogonal. The converged solution has a splitting energy of -5.678 mh. A plot of the first NO in the F-C-F plane is shown in Figure 13. A population of the F hybrid of this NO yields a value of only 16.8% p-character ( $sp^{0.20}$ ), and the average angle between the positive lobe of the pair and the C-F axis is  $116.5^\circ$ . Figure 13 also shows the VB orbitals for the pair, and we see little tendency for either to delocalize in a bonding fashion toward carbon.

We now reconsider the question of the general lone-pair structure in difluoromethane. So far, we have investigated one possible lone-pair set which conforms to the molecular symmetry, but as noted above, there is another possibility: Instead of one 2s-like pair and one out-of-plane 2p pair, we may have two symmetrically related, and nearly sp-hybridized, pairs extending above and below the F-C-F plane. In searching for such a solution, though, we are faced with the problem that the one-pair PGVB approach has no means of treating, in a consistent fashion, the simultaneous splitting of two such symmetrically related pairs. If we attempt to solve for just one of these, we obtain the "best" out-of-plane pair discussed above, which has far too much p-character, and consequently far too large an overlap with its symmetrically related counterpart, to give a reasonable lone-pair description. The only alternative we see is to assume that the two sp-like pairs are well approximated by the appropriate linear combinations of the 2s-like and out-of-plane 2p orbitals which we

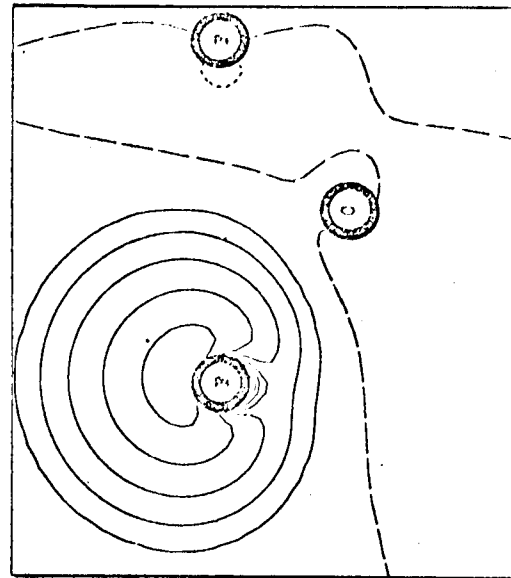
**Figure 13.**  
**The 2s-like F lone**  
**pair in difluoro-**  
**methane (eq. geom.).**  
 See Figure 1 for  
 contour values.



a) The first NO of the PGVB pair.



b) The smaller VB orbital.



c) The larger VB orbital.

have already obtained. This is analogous to forming atomic  $sp$  hybrids from one  $s$  and one  $p$  function, but in our case the "basis functions" are PGVB pairs rather than AO's. Thus, we have formed the normalized sum and difference of the first NO's of these "basis" pairs to obtain two new NO's corresponding to the desired lone-pair structure. The second NO's were treated similarly, and after optimization of the CI coefficients, these new pairs each gave a splitting energy of  $-9.85$  mh, or  $-19.7$  mh for the two. This is  $3.7$  mh below the sum of the  $\Delta E$ 's for the  $2s$ -like pair ( $-5.7$  mh) and the out-of-plane  $2p$  pair ( $-10.3$  mh), which is actually rather remarkable when we consider that these  $sp$ -like pairs have not been variationally optimized. The indication is, then, that the " $2p$ - $2s$ " lone-pair structure is definitely inferior to the " $sp$ - $sp$ " description.

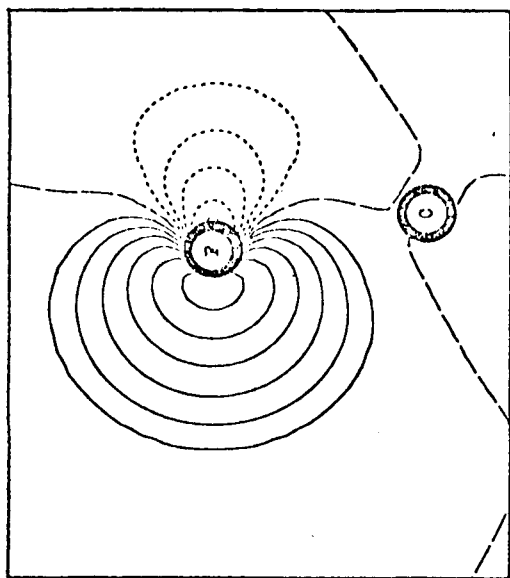
We are not in a position to simultaneously optimize these  $sp$  pairs, but at least we can freeze one of the "constructed" pairs and solve for the second in the first pair's field (the C-F bond pair and in-plane lone pair being fixed also). This process improved the splitting energy of the second pair by only  $0.1$  mh and gave a solution quite similar to the initial guess (two-electron overlap =  $0.99994$ ), with most of the differences appearing in the second NO's (overlap =  $0.9974$ ). The first NO of this optimized pair is an F-centered function with  $sp^{1.35}$  hybridization ( $57.4\%$   $p$ -character). Its average direction is such that it makes an angle of  $100.0^\circ$  with the C-F axis,  $109.4^\circ$  with the in-plane lone pair and  $135.0^\circ$  with its own symmetrically related counterpart. This pair, together with its counterpart,

will be taken as good approximations to the actual out-of-plane lone pairs in all subsequent work.

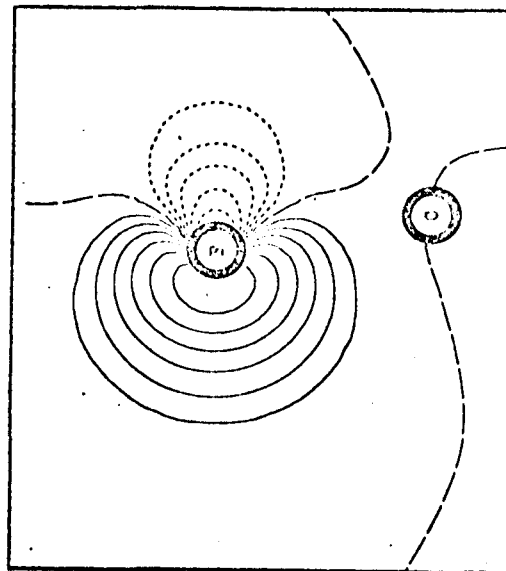
Figure 14 shows plots, in the plane which contains both the C-F axis and the lone pair itself, of the first NO and the VB orbitals for the pair. The outer VB orbital is the only one which even hints of a C-F bonding delocalization, but the effect is by no means pronounced.

So far, we have considered only a portion of the molecule; one C-H bond and the C-F bond pair and F lone pairs associated with one fluorine. By suitably reflecting these orbitals through the H-C-H or F-C-F planes, we may generate an approximate, complete PGVB description of the valence shell of the molecule. The resulting set of first NO's, together with the canonical cores are hopefully similar to the set of naturally localized MO's (NLMO's) which we are ultimately seeking. However, these NLMO's are supposed to be orthogonal, and we have found that the first NO's, as obtained above, show some non-negligible overlaps, the largest (0.20) occurring between the two C-H bonding NO's. In order to obtain properly orthogonal approximations to the NLMO's, we have symmetrically orthogonalized the "raw" set. The approximation may be a rough one, but at least we have managed to obtain localized orbitals which are tied in some fashion to a physically meaningful criterion. We seek now to apply the tools of delocalization energy analysis and population analysis used in the previous section to investigate the NLMO description of the HF wavefunction of difluoromethane.

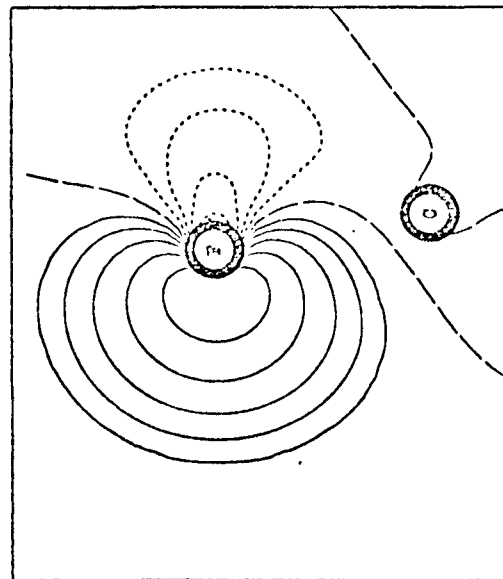
**Figure 14.**  
 The sp-like F lone pair in difluoromethane (eq. geom.). The plot is in the plane which contains the C-F axis and the pair itself (the angle between this plane and the F-C-F plane is  $67.5^\circ$ ). See Figure 1 for contour values.



a) The first NO of the PGVB pair.



b) The smaller VB orbital.



c) The larger VB orbital.

Table 6 gives the delocalization energies of the NLMO's, which are analogous to the LMO values given in Table 1. We see that the total DE for the NLMO's is substantially smaller than the LMO value, and in fact, the truncated NLMO's represent the best bond functions we have yet obtained for this molecule. The core NLMO's are seen to have much smaller DE's than their LMO counterparts, which traces to the fact that we have taken the former to be the well-localized canonical cores. The bonding pairs show very similar values between the two descriptions, while the total lone-pair contribution has dropped by almost a factor of two in the NLMO case. We see that the lone pair NLMO in the F-C-F plane has by far the greatest DE, followed by the out-of-plane pair. Once again, we draw the conclusion that lone-pair delocalization is an important stabilizing factor in the difluoromethane molecule, and that this delocalization is more efficient when the lone pair opposes a C-F bond than when it does not.

We may define NLO's (which are partially corrected for the effects of orthogonality) from the NLMO's just as we did from the LMO's (see equation XXIV). Table 6 includes the DE's for these, and we see that the only major differences between these and the NLMO values appear as lower DE's for the bonding orbitals. We note that, for both sets in Table 6, the non-additivity is substantial.

Table 7 gives the gross and overlap populations for the various NLMO's, for groups thereof and for the entire HF wave function. This is analogous to Table 2, which gives the populations for the LMO's. The core and bond pairs show an excellent parallel between

Table 6. Delocalization Energies for the Naturally Localized Orbitals of Difluoromethane.

<u>Orbital</u>	<u>Number</u>	<u>Delocalization energy (mh)</u>			
		<u>From truncated NLMO's</u>		<u>From TNLO's defined by NLMO's</u>	
		<u>Per orbital</u>	<u>Sum over related orbitals</u>	<u>Per orbital</u>	<u>Sum over related orbitals</u>
All	13	-	68.92 <sup>a</sup>	-	62.08 <sup>a</sup>
F core	2	0.47	0.93	0.40	0.81
C core	1	0.24	0.24	0.37	0.37
C-F bond	2	2.41	4.82	0.72	1.44
C-H bond	2	6.88	13.75	5.25	10.51
F lone pair in F-C-F plane	2	14.32	28.63	14.05	28.11
F lone pair out of plane	4	7.39	<u>29.57</u>	7.07	<u>28.28</u>
		sum =	77.95 <sup>b</sup>	sum =	69.51 <sup>b</sup>
		error =	-9.03 <sup>c</sup>	error =	-7.43 <sup>c</sup>

<sup>a</sup>Actual total DE.

<sup>b</sup>Sum of individual orbital DE's.

<sup>c</sup>Non-additivity error, the difference of the above.

the two descriptions, the only significant difference being that the C-F bonding NLMO gives a much lower C-F OP than the corresponding LMO does. There is also a good parallel between

Table 7. Gross and Overlap Populations for NLMO's and Groups of NLMO's in Difluoromethane (Hartree-Fock Equilibrium Geometry).

Orbital or group	Overlap populations <sup>a</sup>										Gross Populations <sup>a</sup>					
	C-F1	C-F2	C-H1	C-H2	F-F	H-H	F1H1	F1H2	F2H1	F2H2	H1	H2	F1	F2	C	
F1 core	2	0	0	0	0	0	0	0	0	0	0	0	0	1999	0	1
C core	0	0	2	2	0	0	0	0	0	0	1	1	0	0	0	1999
C-F1 bond	468	-13	-6	-6	-8	2	-14	-14	0	0	-4	-4	1504	-2	-2	506
C-H1 bond	-56	-56	852	-59	1	-37	-21	3	-21	3	865	-23	-16	-16	-16	1191
Lone pair on F1, trans to C-F2 bond	95	-33	-3	-3	-8	2	-8	-8	-3	-3	-2	-2	1946	-2	-2	60
Lone pair on F1, "trans" to C-H2 bond	19	-3	-5	-22	-3	-6	-18	0	1	-1	-4	2	1991	0	12	
Core group	1	1	2	2	0	0	0	0	0	0	1	1	1999	1999	2000	
Bond group	343	343	780	780	-13	-70	-31	-31	-31	-31	833	833	1470	1470	3395	
Lone pairs	94	94	-61	-61	-28	-21	-29	-29	-29	-29	-7	-7	5924	5924	166	
All NLMO's	439	439	721	721	-41	-91	-60	-60	-60	-60	826	826	9393	9393	5561	

<sup>a</sup>In units of  $10^{-3}$  electrons.

the LMO and NLMO lone pairs which lie in the F-C-F plane except that the NLMO shows substantially more C-F bonding character than the LMO. The parallel between the out-of-plane pairs is fairly good, though the relative magnitudes of several of the populations differ between the NLMO and the LMO. The total lone pair groups compare very favorably between the two descriptions, except that the NLMO set gives a larger bonding contribution to the C-F OP's.

Thus, the population analysis of the NLMO's supports the conclusions drawn in the previous section that the fluorine lone-pair delocalization "strengthens" the C-F bonds, "weakens" the C-H bonds and causes a charge-transfer from the fluorines to the carbon.

To complete our investigation of the electronic structure of difluoromethane, we now consider the changes which take place in the PGVB orbitals as the F-C-F angle is increased and decreased by 30° from its equilibrium value. We will not analyze the wave-functions in the same detail we used in the equilibrium case, but rather we will concentrate upon the bonding pairs only. For each distorted geometry, the C-F and C-H bonds were split independently, with the canonical cores frozen as they were in the equilibrium geometry. The splitting energies for these pairs proved to vary only modestly as functions of the F-C-F angle. For the C-F bond pair, the  $\Delta E$  values are -25.4, -24.1 and -25.3 mh for the -30°, 0° and +30° distortions, respectively, while the corresponding values for the C-H bond pair are -16.3, -16.5 and -16.7 mh.

Figure 15 shows the first NO and the VB orbitals for the C-F bond pair in the three geometries, and Figure 16 gives the analogous plots for the C-H bond pair. The latter shows rather small changes, most of which involve the "other H" contribution to the pair. The C-F pair, on the other hand, shows substantial bond-bending effects, and we note here, in both the first NO and the VB orbitals, the same sort of fluorine "pivoting" about a relatively static carbon hybrid which we found in the LMO's (see Figure 6).

To make a more quantitative comparison, we may analyze these orbitals in terms of hybridization and direction just as we did the LMO's (see Table 4). Table 8 presents such analyses for the C and F hybrids of the first NO and "shared" VB orbital in the C-F pair, for the F hybrid of the F-centered VB orbital in this pair, and for the C hybrids of the first NO and C-centered VB orbital in the C-H pair. We see by examining these values that the conclusions we drew in the analysis of the LMO's apply well here: The C-H orbitals show relatively little change as the F-C-F angle is altered; the C-F orbitals show a pivoting of the fluorine hybrids while the carbon hybrids tend not to follow the fluorines, but rather to move in the opposite direction. We have not obtained the lone pairs for the distorted geometries, so we cannot verify that the fluorines move as rigid units, but at least we see that the PGVB orbitals, like the LMO's, tend to discount the concept of "orbital following" in the F-C-F angle variation.

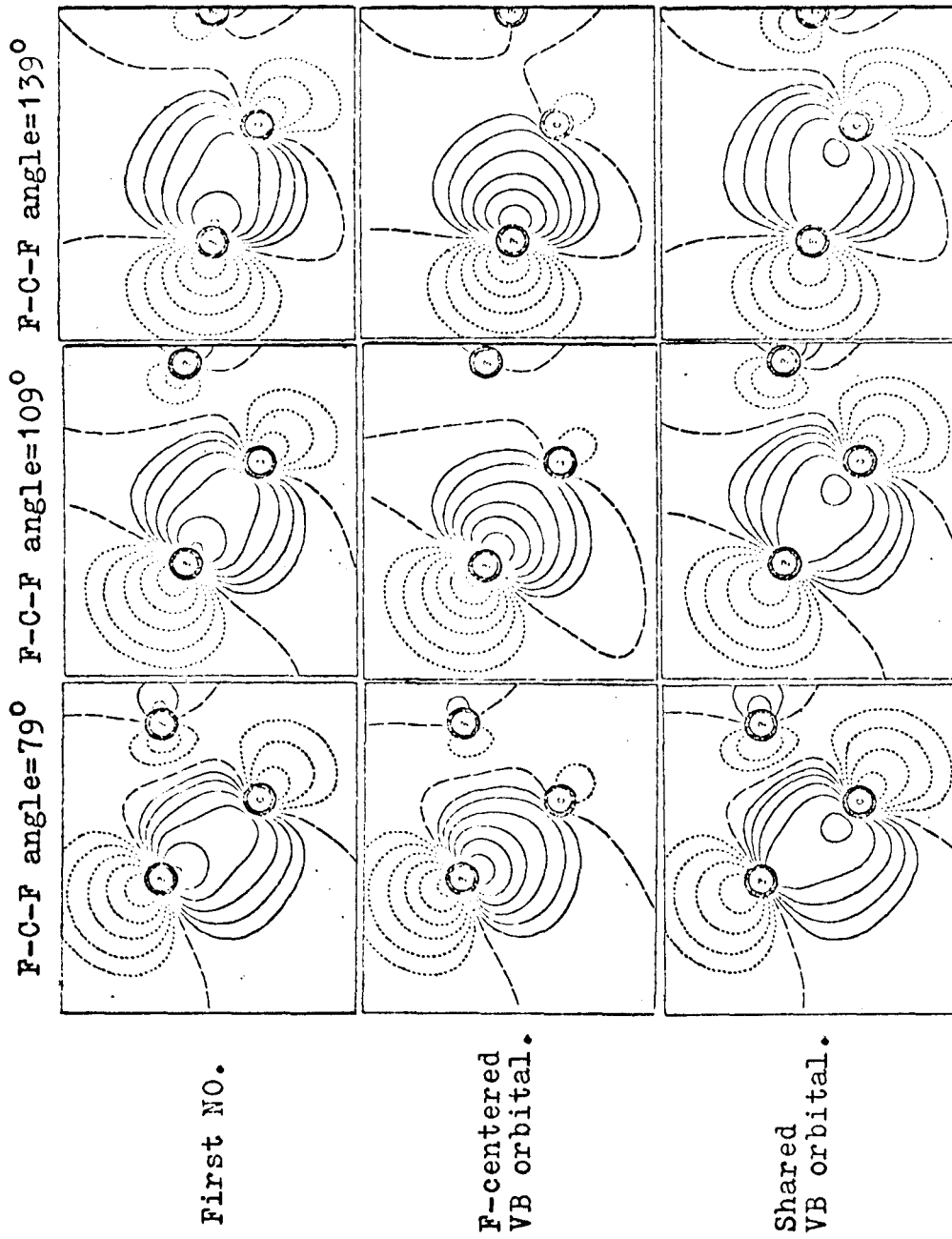


Figure 15. Variation in the orbitals of the C-F bonding pair in difluoromethane as the F-C-F angle is changed.

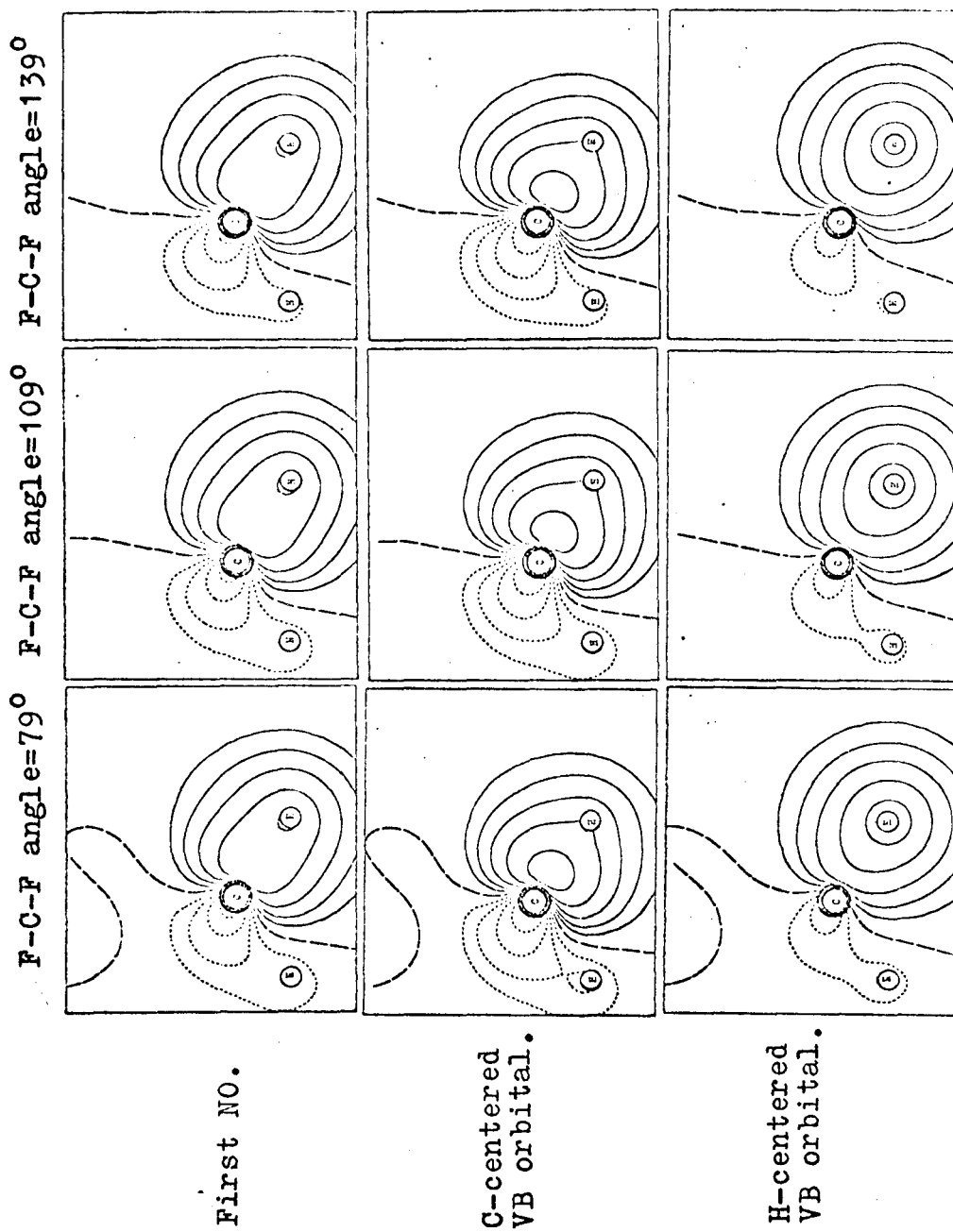


Figure 16. Variation in the orbitals of the C-H bonding pair in difluoromethane as the F-C-F angle is changed

**Table 8.** Geometry Variation of Difluoromethane:  
Hybrid Analysis of the Bonding PGVB Orbitals.

Orbital	F-C-F angle	$\Theta^a$	$\phi^b$	Hybridization <sup>c</sup>	
				C hybrid	F hybrid
C-H bond, first NO	79°	125°(126°,122°)	-	2.0(67%)	-
	109°	124°(125°,122°)	-	2.0(66%)	-
	139°	122°(124°,119°)	-	2.1(68%)	-
C-H bond, C-centered VB orbital	79°	125°(125°,123°)	-	1.6(61%)	-
	109°	123°(124°,122°)	-	1.6(61%)	-
	139°	120°(122°,116°)	-	1.6(62%)	-
C-F bond, first NO	79°	107°(100°,122°)	-10.2°	5.5(85%)	d (100%)
	109°	96°( 98°, 88°)	0.2°	5.7(85%)	d (99%)
	139°	81°( 98°, 37°)	11.2°	4.8(83%)	d (99%)
C-F bond, shared VB orbital	79°	106°(101°,118°)	-9.8°	3.6(78%)	d (98%)
	109°	97°( 99°, 91°)	0.0°	3.5(78%)	d (100%)
	139°	86°( 99°, 52°)	11.3°	2.9(74%)	d (100%)
C-F bond, F-centered VB orbital	79°	-	-10.5°	-	d (97%)
	109°	-	0.4°	-	d (96%)
	139°	-	11.1°	-	d (96%)

<sup>a</sup>This is the angle between the C hybrid of the orbital and the similar hybrid of the symmetrically related bond pair. The value given is based on the average hybrid direction as defined in section B. In parentheses are, respectively, the inner and outer p-contributions to this angle.

<sup>b</sup>This is the average angle between the F hybrid of the orbital and the C-F axis. See p. 118 for sign convention.

<sup>c</sup>The "x" in "sp<sup>x</sup>." Parentheses contain the % p-character.

<sup>d</sup>Greater than 10.0.

#### D. Summary

The following eight points summarize the major topics covered in this chapter:

- 1) A quadratically convergent approach to molecular orbital localization using the Edmiston-Ruedenberg criterion has been developed and has been shown to work satisfactorily for difluoromethane, which gives very slow convergence using the usual two-by-two rotation method.
- 2) An analysis of the localized molecular orbitals for the equilibrium geometry of difluoromethane indicates that the fluorine lone pairs are delocalized in a bonding fashion toward carbon, that this delocalization represents a strong stabilizing influence in the molecule, and that this delocalization is most efficient for those lone pairs which lie in the F-C-F plane. These effects may represent the MO equivalent of the "double bond-no bond" resonance of VB theory.
- 3) The LMO changes which result from the distortion of the F-C-F angle in difluoromethane tend to discount the concept of "orbital following" on the part of carbon. Rather, each fluorine atom appears to "pivot" to maintain high bonding overlap with a relatively static carbon hybrid.

- 4) The Hartree-Fock projected GVB (PGVB) method for splitting one doubly-occupied orbital into a VB-like pair of (optimized) orbitals has been developed in both linearly and quadratically convergent forms. It has been shown to be a very good approximation to the GVB method (though much less time-consuming) in the splitting of the C-F bonding pair of difluoromethane (equilibrium geometry).
- 5) It has been shown that the PGVB solution for the above C-F bond pair is insensitive to the "freezing" of the canonical Hartree-Fock core orbitals. Also, it has been shown that, in the equilibrium geometry of difluoromethane, splitting the C-F bond pair using the PGVB method has little influence upon the optimum C-H bond pair.
- 6) The one-pair PGVB method has been used to give a detailed picture of the electronic structure of each of the unique electron pairs in the equilibrium geometry of difluoromethane.
- 7) The PGVB method has led to an approximate set of naturally localized molecular orbitals which are similar to the LMO's but are tied to a physically meaningful localization criterion. An analysis of these orbitals supports conclusion 2), above, drawn from the LMO's.

- 8) An analysis of the PGVB solutions for the C-F and C-H bond pairs for the geometries of difluoromethane in which the F-C-F angle is distorted supports conclusion 3), above, drawn from the LMO's.

E. REFERENCES

1. W. A. Sheppard and C. M. Sharts, "Organic Fluorine Chemistry," W. A. Benjamin, Inc., New York, 1969, pp. 18-40.
2. L. O. Brockway, J. Phys. Chem., 41, 185, 747 (1937).
3. These values appear in Reference 13 and are collected from a variety of sources.
4. L. Pauling, "The Nature of the Chemical Bond," 3rd ed., Cornell University Press, Ithaca, N. Y., 1960, pp. 314-315.
5. D. Peters, J. Chem. Phys., 38, 561 (1963).
6. A. Streitwieser and D. Holtz, J. Amer. Chem. Soc., 89, 692 (1967).
7. S. Andreades, ibid., 86, 2003 (1964).
8. J. Hine, ibid., 85, 3239 (1963).
9. E. A. C. Lucken, J. Chem. Soc. (A), 2954 (1959).
10. See, e.g., F. L. Pilar, "Elementary Quantum Chemistry," McGraw-Hill, New York, 1968, pp. 551-578.
11. See, e.g., Reference 10, pp. 341-385.
12. See, e.g., Reference 10, p. 611.
13. M. D. Newton, W. A. Lathan, W. J. Hehre and J. A. Pople, J. Chem. Phys., 52, 4046 (1970).
14. M. L. Unland, J. H. Letcher, I. Absar and J. R. van Wazer, J. Chem. Soc. (A), 1328 (1971).
15. R. S. Mulliken, J. Chem. Phys., 23, 1833, 1841 (1955).
16. a) J. E. Lennard-Jones and J. A. Pople, Proc. Roy. Soc. (London), A210, 190 (1951); b) C. Edmiston and K. Ruedenberg, Rev. Mod. Phys., 35, 457 (1963); c) M. D. Newton and E. Switkes, J. Chem. Phys., 54, 3179 (1971) and preceding papers in the series; d) R. M. Pitzer, ibid., 41, 2216 (1964).

17. a) O. J. Sovers, C. W. Kern, R. M. Pitzer and M. Karplus, J. Chem. Phys., 49, 2592 (1968); b) J. R. Hoyland, J. Amer. Chem. Soc., 90, 2227 (1968); c) J. R. Hoyland, J. Chem. Phys., 50, 473 (1969); d) J. D. Petke and J. L. Whitten, ibid., 51, 3166 (1969); e) J. H. Letcher and T. H. Dunning, ibid., 48, 4538 (1969).
18. K. Ruedenberg, "Modern Quantum Chemistry," O. Sinanoglu, Ed., Academic Press, New York, 1965, Part 1, p. 85ff.
19. An enlarged and streamlined version of the localization program written by R. M. Pitzer and W. E. Palke. We thank S. L. Guberman for providing us with a copy of this program.
20. This method is outlined in Reference 16b.
21. W. J. Taylor, J. Chem. Phys., 48, 2385 (1968).
22. This approach was suggested to us by Dr. W. J. Hunt.
23. To show this, we form the product  $\hat{O}^T \hat{O} = 1 + \hat{A}^T + \hat{A} + \hat{A}^T \hat{A}$  and note that the second two terms on the right-hand side cancel one another because  $\hat{A}$  is skew-symmetric. Thus, the left-hand side differs from the unit matrix only in terms which are second-order in the elements of  $\hat{A}$ .
24. A matrix  $\hat{O}$  is symmetrically orthogonalized by forming the symmetric matrix  $\hat{U} = \hat{O}^T \hat{O}$ , then obtaining  $\hat{U}^{-\frac{1}{2}}$ , a symmetric matrix with the same eigenvectors as  $\hat{U}$ , but eigenvalues which are the reciprocal square roots of the corresponding eigenvalues of  $\hat{U}$  (which must all be positive). Then the matrix  $\hat{O}' = \hat{O} \hat{U}^{-\frac{1}{2}}$  is truly orthogonal.
25. See, e.g., W. A. Bennett, J. Org. Chem., 34, 1772 (1969).
26. See, e.g., Reference 4, p. 122.
27. M. D. Newton, E. Switkes and W. N. Lipscomb, J. Chem. Phys., 53, 2645 (1970).
28. P. O. Löwdin, ibid., 18, 365 (1950).
29. That is,  $\hat{S}^{\frac{1}{2}}$  has the same eigenvectors as  $\hat{S}$ , but eigenvalues which are the square roots of the corresponding eigenvalues of  $\hat{S}$ .

30. See, e.g., J. D. Roberts, "Notes on Molecular Orbital Calculations," W. A. Benjamin, Inc., New York, 1962, p. 47.
31. For a discussion of the orbital following concept as it applies to the problem of harmonic force constant definition, see I. M. Mills, Spectrochim. Acta, 19, 1585 (1963).
32. a) W. J. Hunt, P. J. Hay and W. A. Goddard III, J. Chem. Phys., 57, 738 (1972); b) P. J. Hay, W. J. Hunt and W. A. Goddard III, J. Amer. Chem. Soc., in press; c) W. A. Goddard III, ibid., 94, 793 (1972); d) P. J. Hay, W. J. Hunt and W. A. Goddard III, Chem. Phys. Letters, 13, 30 (1972); e) W. A. Goddard III and R. C. Ladner, J. Amer. Chem. Soc., 93, 6750 (1971).
33. A. C. Hurley, J. E. Leonard-Jones and J. A. Pople, Proc. Roy. Soc. (London), A220, 446 (1953).
34. H. F. Schaeffer III, "The Electronic Structure of Atoms and Molecules," Addison-Wesley Publ. Co., Menlo Park, California, 1972, p. 37.
35. As discussed in References 32a and 32d, the cores can be left unsplit without significantly altering the splitting of the valence pairs, and the optimum doubly-occupied core pairs are essentially unmodified 1s functions.
36. W. A. Goddard III, W. J. Hunt and T. H. Dunning, private communication.
37. See Reference 10, pp. 279-282.
38. If  $D_i$  represents a measure of the change in the wavefunction during iteration  $i$ , then linear convergence is characterized by the approximate relationship
- $$D_{i+1} = KD_i$$
- where  $K$  is usually in the range 0.1-0.8.
39. a) A. Veillard, "IBMOL: Computation of Wave-Function for Molecules of General Geometry. Version 4," Large Scale Scientific Computations Department, IBM Research Laboratory, San Jose, California, 95114, part 1, pp. 33-34; b) C. C. J. Roothaan and P. S. Bagus, "Methods in Computational Physics," B. Alder, S. Fernbach and M. Rotenberg, Eds., Academic Press, New York, 1963, pp. 62-64.

40. If  $D_i$  is as in 38, above, then quadratic convergence is characterized by the approximate relationship

$$D_{i+1} = KD_i^2$$

The value of  $K$  depends upon the units of  $D$ , but as convergence is approached,  $K$  is such that  $D_{i+1}$  is much smaller than  $D_i$ .

41. See, e.g., T. M. Apostol, "Mathematical Analysis," Addison Wesley Publ. Co., Inc., Palo Alto, California, 1964, pp. 112-114.
42. This may be derived from the expression for the energy of a general determinantal wavefunction given in Reference 10, p. 333.
43. See, e.g., Reference 32a.
44. T. H. Dunning, private communication.
45. W. A. Goddard III, T. H. Dunning and W. J. Hunt, private communication.